



NEUROSCIENCE  
**2017**

# **SHORT COURSE 1**

## **Intersections Between Brain and Immune System in Health and Disease**

Organizers: Carla Shatz, PhD,  
and Beth Stevens, PhD



SOCIETY *for*  
NEUROSCIENCE

# Short Course 1

## Intersections Between Brain and Immune System in Health and Disease

Organized by Carla Shatz, PhD, and Beth Stevens, PhD

---



SOCIETY *for*  
NEUROSCIENCE

Please cite articles using the model:  
[AUTHOR'S LAST NAME, AUTHOR'S FIRST & MIDDLE INITIALS] (2017)  
[CHAPTER TITLE] In: Intersections Between Brain and Immune System in Health and Disease.  
(Shatz C, Stevens B, eds) pp. [xx-xx]. Washington, DC: Society for Neuroscience.

All articles and their graphics are under the copyright of their respective authors.

Cover graphics and design © 2017 Society for Neuroscience.



## SHORT COURSE 1

### Intersections Between Brain and Immune System in Health and Disease

Organized by Carla Shatz, PhD and Beth Stevens, PhD

Friday, November 10, 2017

8:30 a.m.—6 p.m.

Location: Washington, DC Convention Center • Room: Ballroom A

TIME	TOPIC	SPEAKER
8 – 8:30 a.m.	CHECK-IN	
8:30 – 8:40 a.m.	Opening Remarks	Carla Shatz, PhD • Stanford University Beth Stevens, PhD • Harvard University
8:40 – 9:30 a.m.	Multiple Sclerosis: From Bench to Bedside and Back Again	Stephen Hauser, MD • University of California, San Francisco
9:30 – 10:20 a.m.	What Do Reactive Astrocytes Do, and How Should We Study Them?	Shane Liddelow, PhD • Stanford University
10:20 – 10:50 a.m.	MORNING BREAK	
10:50 – 11:40 a.m.	Glymphatic–Lymphatic Connections	Maiken Nedergaard, PhD • University of Rochester
11:40 a.m. – 12:30 p.m.	Microbiota, CNS Development, and the Enteric Nervous System	Dan Littman, PhD • New York University
12:30 – 1:30 p.m.	LUNCH – ROOM 151 AB	
1:30 – 2:20 p.m.	Innate Immune Receptors in Microglia Biology	Marco Colonna, MD • Washington University in St. Louis
2:20 – 3:10 p.m.	Microglia: Synaptic Sculptors and Saboteurs	Beth Stevens, PhD • Harvard University
3:10 – 4 p.m.	Surprise at the Synapse: Developmentally Critical Periods and Alzheimer's Disease	Carla Shatz, PhD • Stanford University
4 – 4:15 p.m.	AFTERNOON BREAK	

#### AFTERNOON BREAKOUT SESSIONS • PARTICIPANTS SELECT DISCUSSION GROUPS AT 4:15 AND 5:15 P.M.

TIME	BREAKOUT SESSIONS	SPEAKERS	ROOM
4:15 – 5 p.m.	Group 1: Modeling Human Disease: Revising Assumptions About Molecules and Mechanisms	Carla Shatz, Stephen Hauser, & Shane Liddelow	143A
	Group 2: What Are the Interactions Between the Brain and the Periphery?	Maiken Nedergaard & Dan Littman	143B
	Group 3: How Normal Immune Processes Go Awry in Brain Disease: Implications for New Therapies and Biomarkers	Beth Stevens & Marco Colonna	143C
5 – 5:15 p.m.	AFTERNOON BREAK		
5:15 – 6 p.m.	Repeat sessions above. Select a second breakout group.		

# Table of Contents

---

Introduction <i>Carla Shatz, PhD, and Beth Stevens, PhD</i> . . . . .	5
Multiple Sclerosis: From Bench to Bedside and Back Again <i>Stephen L. Hauser, MD</i> . . . . .	6
Purification and Culture Methods for Astrocytes <i>Shane Liddelow, PhD</i> . . . . .	19
The Glymphatic System <i>Nadia Aalling, MSc, Anne Sofie Finmann Munk, BSc, Iben Lundgaard, PhD, and Maiken Nedergaard, MD, DMSc</i> . . . . .	27
The Maternal Interleukin-17a Pathway in Mice Promotes Autism-Like Phenotypes in Offspring <i>Gloria B. Choi, PhD, Yeong S. Yim, PhD, Helen Wong, PhD, Sangdoon Kim, PhD, Hyun Ju Kim, PhD, Sangwon V. Kim, PhD, Charles A. Hoeffler, PhD, Jun R. Huh, PhD, and Dan R. Littman, MD, PhD</i> . . . . .	37
TREM2 Variants: New Keys to Decipher Alzheimer's Disease Pathogenesis <i>Marco Colonna, MD, and Yaming Wang, PhD</i> . . . . .	49
Microglia: Phagocytosing to Clean, Sculpt, and Destroy <i>Soyon Hong, PhD, and Beth Stevens, PhD</i> . . . . .	64
Synapse Elimination and Learning Rules Coregulated by Major Histocompatibility Class I Protein H2-D <sup>b</sup> <i>Hanmi Lee, PhD, Lowry A. Kirkby, PhD, Barbara K. Brott, PhD, Jaimie D. Adelson, PhD, Sarah Cheng, BS, Marla B. Feller, PhD, Akash Datwani, PhD, and Carla J. Shatz, PhD</i> . . . . .	70

# Introduction

---

Communication between brain cells and immune system cells plays a critical role in neural development, homeostasis, and disease. The intersections between the nervous and immune systems are complex and can have either beneficial or detrimental impacts on brain function, depending on the context.

The nervous and immune systems share an array of molecules that have both specialized and analogous functions in the other system. Many immune-related molecules are expressed in the healthy brain and have homeostatic and physiological functions. For example, molecules traditionally associated with adaptive and innate immunity regulate circuit development and plasticity. Microglia, resident immune cells, and phagocytes actively signal along with neurons and astrocytes and sculpt developing synapses. Conversely, aberrant regulation of neural-immune interactions can damage the brain by mediating neuroinflammation, autoimmune reactions, vascular breakdown, synapse loss, and neurodegeneration. It is thus crucial that we understand the mechanisms that give rise to these divergent outcomes.

This course will bring together an interdisciplinary team of faculty and researchers to discuss these and other emerging topics in neuroimmunology, with an emphasis on the mechanisms underlying neural-immune system cross talk in health and disease. Faculty will highlight new discoveries, tools, and approaches to study and model neural-immune signaling in different contexts, including human disease. Lecture topics include the interactions between the brain and the periphery; mechanisms and implications of reactive gliosis; glymphatic-lymphatic system connections; microglia function and dysfunction; the microbiome and the gut-brain axis; and immune mechanisms of synapse loss during developmentally critical periods and in neurodegeneration.

# **Multiple Sclerosis: From Bench to Bedside and Back Again**

Stephen L. Hauser, MD

---

Weill Institute for Neurosciences  
University of California, San Francisco  
San Francisco, California

## Introduction

The goal of a career in biomedical research is to contribute meaningfully to medically useful discoveries: something that happens, if one is fortunate, perhaps a few times over the course of a career. For those of us involved in the B-cell story in multiple sclerosis (MS), this occurred in September 2006 with the unblinding of the phase II anti-CD20 rituximab (RTX) study (Hauser et al., 2008). First, we saw evidence of a potentially powerful new approach for treating relapsing MS (RMS). Second, despite this success, it was also clear that the rationale behind the clinical testing of RTX for MS was almost certainly incorrect. In many respects, this was the best possible result that one could wish for. A novel approach appeared to offer significant benefits for patients, and yet the data also sent us back to the bench in new and unexpected directions. The rubber meets the road when ideas born in the lab are formally tested at the bedside, and when data from real-life patients create new, testable ideas for research. Translational medicine is most effective when information flow is bidirectional, linking the laboratory with the clinic.

## The Early Days

In the late 1970s, during my neurology residency, I was in a conference room at Massachusetts General Hospital in Boston with the chair of neurology, Raymond D. Adams. A postdoctoral fellow was presenting some work in experimental autoimmune encephalomyelitis (EAE) induced by myelin basic protein. Adams noted, with a touch of sarcasm, that the paralysis observed in the rodents likely resulted from peripheral nerve, and not CNS, disease. Indeed, he emphasized that the pathology of EAE and MS was quite different. T-cell-mediated acute EAE models in mice were dominated by an inflammatory panencephalitis with relatively sparse demyelination, unlike the primary macrophage-mediated demyelinating pathology typical of human MS. This experience motivated me to begin a long-term effort to model MS-like pathology in the laboratory.

## Developing a Better Disease Model

In partnership with Norman Letvin, we began immunizing different species of nonhuman primates to search for pathologies that closely mimicked MS (Genain and Hauser, 1997). We were hopeful that a model could be generated in the New World marmoset *Callithrix jacchus*, a small primate approximately the size of a guinea pig but with a unique defining characteristic. *C. jacchus* pregnancies are typically multiple, involving gestation of several nonidentical

embryos at a time. Each fetus shares a common blood supply, leading to the establishment of a permanent, stable, lifelong bone marrow chimerism among fraternal twins or triplets. We found that this chimeric state, as predicted, permitted the transfer of T-lymphocytes from one sibling to another without eliciting an alloresponse in the recipient. These data set the stage for adoptive transfer of encephalitogenic T-cells in a species phylogenetically close to humans, analogous to earlier experiments in inbred mice that were critical for defining the immunology of murine EAE.

After several years of starts and stops, a model of MS was successfully developed by Luca Massacesi, a postdoctoral fellow, in 1995 (Massacesi et al., 1995). The key step, which had eluded us before Luca's arrival, was the creative use of different immune adjuvants (Genain and Hauser, 1996). Following immunization with a myelin extract in incomplete Freund's adjuvant, and later with myelin oligodendrocyte glycoprotein (MOG), animals developed a mild relapsing–remitting disease and an acute pathology characterized by large concentric areas of macrophage-mediated demyelination with relative axonal sparing and foci of remyelination; the myelin membrane was destroyed and reconstituted into vesicular fragments (Fig. 1), a pattern termed “vesicular demyelination” (Prineas and Connell, 1978). This was our first eureka moment—we had replicated the MS-like pathology that we had sought for a decade.

However, when we adoptively transferred MOG-reactive T-cell clones from an immunized *C. jacchus* animal into a chimeric sibling, we replicated the acute murine pathology of panencephalitis but not the distinctive MS-like pathology of vesicular demyelination (Massacesi et al., 1995). The explanation for this apparent conundrum was quickly solved by another postdoctoral fellow at the time, Claude Genain. Only by coadministering encephalitogenic T-cells plus pathogenic antibodies (Abs) could the MS-like demyelinating phenotype be reconstituted. This finding led us to focus on the concept that an MS-like, demyelinating lesion required both pathogenic T-cells plus autoantibodies; the autoantibodies alone were nonpathogenic, presumably because they required encephalitogenic T-cells to open the blood–brain barrier (BBB) and permit their passage into the CNS (Genain et al., 1995, 1996). Our confidence that these mechanisms were operational in MS was strengthened by older literature in guinea pig optic neuritis first described by Appel and Bornstein (1964), and much later by Linington, Olssen, and Wekerle in work with rat

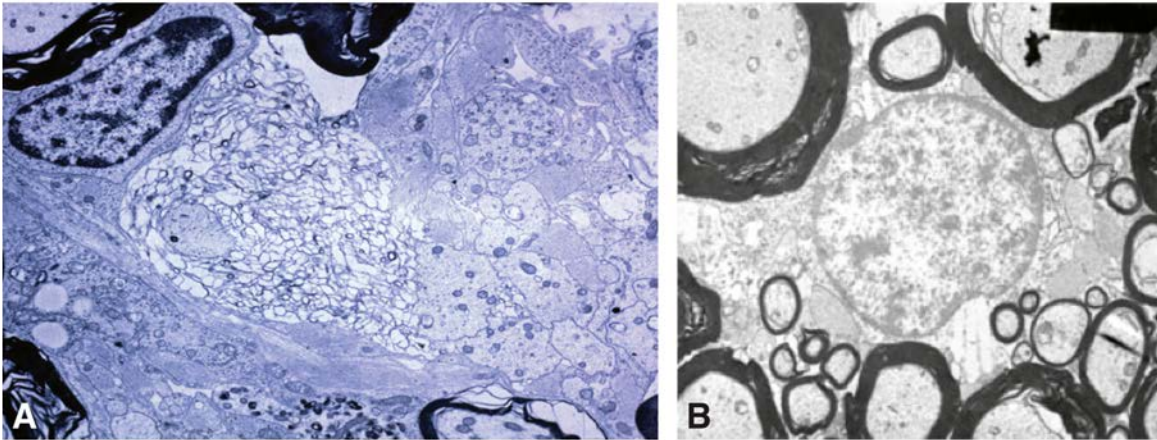


**Figure 1.** Ultrastructural features of *C. jacchus* EAE. In **A**, primary demyelination with preservation of axons, macrophage infiltration (macrophage nucleus visible at the top right), and astrogliosis are present. In the center, morphological changes of myelin dissolution and fasciculation are visible. In **B**, findings in chronic *C. jacchus* EAE are shown, illustrating areas of thin, compact myelin-encircling axons, indicative of remyelination. Reprinted with permission from Hauser (2015), Fig. 3. Copyright 2015, SAGE Publications.

EAE models (Linington et al., 1993; Lorentzen et al., 1995).

In 1999, we completed a deeper study of the lesion with Cedric Raine, revealing the presence of bound Abs in the demyelinated lesions of *C. jacchus* that recognized the immunizing antigen (Ag) MOG. However, when we then turned to human MS tissue, we found that deposited Abs were also bound to the myelin membrane but had specificities that were far more diverse than in EAE (Genain et al., 1999; Raine et al., 1999). This suggested that a highly focused immunotherapy is unlikely to be successful for MS.

## Back to the Bedside

Given the heterogeneous nature of the Ab repertoire associated with myelin destruction in MS, it became clear that targeting any specific protein or epitope was a dubious therapeutic strategy. Thus, we turned to methods that could deplete or inactivate a broad range of Abs, plasma cells, or perhaps their progenitors, B-lymphocytes. The first two options were not feasible with available therapeutics, and we had previously found that indiscriminate Ab removal via plasmapheresis had little meaningful effect on chronic MS (Hauser et al., 1982, 1983); thus, our thoughts turned to B-cell-based therapy, and specifically to the anti-CD20 monoclonal Ab (MAb) RTX.

RTX was synthesized at Idec Pharmaceuticals in 1986. Idec entered into a codevelopment partnership with Genentech in 1995, and two years later, RTX

(marketed as Rituxan) received U.S. Food and Drug Administration (FDA) approval for the treatment of B-cell lymphoma. In 2001, I began discussions with Genentech around RTX therapeutics for MS after our failed application to the National Institutes of Health (championed by Claude Genain with Michael Racke and Nancy Monson at University of Texas Southwestern Medical Center) had left us little hope that public resources could be found to support this trial. The referee comments from the application were dismissive, reflecting profound skepticism of the proposition that humoral immune mechanisms might be central to MS pathogenesis. Across much of academia at the time, MS research was dominated by concepts of T-cell mediation, analogy to murine EAE models, and a belief that CNS Igs, including oligoclonal bands (OCBs), represented meaningless “nonsense” Abs (Mattson et al., 1980). The field was not yet ready.

Industry proved to be a more flexible, and less risk-averse, partner. Discussions with Genentech progressed well, although the company estimated our chance of success at “less than 15%.” Even if one accepted that autoantibodies were responsible for MS, a B-cell-based therapy would not immediately knock down Ab production by long-lived plasma cells. Their experience with RTX indicated that IgG Ab levels were largely unchanged following treatment, although lower-affinity IgM was modestly reduced by approximately 15%. At least in theory, one would need many years of treatment to reduce circulating levels of Ig. Our original plan was to begin with a placebo-controlled phase IIB clinical trial of

two courses of RTX spaced six months apart, and a primary endpoint at 12 months, or six months after the final infusion. The FDA balked at this design, advising us that it was unethical to maintain MS patients on placebo therapy for one year. In response to these concerns, the trial was scaled back; fewer patients would be enrolled, only a single course of RTX would be administered, and the primary endpoint would be measured at six months. Our prospects for success seemed ever dimmer.

As noted earlier, when the data were unblinded in 2006, we observed a dramatic and almost immediate 91% reduction in gadolinium-enhancing magnetic resonance imaging (MRI) activity (the primary endpoint) plus a significant reduction in the rate of new relapses (Hauser et al., 2008). This was our second eureka moment. Perhaps the rapid onset of the benefit conferred by RTX was the most stunning aspect of the trial. Because the clinical effects happened so quickly, they were almost certainly not the result of any reduction in long-lived Abs but were more likely explained by some direct effect on B-cells themselves. In many respects, this was the best of all possible results for a clinical experiment. The data raised hope that an impactful new approach to MS therapy would result, but they were also perplexing, sending us back to the lab with information that the underlying hypothesis behind the clinical trial was almost certainly wrong. We now had a new focus on B-cell biology.

### The Multifunctional B-Cell

B-cells are extremely diverse members of the universe of adaptive immunity. Although targeting autoantibodies provided the original conceptual framework for testing RTX in RMS, the resulting data made it likely that the robust efficacy was somehow related to a direct effect on B-cells themselves (von Büdingen et al., 2011). B-cells have numerous effector functions independent of their differentiation from Ab-secreting plasma cells (Fig. 2). B-cells are highly effective Ag-presenting cells (APCs), but unlike other conventional APCs that are promiscuous Ag presenters, B-cells are most

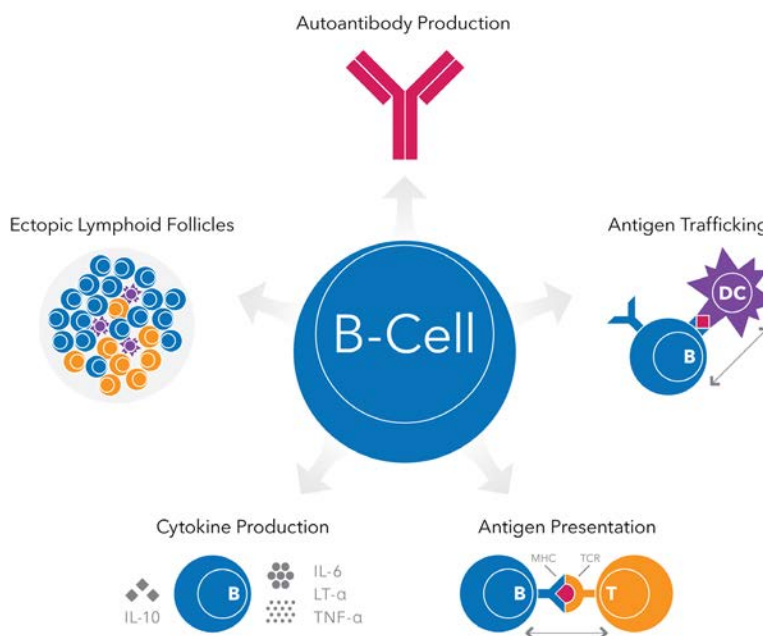


**Figure 2.** An overview of the diverse functional roles of B-cells. LT- $\alpha$ , lymphotoxin-alpha; TCR, T-cell receptor. Reprinted with permission from Hauser (2015), Fig. 4. Copyright 2015, SAGE Publications.

efficient at presenting Ag that is initially recognized by the surface B-cell receptor (BCR), i.e., the clonally specific Ig molecule. Thus, B-cells can be viewed as extremely selective APCs. Ag initially bound to surface BCRs is internalized, complexed in endosomes with class II major histocompatibility complex (MHCII) molecules, and returned to the surface for Ag presentation to T-cells. B-cells are also highly motile, and in secondary lymphoid structures, they play a role in “Ag shuttling,” a process in which Ag is grabbed from macrophages by B-cells via the BCR and transported to follicular dendritic cells (DCs), another class of APCs. Through secretion of cytokines, B-cells can also regulate, as bystanders, various effector immune functions mediated by both B-cells and T-cells. Some B-cells support pro-inflammatory function through secretion of tumor necrosis factor alpha (TNF- $\alpha$ ) and lymphotoxin, whereas a different interleukin (IL)-10-producing B-cell population has a regulatory, anti-inflammatory role. Interestingly, MS B-cells may be inherently polarized toward a pro-inflammatory functional phenotype (Bar-Or et al., 2010). As noted earlier, the rapid response to B-cell depletion therapy for focal disease activity in RMS indicated that the mechanism of action was likely not, as initially hypothesized, inhibiting autoantibodies. Instead, it was more likely blocking B-cell APC function and subsequent T-cell activation, or perhaps acting via

bystander effects on adaptive immunity. However, the potential inhibition of an as-yet unidentified autoantibody in MS could not be completely excluded (Khosroshahi et al., 2010).

B-cell development begins in the bone marrow and proceeds through stages of pro-B-cells and pre-B-cells before the cells exit into the circulation as naive, Ag-inexperienced B-cells. The vast majority of B-cells are located in follicles in secondary lymphoid tissues, including lymph nodes and spleen, and in mucosal sites. Binding of Ag through the BCR triggers activation, proliferation, and somatic hypermutation (SHM) of BCRs, resulting in maturation to memory (Ag-experienced) B-cells and differentiation to Ab-secreting plasma cells. B-cells are believed to reside in lymphoid follicles for only ~1 d before returning to the circulation, highlighting the dynamic nature of B-cell Ag capture, activation, and SHM of the BCR. It is thought that both memory B-cells and Ab-secreting plasmablasts and plasma cells can cross the BBB and enter the CNS in low numbers, and once there can reside in protective niches for long periods of time—a concept that has become increasingly relevant to research in progressive MS.

CD20 is an ideal target for B-cell immunotherapy. The CD20 molecule is expressed on pre-B-cells and throughout the life cycle of naive and memory B-cells; CD20 is not expressed on stem cells or pro-B-cells at the earliest stages of the B-cell differentiation program, nor is it expressed on plasmablasts or terminally differentiated plasma cells (Fig. 3, top). Following removal of CD20 B-cells with RTX, there is consistent repletion from early B-cell progenitors residing in the bone marrow, generally beginning four to six months after treatment (Fig. 3, bottom). Because long-lived plasma cells are unaltered, Ab responses to infectious agents or to vaccinations are largely preserved during periods of B-cell depletion. This feature may also explain the favorable safety record (after ~3 million doses) of RTX. MAbs against CD20 do not effectively remove B-cells residing in protective niches within secondary lymphoid structures. Circulating B-cells, representing only ~2% of the total B-cell pool in humans, are the B-cell compartment most efficiently depleted by these agents.

If B-cells residing in pathogenic niches (e.g., the CNS in MS, or synovium in rheumatoid arthritis [RA]) are relatively protected from anti-CD20 therapy, then how does the treatment work? The most likely explanation is that sustained depletion of circulating B-cells, which in autoimmune disease likely includes recirculating, restimulated memory B-cells destined

to return to the target tissue, prevents their reentry into white matter regions in MS or joint tissue in RA (Silverman and Boyle, 2008).

## Technology Moves Faster Than Clinical Research

It took 18 months for the RTX data to find their way into final print (Hauser et al., 2008), but by this time, the prospects for advancing to phase III clinical trials of RTX were dead. The reasons for this were multiple but included complex governance of the RTX franchise between the two participating pharmaceutical companies, Biogen Idec and Genentech (Biogen and Idec Pharmaceutical agreed to merge in 2003) and RTX's expiring patent life; an FDA requirement that we carry out a dose-finding study of RTX before moving forward with phase III; the development of a new humanized anti-CD20 MAb, ocrelizumab (OCR), by Genentech; and lastly, Roche's acquisition of Genentech in 2009. A plan was put forward to no longer pursue RTX but instead to develop OCR for MS.

Different MAbs are not necessarily biologically identical even if they target the same molecule; this is certainly the case for Abs that target CD20. RTX and OCR target different epitopes of CD20 and kill B-cells through different cytolytic pathways. RTX has stronger complement-dependent cytotoxicity (CDC) and less Ab-dependent cell-mediated cytotoxicity (ADCC), whereas the converse is true for OCR. Greater ADCC activity by OCR results from a higher affinity of Fc binding to the Fc-gamma receptor IIIa (FcγRIIIa) on host natural killer cells. The dose of Ab used, and the frequency of administration, may also influence ADCC activity. These differences between RTX and OCR, as well as differences in dose plus the use of polytherapy, may help to explain a complication observed in a trial of OCR as add-on therapy for RA in which several serious opportunistic infections developed in older Asian RA patients treated with high doses of OCR (Rigby et al., 2012). This complication in the OCR trial was quite unexpected, as no safety signal of this type had been noted in the nearly 200,000 RA patients treated with RTX as add-on therapy (Rubbert-Roth et al., 2010). Although the RA trial of OCR was halted, the MS phase II trial of low-dose OCR as monotherapy proceeded, and when the results were unblinded, a robust treatment response identical to that found for RTX was observed with acceptable safety (Kappos et al., 2011). Also important, our hope that OCR, a humanized MAb working primarily through ADCC, would produce a lower incidence of infusion reactions compared

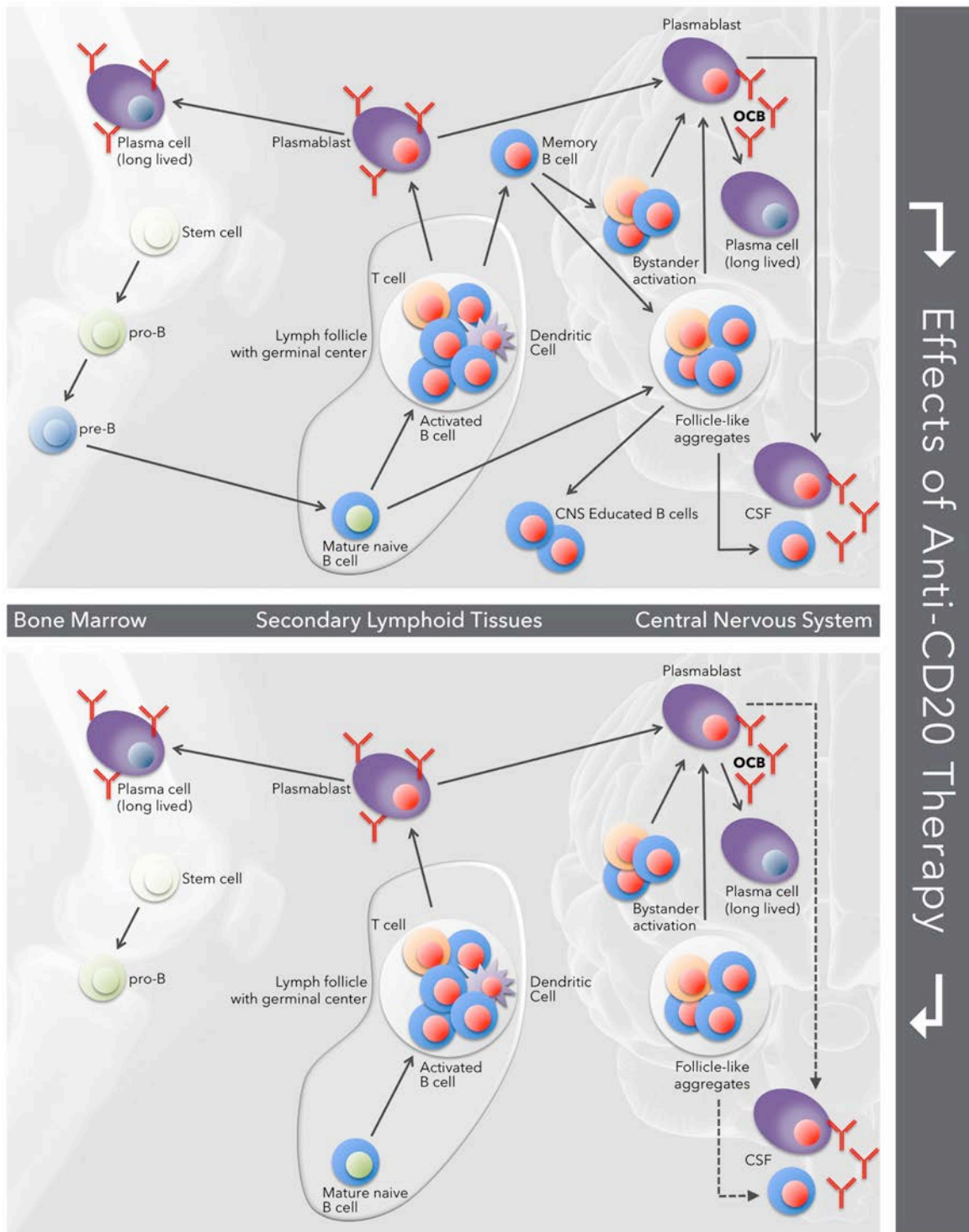


**Figure 3.** The effects of anti-CD20 therapy on recirculating B-cells. Top panel, summary of the life cycle of B-cells destined for the CNS. Bottom panel, highlights of the effects of depletion of circulating B-cells with anti-CD20 therapy; B-cells residing in lymphoid tissues and the CNS are likely to be resistant to depletion with anti-CD20 therapy. Reprinted with permission from Hauser (2015), Fig. 5. Copyright 2015, SAGE Publications.

with the chimeric RTX mediating lysis via CDC, was confirmed, making OCR a far more attractive agent for chronic use. All involved breathed a deep collective sigh of relief as we advanced to the pivotal phase III clinical trials.

Although OCR's success was anticipated in RMS, the results of the two pivotal OCR trials, published earlier this year, exceeded expectations (Hauser et al., 2017; Montalban et al., 2017). The trials revealed dramatic effects on all key clinical and MRI outcomes in RMS and demonstrated clear benefits for the previously untreatable form of the disease, primary progressive MS (PPMS). In the RMS trials, OCR produced stunning reductions in the MRI endpoint of gadolinium enhancement and new lesion formation: almost 99% compared with baseline levels, indicating nearly complete elimination of new lesion formation in brain white matter. In a single pivotal study in PPMS, confirmed progression of disability (the primary endpoint) favored OCR. However, a modest risk reduction of 24% and multiple secondary clinical and MRI endpoints, including timed walk, white matter lesion volume, and brain atrophy, also showed benefits favoring treatment. OCR (marketed as Ocrevus) was recently approved by the FDA for RMS and PPMS, and decisions by other regulatory agencies are expected to be forthcoming.

### Additional Insights from the Trials

In the original phase II RTX study in MS, focal disease activity remained reduced even after B-cells had returned to the peripheral blood (PBL). This point was driven home in a preliminary open-label, open-extension phase of the OCR phase II study. After four courses of treatment with OCR, MRI and clinical disease activity remained quiescent 18 months after the last dose. Equally important, in the phase II studies, no evidence of rebound was present at any time point. These data suggest that anti-CD20 treatment might reset the immune system in some way and confer protection against the development of new focal MS lesions beyond the period of B-cell depletion. Studies of PBL in RTX-treated individuals indicated that, following repletion, there are persistent changes in both B-cell and T-cell subpopulations that could, at least in theory, promote immune homeostasis and reduce pro-inflammatory responses. Repleting B-cells express predominantly naive and immature (CD5, CD38hi) phenotypes (Duddy et al., 2007); pro-inflammatory T-cells are decreased (Bar-Or et al., 2010); and regulatory T-cells are increased (Vallerskog et al., 2007). Reductions in pro-inflammatory immune cells are also present in CSF, with reduced numbers of T-cells and B-cells (Cross et al., 2006; Piccio et al., 2010)

and a predominance of resting B-cells (Monson et al., 2005).

### Another Surprise: CD20-Positive T-Cells

Work led by Christian von Büdingen confirmed earlier suggestions that CD20 T-cells exist in the healthy human circulation (Palanichamy et al., 2014b). This heterogeneous population, representing ~7% of total mature circulating T-cells, is composed of numerous T-cell subsets, including both CD4 helper and CD8 cytotoxic T-cells as well as naive and various memory T-cell populations. CD20<sup>+</sup> T-cells have a lower surface density of CD20 compared with B-cells (hence the designation CD3<sup>+</sup>CD20<sup>dim</sup>), but nonetheless, the vast majority of these cells are depleted from the peripheral circulation with anti-CD20 therapy. It remains possible—and would certainly be ironic if true—that the effects of anti-CD20 therapy on MS result from elimination of pathogenic CD20<sup>+</sup> T-cells.

### Back to the Bench

Scott Zamvil developed bone marrow (BM) chimeric mice containing B-cells that were selectively deficient in expression of MHCII molecules; other APCs, including DCs and monocytes, expressed MHCII normally. Following immunization with the extracellular region of mouse MOG, or with an immunodominant p35–55 MOG peptide, mice lacking MHCII on B-cells developed EAE normally. However, following immunization with recombinant human MOG, these mice became resistant to EAE induction, and susceptibility could not be restored by administering MOG Ab (Molnarfi et al., 2013). How can one interpret the finding that B-cells competent to serve as APCs were absolutely required for EAE against human MOG (hMOG) but not against murine MOG? This B-cell dependence can probably be attributed to a single amino acid change in the immunodominant region of MOG (e.g., a substitution of proline in place of serine at position 42 in human MOG). Moreover, transgenic mice that expressed surface MOG-reactive Ig on their B-cells could not secrete Ab. When crossed with a transgenic MOG-reactive T-cell line, progeny developed spontaneous EAE (associated with Th17 polarization, B-cell activation, and formation of ectopic germinal centers in the meninges), all in the absence of secreted Ab. Thus, B-cell APC function, in the absence of autoantibodies, is sufficient to promote T-cell activation and an MS-like disorder.

In EAE, B-cells tend to be involved as APCs when the immunization regimen employs whole myelin

proteins such as hMOG, but not when myelin peptides (e.g., p35–55 MOG) are used. Peptide immunization models are B-cell independent because the BCR that binds mostly conformational rather than short linear epitopes is not involved in Ag capture (Lyons et al., 1999; Fillatreau et al., 2002). Interestingly, in EAE induced by whole MOG protein, B-cell depletion is protective, but in EAE induced by MOG peptide, B-cell depletion worsens disease severity, probably by depleting IL-10-secreting regulatory B-cells (Weber et al., 2010). In humans, a clinical trial of atacept—a decoy receptor for the B-cell growth factors B-cell activating factor of the TNF family (BAFF) and a proliferation-inducing ligand (APRIL)—paradoxically worsened MS, possibly by altering regulatory B-cell tone (Kappos et al., 2014). These cautionary data emphasize that B-cell depletion can be deleterious in some situations, and they highlight the potential clinical relevance of information gleaned from EAE even when the models are imperfect representations of human MS.

Thus, B-cells can be pro-inflammatory or regulatory, and the predominance of one or another function is one determinant of the outcome of an ongoing immune response. Clearly what is needed is to better understand how B-cell polarization might be aberrant in MS. Gene variants that are expressed by B-cells make up an important component of the more than 200 variants thus far known to be associated with inherited risk for MS (International Multiple Sclerosis Genetics Consortium et al., 2013; Farh et al., 2015). Similarly, a number of functional changes in B-cells have been described in MS patients, including changes in cytokine profiles indicating a pro-inflammatory bias, and a defect in inducing B-cell tolerance in PBL (Kinnunen et al., 2013).

## Identifying and Tracking Culprit B-Cells

BCRs are heterodimeric proteins with the Ag-binding portion formed by the variable regions of heavy and light chains. With respect to Ag recognition, the heavy-chain variable region (VH) is generally believed to play the primary role; VH results from the splicing of three gene segments into a mature transcript: one copy of a variable (*V*), diversity (*D*), and joining (*J*) gene segment. *V*, *D*, and *J* genes exist as multiple copies in each genome, contributing significantly to the diversity of Ab transcripts. Most Ab diversity is generated by variation in how gene segments splice together, and especially by somatic mutations in the complementarity-determining regions of *V* genes that shape the Ab response. Following Ag contact in secondary, and possibly in

ectopic, lymphoid tissues, BCRs undergo somatic diversification as their phenotype advances from naive to memory B-cells, and then to Ab-secreting plasmablasts and plasma cells. The propensity of B-cells to select some members of *V* gene families over others is highly heritable, but the clonal repertoire of BCRs expressed by any individual is stochastic and not influenced by differences in the architecture of germline genes (Baranzini et al., 2010; Glanville et al., 2011).

Sequencing IgG-VH repertoires in MS patients revealed that CSF B-cells represent a clonally restricted population that had undergone highly selective activation and affinity maturation within the CNS compartment. By performing parallel sequencing of many thousands of IgG-VH transcripts per sample, it was possible to construct lineage trees representing clonally related CSF B-cells defined by their BCRs and to identify clonally related BCR sequences from PBL in the same individual. Results revealed a deep connection of these highly selected, clonally related B-cells between the CSF and PBL compartments (Fig. 4) (von Büdingen et al., 2012; Palanichamy et al., 2014b). Further, when CSF IgG-VH sequences were matched with mass-spectrometric proteomic analyses of isoelectric-focused CSF IgG, remarkably, the proteomic data and IgG-VH transcripts matched (Obermeier et al., 2008). Most peptides sequenced from OCBs could be shown to map to CSF-derived IgG-VH sequences, and in a given individual, different bands composing the OCBs were shown to be clonally related—that is, they belonged to the same BCR lineage tree (Obermeier et al., 2008; von Büdingen et al., 2012; Bankoti et al., 2014). Thus, there is evidence that ongoing stimulation and maturation to clonally restricted Ab-expressing B-cells occur primarily inside the CNS compartment. In some individuals, B-cells participating in OCB production can also be identified in PBL; these cells appear to migrate across the BBB and may undergo further Ag stimulation in the periphery (Bankoti et al., 2014; Palanichamy et al., 2014a). Thus, OCBs are not merely the terminal result of a focused immune response in MS but represent a component of active B-cell immunity that is dynamically supported on both sides of the BBB. Although it is unclear where in the periphery activation and/or SHM of B-cells responding to brain Ags might occur, recent data suggest that draining cervical lymph nodes are one potential site (Stern et al., 2014).

Our work in CSF (von Büdingen et al., 2012; Bankoti et al., 2014; Palanichamy et al., 2014a) and

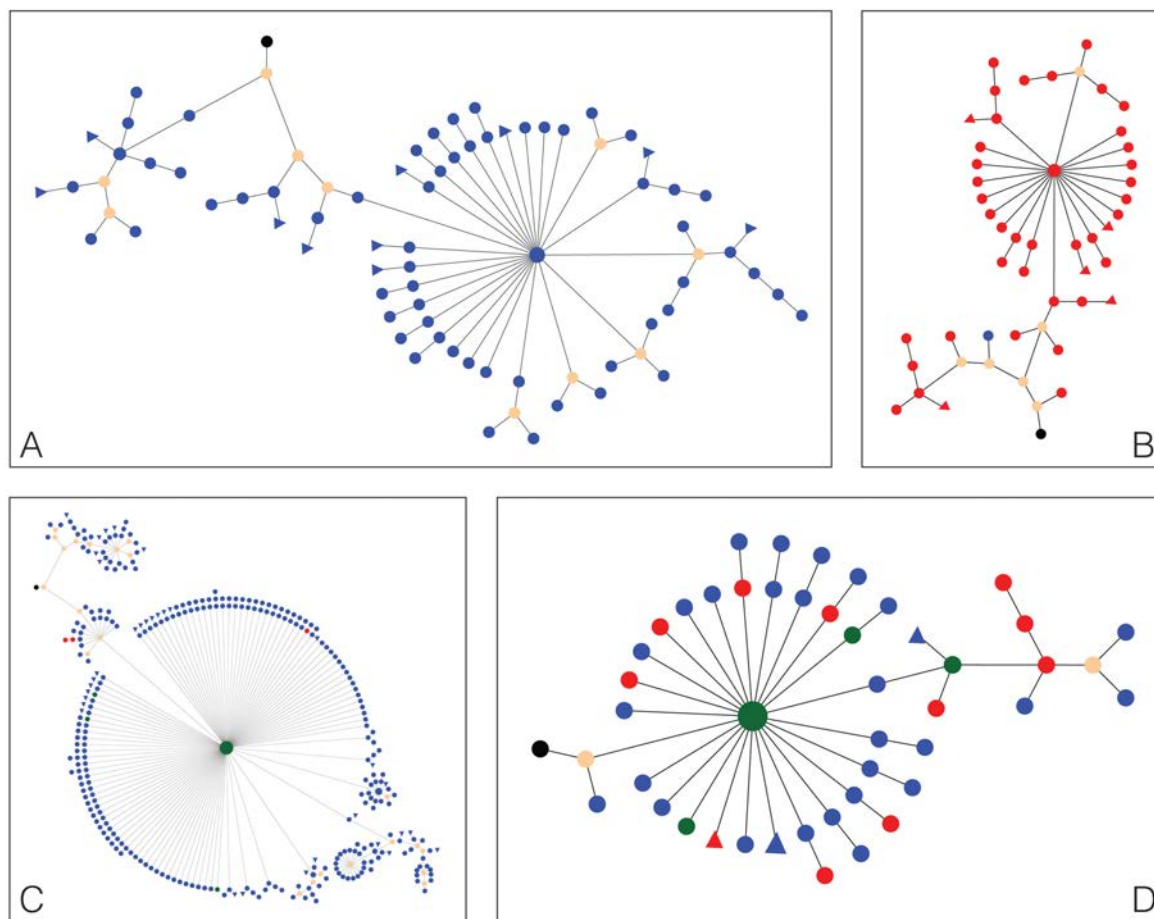


**Figure 4.** Intimate connections between CNS and peripheral B-cells in MS. Representative lineages of clonally related IgG-VH found in CSF (A), or in CSF and PBL (B–D) of MS patients as calculated by IgTree software and visualized in Cytoscape version 3.1 (organic layout) (Cytoscape Consortium, San Diego, CA). Each round node represents at least one unique IgG-VH sequence ranging from at least the 5' end of H-CDR1 to the 3' end of H-CDR3; larger nodes represent up to hundreds of identical sequences. Blue nodes, CSF-derived IgG-VH sequences; red nodes, PBL-derived sequences; green nodes, identical sequences found in both compartments. Black nodes, putative germline sequences represent the lineage root; beige nodes, hypothetical intermediates calculated by IgTree. Triangular nodes contain two or more singleton sequences in leaves. A, intrathecal affinity maturation; B, IgG-VH lineage with predominantly PBL-derived IgG-VH suggestive of B-cell migration from the CNS to the PBL or seeding from the PBL into the CNS; C suggests B-cell migration from the PBL into the CNS, with traces of the clusters remaining in the PBL and with extensive intrathecal B-cell SHM; D suggests ongoing B-cell exchange across the BBB, or affinity maturation occurring in both compartments in parallel. H-CDR1, heavy-chain complementarity-determining region 1. Reprinted with permission from Hauser (2015), Fig. 7. Copyright 2015, SAGE Publications.

that of others studying CSF (Owens et al., 2007) and brain tissue (Owens et al., 1998) clearly show that the activated B-cell clones in the CNS of MS patients display a bias in terms of increased usage of members of the IgG VH4 family. These data raise the possibility that even more-selective therapies based on targeting restricted populations of B-cells defined by their surface Ab receptors could be effective.

### B-Cells and Progressive MS

As discussed earlier, the anti-CD20 therapies eliminate mostly circulating B-cells, leaving B-cells

in secondary lymphoid organs and other sites partially unaffected. This feature could account for their favorable safety profile; however, at least in theory, it could also pose a challenge to effectively treating progressive MS (Hauser et al., 2013). If established B-cell nests residing in lymphoid follicle-like structures in the meninges are drivers of a chronic neurodegenerative process that ultimately results in progressive MS (Magliozzi et al., 2007), then anti-CD20 therapy would likely fail to deplete B-cells from these sites. This resistance of B-cells in protective niches could explain the relatively meager

response of PPMS (Hawker et al., 2009; Montalban et al., 2017) and the observation that RMS can evolve to secondary progressive MS despite ongoing RTX treatment. It is also possible that long-lived, CD20-negative plasma cells and their Ab products play some role in progressive MS. OCBs can persist in the CSF even after chronic treatment with RTX, indicating that aberrant humoral immune responses have not been eliminated from the CNS. Eliminating these CNS-restricted humoral immune responses might require the development of MAbs that disrupt protective niches (Radford et al., 2013), penetrate the BBB more effectively, and/or directly lyse Ig-secreting plasma cells. Another area of promise is to develop small molecules that inhibit critical B-cell signaling pathways (Puri et al., 2013; Byrd et al., 2014; Furman et al., 2014).

## Conclusions

Looking back to that distant seminar room in Boston, it would have been impossible to imagine that almost 40 years later, B-cells would rest, arguably, at the epicenter of MS immunology. The B-cell saga in MS has provided a cornucopia of surprises, thrilling insights, several disappointments, numerous unsolved conundrums, and a few generic lessons. Foremost among the latter is the importance of road-testing ideas developed in the laboratory in real-life clinical situations and vice versa. Finally, the long process from conception to an initial clinical suggestion of efficacy, to completing the definitive clinical trials, amply demonstrates the bumpy and uncertain road that accompanies forays between academia and industry. This bidirectional process must be made more efficient if we are to effectively translate new discoveries into treatments and cures for our patients.

## Acknowledgments

I thank the Multiple Sclerosis International Federation and the European Committee for Treatment and Research in Multiple Sclerosis (ECTRIMS) and Andrew Barnecut, who provided invaluable editorial assistance with preparation of the manuscript. This work was supported by funding from the National Institutes of Health (Grants R01 NS049477 and 1U19A1067152) and the National Multiple Sclerosis Society (Grant RG 2899-D11). This chapter was excerpted and modified from a previously published article: Hauser SL (2015) The Charcot Lecture | beating MS: a story of B cells, with twists and turns. *Mult Scler* 21:8–21. Copyright 2015, SAGE Publications.

## References

- Appel SH, Bornstein MB (1964) The application of tissue culture to the study of experimental allergic encephalomyelitis. II. Serum factors responsible for demyelination. *J Exp Med* 119:303–312.
- Bankoti J, Apeltsin L, Hauser SL, Allen S, Albertolle ME, Witkowska HE, von Büdingen HC (2014) In multiple sclerosis, oligoclonal bands connect to peripheral B-cell responses. *Ann Neurol* 75:266–276.
- Baranzini SE, Mudge J, van Velkinburgh JC, Khankhanian P, Khrebtukova I, Miller NA, Zhang L, Farmer AD, Bell CJ, Kim RW, May GD, Woodward JE, Caillier SJ, McElroy JP, Gomez R, Pando MJ, Clendenen LE, Ganusova EE, Schilkey FD, Ramaraj T, et al. (2010) Genome, epigenome and RNA sequences of monozygotic twins discordant for multiple sclerosis. *Nature* 464:1351–1356.
- Bar-Or A, Fawaz L, Fan B, Darlington PJ, Rieger A, Ghorayeb C, Calabresi PA, Waubant E, Hauser SL, Zhang J, Smith CH (2010) Abnormal B-cell cytokine responses a trigger of T-cell-mediated disease in MS? *Ann Neurol* 67:452–461.
- Byrd JC, Brown JR, O'Brien S, Barrientos JC, Kay NE, Reddy NM, Coutre S, Tam CS, Mulligan SP, Jaeger U, Devereux S, Barr PM, Furman RR, Kipps TJ, Cymbalista F, Pocock C, Thornton P, Caligaris-Cappio F, Robak T, Delgado J, et al. (2014) Ibrutinib versus ofatumumab in previously treated chronic lymphoid leukemia. *N Engl J Med* 371:213–223.
- Cross AH, Stark JL, Lauber J, Ramsbottom MJ, Lyons JA (2006) Rituximab reduces B cells and T cells in cerebrospinal fluid of multiple sclerosis patients. *J Neuroimmunol* 180:63–70.
- Duddy M, Niino M, Adatia F, Hebert S, Freedman M, Atkins H, Kim HJ, Bar-Or A (2007) Distinct effector cytokine profiles of memory and naive human B cell subsets and implication in multiple sclerosis. *J Immunol* 178:6092–6099.
- Farh KK, Marson A, Zhu J, Kleinewietfeld M, Housley WJ, Beik S, Shores N, Whitton H, Ryan RJ, Shishkin AA, Hatan M, Carrasco-Alfonso MJ, Mayer D, Luckey CJ, Patsopoulos NA, De Jager PL, Kuchroo VK, Epstein CB, Daly MJ, Hafler DA, et al. (2015) Genetic and epigenetic fine mapping of causal autoimmune disease variants. *Nature* 518:337–343.

- Fillatreau S, Sweenie CH, McGeachy MJ, Gray D, Anderton SM (2002) B cells regulate autoimmunity by provision of IL-10. *Nat Immunol* 3:944–950.
- Furman RR, Sharman JP, Coutre SE, Cheson BD, Pagel JM, Hillmen P, Barrientos JC, Zelenetz AD, Kipps TJ, Flinn I, Ghia P, Eradat H, Ervin T, Lamanna N, Coiffier B, Pettitt AR, Ma S, Stilgenbauer S, Cramer P, Aiello M, et al. (2014) Idelalisib and rituximab in relapsed chronic lymphocytic leukemia. *N Engl J Med* 370:997–1007.
- Genain CP, Hauser SL (1996) Allergic encephalomyelitis in common marmosets: pathogenesis of a multiple sclerosis–like lesion. *Methods* 10:420–434.
- Genain CP, Hauser SL (1997) Creation of a model for multiple sclerosis in *Callithrix jacchus* marmosets. *J Mol Med (Berl)* 75:187–197.
- Genain CP, Nguyen MH, Letvin NL, Pearl R, Davis RL, Adelman M, Lees MB, Lington C, Hauser SL (1995) Antibody facilitation of multiple sclerosis–like lesions in a nonhuman primate. *J Clin Invest* 96:2966–2974.
- Genain CP, Abel K, Belmar N, Villinger F, Rosenberg DP, Lington C, Raine CS, Hauser SL (1996) Late complications of immune deviation therapy in a nonhuman primate. *Science* 274:2054–2057.
- Genain CP, Cannella B, Hauser SL, Raine CS (1999) Identification of autoantibodies associated with myelin damage in multiple sclerosis. *Nat Med* 5:170–175.
- Glanville J, Kuo TC, von Büdingen HC, Guey L, Berka J, Sundar PD, Huerta G, Mehta GR, Oksenberg JR, Hauser SL, Cox DR, Rajpal A, Pons J (2011) Naive antibody gene-segment frequencies are heritable and unaltered by chronic lymphocyte ablation. *Proc Natl Acad Sci USA* 108:20066–20071.
- Hauser SL (2015) The Charcot Lecture | beating MS: a story of B cells, with twists and turns. *Mult Scler* 21:8–21.
- Hauser SL, Fosburg M, Kevy S, Weiner HL (1982) Plasmapheresis, lymphocytapheresis, and immunosuppressive drug therapy in multiple sclerosis. *Prog Clin Biol Res* 106:239–254.
- Hauser SL, Dawson DM, Leirich JR, Beal MF, Kevy SV, Pröpper RD, Mills JA, Weiner HL (1983) Intensive immunosuppression in progressive multiple sclerosis. A randomized, three-arm study of high-dose intravenous cyclophosphamide, plasma exchange, and ACTH. *N Engl J Med* 308:173–180.
- Hauser SL, Waubant E, Arnold DL, Vollmer T, Antel J, Fox RJ, Bar-Or A, Panzara M, Sarkar N, Agarwal S, Langer-Gould A, Smith CH; HERMES Trial Group (2008) B-cell depletion with rituximab in relapsing–remitting multiple sclerosis. *N Engl J Med* 358:676–688.
- Hauser SL, Chan JR, Oksenberg JR (2013) Multiple sclerosis: Prospects and promise. *Ann Neurol* 74:317–327.
- Hauser SL, Bar-Or A, Comi G, Giovannoni G, Hartung HP, Hemmer B, Lublin F, Montalban X, Rammohan KW, Selmaj K, Traboulsee A, Wolinsky JS, Arnold DL, Klingelschmitt G, Masterman D, Fontoura P, Belachew S, Chin P, Mairon N, Garren H, et al. (2017) Ocrelizumab versus interferon beta-1a in relapsing multiple sclerosis. *N Engl J Med* 376:221–234.
- Hawker K, O'Connor P, Freedman MS, Calabresi PA, Antel J, Simon J, Hauser S, Waubant E, Vollmer T, Panitch H, Zhang J, Chin P, Smith CH; OLYMPUS Trial Group (2009) Rituximab in patients with primary progressive multiple sclerosis: results of a randomized double-blind placebo-controlled multicenter trial. *Ann Neurol* 66:460–471.
- International Multiple Sclerosis Genetics Consortium (IMSGC), Beecham AH, Patsopoulos NA, Xifara DK, Davis MF, Kempainen A, Cotsapas C, Shah TS, Spencer C, Booth D, Goris A, Oturai A, Saarela J, Fontaine B, Hemmer B, Martin C, Zipp F, D'Alfonso S, Martinelli-Boneschi F, Taylor B, et al. (2013) Analysis of immune-related loci identifies 48 new susceptibility variants for multiple sclerosis. *Nat Genet* 45:1353–1360.
- Kappos L, Li D, Calabresi PA, O'Connor P, Bar-Or A, Barkhof F, Yin M, Leppert D, Glanzman R, Tinbergen J, Hauser SL (2011) Ocrelizumab in relapsing–remitting multiple sclerosis: a phase 2, randomised, placebo-controlled, multicentre trial. *Lancet* 378:1779–1787.
- Kappos L, Hartung HP, Freedman MS, Boyko A, Radü EW, Mikol DD, Lamarine M, Hyvert Y, Freudensprung U, Plitz T, van Beek J; ATAMS Study Group (2014) Atacicept in multiple sclerosis (ATAMS): a randomised, placebo-controlled, double-blind, phase 2 trial. *Lancet Neurol* 13:353–363.
- Khosroshahi A, Bloch DB, Deshpande V, Stone JH (2010) Rituximab therapy leads to rapid decline of serum IgG4 levels and prompt clinical improvement in IgG4-related systemic disease. *Arthritis Rheum* 62:1755–1762.

- Kinnunen T, Chamberlain N, Morbach H, Cantaert T, Lynch M, Preston-Hurlburt P, Herold KC, Hafler DA, O'Connor KC, Meffre E (2013) Specific peripheral B cell tolerance defects in patients with multiple sclerosis. *J Clin Invest* 123:2737–2741.
- Linnington C, Berger T, Perry L, Weerth S, Hinze-Selch D, Zhang Y, Lu HC, Lassmann H, Wekerle H (1993) T cells specific for the myelin oligodendrocyte glycoprotein mediate an unusual autoimmune inflammatory response in the central nervous system. *Eur J Immunol* 23:1364–1372.
- Lorentzen JC, Issazadeh S, Storch M, Mustafa MI, Lassmann H, Linnington C, Klareskog L, Olsson T (1995) Protracted, relapsing and demyelinating experimental autoimmune encephalomyelitis in DA rats immunized with syngeneic spinal cord and incomplete Freund's adjuvant. *J Neuroimmunol* 63:193–205.
- Lyons JA, San M, Happ MP, Cross AH (1999) B cells are critical to induction of experimental allergic encephalomyelitis by protein but not by a short encephalitogenic peptide. *Eur J Immunol* 29:3432–3439.
- Magliozzi R, Howell O, Vora A, Serafini B, Nicholas R, Puopolo M, Reynolds R, Aloisi F (2007) Meningeal B-cell follicles in secondary progressive multiple sclerosis associate with early onset of disease and severe cortical pathology. *Brain* 130:1089–1104.
- Massacesi L, Genain CP, Lee-Parritz D, Letvin NL, Canfield D, Hauser SL (1995) Active and passively induced experimental autoimmune encephalomyelitis in common marmosets: a new model for multiple sclerosis. *Ann Neurol* 37:519–530.
- Mattson DH, Roos RP, Arnason BG. (1980) Isoelectric focusing of IgG eluted from multiple sclerosis and subacute sclerosing panencephalitis brains. *Nature* 287:335–337.
- Molnarfi N, Schulze-Topphoff U, Weber MS, Patarroyo JC, Prod'homme T, Varrin-Doyer M, Shetty A, Linnington C, Slavin AJ, Hidalgo J, Jenne DE, Wekerle H, Sobel RA, Bernard CC, Shlomchik MJ, Zamvil SS (2013) MHC class II-dependent B cell APC function is required for induction of CNS autoimmunity independent of myelin-specific antibodies. *J Exp Med* 210:2921–2937.
- Monson NL, Cravens PD, Frohman EM, Hawker K, Racke MK (2005) Effect of rituximab on the peripheral blood and cerebrospinal fluid B cells in patients with primary progressive multiple sclerosis. *Arch Neurol* 62:258–264.
- Montalban X, Hauser SL, Kappos L, Arnold DL, Bar-Or A, Comi G, de Seze J, Giovannoni G, Hartung HP, Hemmer B, Lublin F, Rammohan KW, Selmaj K, Traboulsee A, Sauter A, Masterman D, Fontoura P, Belachew S, Garren H, Mairon N, et al. (2017) Ocrelizumab versus placebo in primary progressive multiple sclerosis. *N Engl J Med* 376:209–220.
- Obermeier B, Mentele R, Malotka J, Kellermann J, Kämpfel T, Wekerle H, Lottspeich F, Hohlfeld R, Dornmair K (2008) Matching of oligoclonal immunoglobulin transcriptomes and proteomes of cerebrospinal fluid in multiple sclerosis. *Nat Med* 14:688–693.
- Owens GP, Kraus H, Burgoon MP, Smith-Jensen T, Devlin ME, Gilden DH (1998) Restricted use of VH4 germline segments in an acute multiple sclerosis brain. *Ann Neurol* 43:236–243.
- Owens GP, Wings KM, Ritchie AM, Edwards S, Burgoon MP, Lehnhoff L, Nielsen K, Corboy J, Gilden DH, Bennett JL (2007) VH4 gene segments dominate the intrathecal humoral immune response in multiple sclerosis. *J Immunol* 179:6343–6351.
- Palanichamy A, Apeltsin L, Kuo TC, Sirota M, Wang S, Pitts SJ, Sundar PD, Telman D, Zhao LZ, Derstine M, Abounasr A, Hauser SL, von Büdingen HC (2014a) Immunoglobulin class-switched B cells form an active immune axis between CNS and periphery in multiple sclerosis. *Sci Transl Med* 6:248ra106.
- Palanichamy A, Jahn S, Nickles D, Derstine M, Abounasr A, Hauser SL, Baranzini SE, Leppert D, von Büdingen HC (2014b) Rituximab efficiently depletes increased CD20-expressing T cells in multiple sclerosis patients. *J Immunol* 193:580–586.
- Piccio L, Naismith RT, Trinkaus K, Klein RS, Parks BJ, Lyons JA, Cross AH (2010) Changes in B- and T-lymphocyte and chemokine levels with rituximab treatment in multiple sclerosis. *Arch Neurol* 67:707–714.
- Prineas JW, Connell F (1978) The fine structure of chronically active multiple sclerosis plaques. *Neurology* 28(9 Pt 2):68–75.
- Puri KD, Di Paolo JA, Gold MR (2013) B-cell receptor signaling inhibitors for treatment of autoimmune inflammatory diseases and B-cell malignancies. *Int Rev Immunol* 32:397–427.

- Radford J, Davies A, Cartron G, Morschhauser F, Salles G, Marcus R, Wenger M, Lei G, Wassner-Fritsch E, Vitolo U (2013) Obinutuzumab (GA101) plus CHOP or FC in relapsed/refractory follicular lymphoma: results of the GAUDI study (BO21000). *Blood* 122:1137–1143.
- Raine CS, Cannella B, Hauser SL, Genain CP (1999) Demyelination in primate autoimmune encephalomyelitis and acute multiple sclerosis lesions: a case for antigen-specific antibody mediation. *Ann Neurol* 46:144–160.
- Rigby W, Tony HP, Oelke K, Combe B, Laster A, von Muhlen CA, Fischeleva E, Martin C, Travers H, Dummer W (2012) Safety and efficacy of ocrelizumab in patients with rheumatoid arthritis and an inadequate response to methotrexate: results of a forty-eight-week randomized, double-blind, placebo-controlled, parallel-group phase III trial. *Arthritis Rheum* 64:350–359.
- Rubbert-Roth A, Tak PP, Zerbini C, Tremblay JL, Carreño L, Armstrong G, Collinson N, Shaw TM; MIRROR Trial Investigators (2010) Efficacy and safety of various repeat treatment dosing regimens of rituximab in patients with active rheumatoid arthritis: results of a phase III randomized study (MIRROR). *Rheumatology (Oxford)* 49:1683–1693.
- Silverman GJ, Boyle DL (2008) Understanding the mechanistic basis in rheumatoid arthritis for clinical response to anti-CD20 therapy: the B-cell roadblock hypothesis. *Immunol Rev* 223:175–185.
- Stern JN, Yaari G, Vander Heiden JA, Church G, Donahue WF, Hintzen RQ, Huttner AJ, Laman JD, Nagra RM, Nylander A, Pitt D, Ramanan S, Siddiqui BA, Vigneault F, Kleinstein SH, Hafler DA, O'Connor KC (2014) B cells populating the multiple sclerosis brain mature in the draining cervical lymph nodes. *Sci Transl Med* 6:248ra107.
- Vallerskog T, Gunnarsson I, Widhe M, Risselada A, Klareskog L, van Vollenhoven R, Malmström V, Trollmo C (2007) Treatment with rituximab affects both the cellular and the humoral arm of the immune system in patients with SLE. *Clin Immunol* 122:62–74.
- von Büdingen HC, Bar-Or A, Zamvil SS (2011) B cells in multiple sclerosis: connecting the dots. *Curr Opin Immunol* 23:713–720.
- von Büdingen HC, Kuo TC, Sirota M, van Belle CJ, Apeltsin L, Glanville J, Cree BA, Gourraud PA, Schwartzburg A, Huerta G, Telman D, Sundar PD, Casey T, Cox DR, Hauser SL (2012) B cell exchange across the blood-brain barrier in multiple sclerosis. *J Clin Invest* 122:4533–4543.
- Weber MS, Prod'homme T, Patarroyo JC, Molnarfi N, Karnezis T, Lehmann-Horn K, Danilenko DM, Eastham-Anderson J, Slavin AJ, Linington C, Bernard CC, Martin F, Zamvil SS (2010) B-cell activation influences T-cell polarization and outcome of anti-CD20 B-cell depletion in central nervous system autoimmunity. *Ann Neurol* 68:369–383.

# Purification and Culture Methods for Astrocytes

Shane Liddelow, PhD

---

Department of Neurobiology  
Stanford University School of Medicine  
Stanford, California

## Introduction

Inflammatory responses are a major part of all CNS insults, including acute trauma, infection, and chronic neurodegenerative disease (Sofroniew, 2015). In trauma and infection, the principle culprits in initiating and propagating this inflammatory response are circulating bone-marrow-derived leukocytes. In chronic neurodegenerative disease, the concept of neuroinflammation has evolved and implies an inflammatory process thought to originate primarily from CNS cell types. Chief among these CNS glial cells are microglia, the resident myeloid cells of the brain. It is also becoming apparent, however, that this response involves astrocytes. Microglia and astrocytes have both pro-inflammatory and anti-inflammatory functions, depending on the mode of injury (Zamanian et al., 2012; Anderson et al., 2016; Crotti and Ransohoff, 2016; Liddelow et al., 2017). Acute trauma, chronic infection, and other diseases of the CNS trigger a coordinated multicellular inflammatory response that involves glia as well as neurons and other nonneuronal CNS cells.

As techniques for astrocyte purification and visualization have improved, recent advances have shown that astrocytes are able to respond to a vast array of CNS insults. Such insults include, but are not limited to, traumatic brain injury, spinal cord injury, stroke, brain tumor, inflammation, and a wide range of neurodegenerative diseases (for references, see Sofroniew, 2015; Liddelow and Barres, 2017). These injuries coincide with robust activation of astrocytes as well as microglia and other peripheral immune cells, and therefore it has been difficult to discern the relative importance and function of individual cell-type responses. We now know that the astrocyte response machinery includes phagocytosis of synapses, changes in the secretion of neurotrophins, clearance of debris and dead cells, repair of the blood–brain barrier (BBB), and formation of a scar to enclose the necrotic lesion of such injuries or infection. These effects benefit the CNS, but as we will discuss, mounting evidence points to negative outcomes of reactive astrocyte responses as well.

The large number of cell types involved in inflammatory responses in CNS injury and disease, as well as the complex cell–cell interactions among these and other neural cell types, has hampered mechanistic understanding of glial reactivity. The main focus of recent work has been to address the lack of appropriate models for studying the mechanisms of glial dysfunction. How heterogeneous is the glial response to injury and disease, and how is this heterogeneity induced? Are reactive glia helpful

or harmful and, if so, how are their effects mediated? Advances in these areas have implications for the development of new therapies for CNS injury and disease.

This chapter will run through the most commonly employed methods to purify and culture astrocytes *in vitro*. The main goal is to begin comparing the new suites of cell purification and culturing methods that have been developed and to highlight key areas in which they could be improved in the future.

## Purification and Cell Culture Methods to Study Astrocyte Function

Cell purification provides a powerful method that enables the study of the intrinsic properties of a cell type in isolation, as well as enabling the investigation of interactions between different cell types. Despite their abundance in the CNS, the study of astrocytes has been hindered by the lack of appropriate methods for their purification and culture. This section briefly reviews the main methods for astrocyte purification. It should be noted that this list is not exhaustive, and there are many alterations to each of these methods. What should be considered at all times is which method is going to most appropriately enable you to distinguish the astrocyte function under investigation. Equally important is whether the model you choose is an appropriate proxy for this function, as observed in astrocytes *in vivo*—either in rodents or, more specifically, in humans. A brief overview of each method, including pros and cons, is provided in Figure 1.

### The McCarthy and de Vellis astrocyte model

The MD-astrocyte model, so named for its authors Ken McCarthy and Jean De Vellis (1980), was the first *in vitro* system to allow for the widespread study of isolated astrocytes. These MD astrocytes have been extremely powerful and useful but have several shortcomings. First, purification takes several weeks and lends itself to considerable contamination of other CNS cell types, including microglia and progenitor cells. Second, these cultures are maintained in serum-containing media, and owing to the presence of the BBB, serum components are usually excluded from the CNS (except in instances of trauma or vascular distress following stroke). Serum exposure appears to alter astrocyte transcriptomes and morphology in various ways, leading to fewer processes and larger hypertrophied cell bodies akin to reactive astrocytes or fibroblasts *in vivo* (Foo et al., 2011). Although MD cells are largely used as the

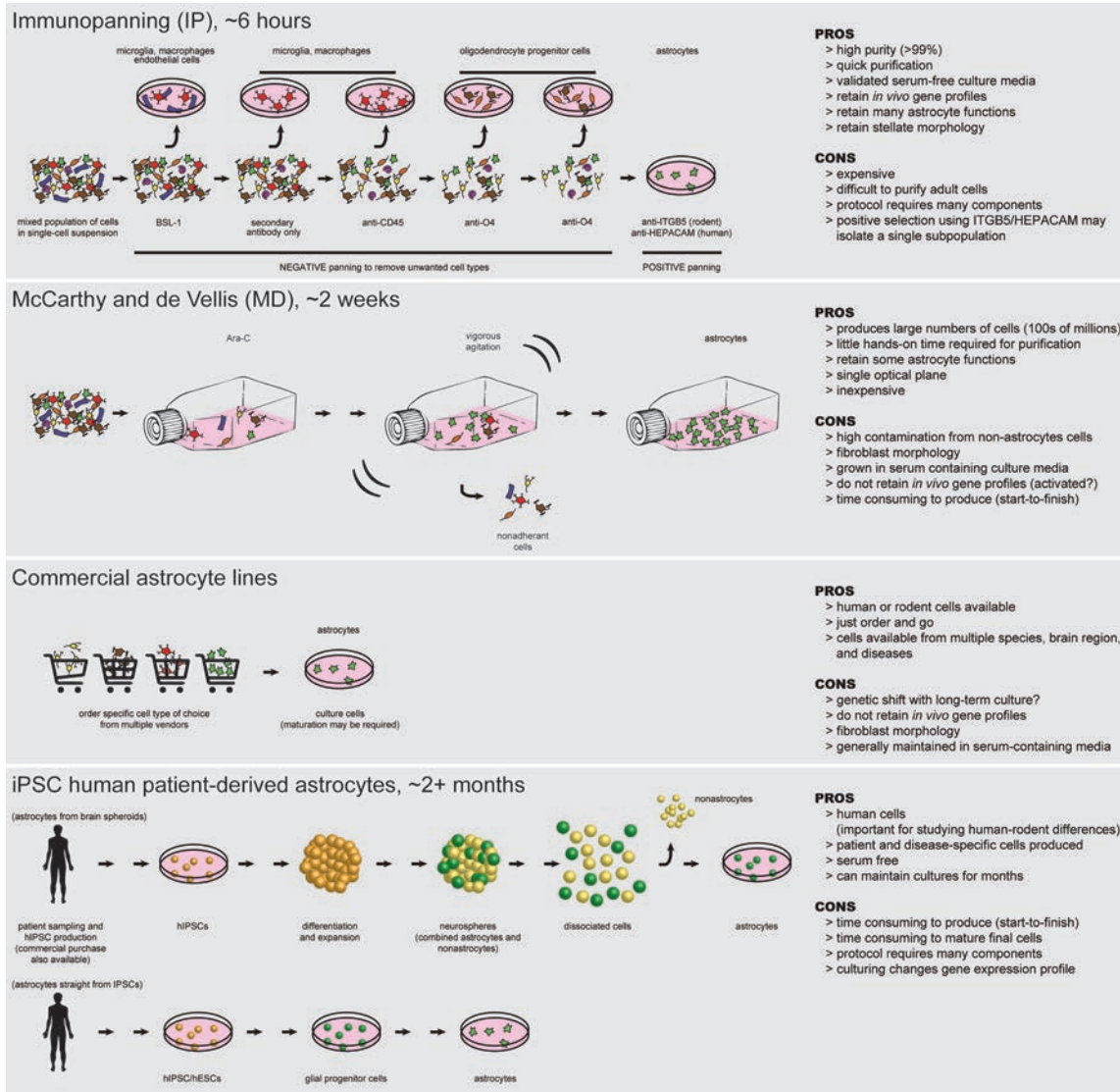


**Figure 1.** Methods for purifying and culturing postnatal astrocytes. Top row, IP reliably provides high-yield, high-viability cells in three steps: (1) enzymatic preparation of a cell suspension, (2) passing this suspension over a series of antibody-coated panning (Petri) dishes, and (3) removing the purified cells from the final dish. Second row, the MD-astrocyte model (McCarthy and De Vellis, 1980) comprises mainly (1) the death of neurons in cultures prepared from postnatal rat cerebra; (2) the rapid proliferation of astrocytes and oligodendrocytes in culture; and (3) the selective detachment of the overlying oligodendrocytes when exposed to sheer forces generated by shaking the cultures. Third row, commercially available cell lines grown in serum-containing media, from patients with verified disease states. Bottom, human patient-derived embryonic stem cells or adult fibroblasts are retro-engineered to iPSC states that can then be enticed to differentiate into astrocytes. BSL-1, Griffonia (Bandeiraea) Simplicifolia Lectin 1; hESC, human embryonic stem cell; hiPSC, human induced pluripotent stem cell.

premiere astrocyte purification and culture system of choice, it is becoming more apparent that these cells do not adequately model many aspects of *in vivo* astrocytes. Additionally, because these MD astrocytes can be isolated only from neonatal brain, they are highly mitotic, unlike mature astrocytes *in vivo*. Hence, it is speculated that these cells may be more akin to radial glia or astrocyte progenitor cells. Recent transcriptome databases of astrocytes purified by fluorescence-activated cell sorting (FACS) show

that MD astrocytes highly express hundreds of genes that are not normally expressed *in vivo* (Cahoy et al., 2008). In addition, their profiles indicate that they may consist of a combination of reactive and developing astrocytes (Zamanian et al., 2012; Zhang et al., 2016) as opposed to resting, mature astrocytes.

This original method of purifying “astrocytes” is based on three main steps: (1) the death of neurons in cultures prepared from postnatal rat cerebra; (2) the

rapid proliferation of astrocytes and oligodendrocytes in culture; and (3) the selective detachment of the overlying oligodendrocytes when exposed to shear forces generated by shaking the cultures (Fig. 1). These three steps leave a highly proliferative, dense monolayer of astrocyte-like cells that can be replated and passaged to provide an enormous number of additional cells.

Several alterations to the original MD protocol go some way to improving the method. Each amendment has been produced to improve a specific readout of astrocyte function. Several three-dimensional matrices of MD astrocytes using high concentrations of HB-EGF (heparin-binding epidermal growth factor, an astrocyte trophic support molecule) (Foo et al., 2011) have yielded cultures with far more processes-bearing morphologies (Puschmann et al., 2013; Placone et al., 2015). Follow-up studies, however, showed that such high concentrations of HB-EGF can cause these astrocytes to de-differentiate (Puschmann et al., 2014). Alternative approaches that use the original MD purification steps but then grow the acquired cells in serum-free media have also been used. Morita and colleagues (2003) first used serum-free media for growing astrocytes. These produced thin processes and glutamate-inducible, but not spontaneous,  $\text{Ca}^{2+}$  fluctuations (spontaneous astrocyte  $\text{Ca}^{2+}$  fluctuations occur in brain slices) (Nett et al., 2002; Foo et al., 2011). Further additions to the serum-free approach included other growth factors (e.g., EGF and TGF- $\alpha$ ); however, these largely produced “reactive” astrocytes with increased GFAP immunoreactivity (Tsugane et al., 2007). The latest alteration to the MD protocol, so-called AWESAM (a low-cost easy stellate astrocyte method), has proven better for measuring  $\text{Ca}^{2+}$  dynamics (Wolfes et al., 2016). Unfortunately, the authors did not present a transcriptome analysis of their astrocyte cultures, so it is unknown whether these are representative of more “normal” astrocyte functions.

What is unknown is whether the MD method produces astrocytes that are irreversibly changed from their *in vivo* counterparts—and whether they can perhaps be enticed to change back into a nonreactive, process-bearing form.

### Immunopanning astrocytes

The use of immunopanning (IP) to purify CNS cells was developed by Ben Barres in the 1980s (Barres et al., 1988) and has been modified continuously for multiple CNS cell types in the decades since. Once proficiency is achieved, IP reliably provides high-yield, high-viability cells. Panning is, at its

heart, rather trivial and involves only three steps: (1) enzymatic preparation of a cell suspension, (2) passing this suspension over a series of antibody-coated panning (Petri) dishes, and (3) removing the purified cells from the final dish. Having said this, although purification of cells by panning is simple, it does take practice, as every step needs to be done correctly to achieve high viability by the end of the procedure. A detailed outline of the major pitfalls of IP, key tips for producing personalized panning protocols, and references to IP protocols for multiple CNS cell types are provided elsewhere (Barres, 2014).

In a typical IP purification, cell-type-specific antibodies are adsorbed to the surface of a Petri dish, and a cell suspension from the tissue sample of interest is then consecutively passed over several of these coated IP dishes (Fig. 1). The first “negative panning” dishes deplete unwanted cell types, such as microglia, and the final “positive” dish selects for the cell type of interest (e.g., astrocytes). Because the protocol is based on prospectively catching your cell of interest, there is a requirement for a cell-type-specific cell-surface antigen to which an appropriate antibody has been raised. There are many searchable cell-type-specific transcriptome databases; for example, mouse and human CNS glia datasets are freely accessible and downloadable at <http://www.brainseq.org> (Cahoy et al., 2008; Zhang et al., 2016). More brain-region-specific astrocyte transcriptome databases can be accessed at <http://astrocytarnaseq.org> (Chai et al., 2017).

Unlike the weeks-long MD purification methods, IP rapidly purifies astrocytes from postnatal rodent brain in  $< 1$  d (Foo et al., 2011). Panning for astrocytes is possible in the rodent using antibodies to the cell-surface antigen ITGB5 (Foo et al., 2011, 2013) and in the human using HEPACAM (Zhang et al., 2016). Rodent cells can also be grown in serum-free conditions (a minimal base media with the addition of the astrocyte trophic factor HBEGF), which enables them to retain their *in vivo* gene profiles for extended periods. In addition to retaining gene profiles, IP rodent astrocytes maintain their distinct tiling domains in culture, are multiprocess bearing, have polarized aquaporin 4 (AQP4) protein localization, conduct  $\text{Ca}^{2+}$  transients, are connected via gap junctions, and maintain many other normal physiological functions (Foo et al., 2011; Liddel et al., 2017). Although human astrocytes can easily be purified using HEPACAM antibodies (Zhang et al., 2016), maintaining their nonactivated transcriptome profiles remains elusive.

To date, IP astrocytes (and other IP purified cells discussed in Barres, 2014) remain the best way to obtain highly pure populations of cells that can be maintained in a nonactivated state. Although expensive, the data obtained from these culture methods are largely reproducible in *in vivo* models, making the difficulties of setting up cultures and maintaining a serum-free culture system well worth the effort.

Recently, we used base IP methods to develop a new model system that enables pure neuroinflammatory reactive (A1) astrocytes to be studied in a culture dish (Liddel et al., 2017). This was possible thanks to our ability to rapidly purify astrocytes from the uninjured postnatal brain, grow them in serum-free cultures, and finally supplement these cultures with a reactive astrocyte-inducing, microglial-derived cytokine cocktail. Microglial activation (by either acute CNS injury or systemic lipopolysaccharides injection) induces A1 reactive astrocytes both *in vitro* and *in vivo*. We found that microglia induce these A1s by releasing three cytokines: interleukin 1 alpha (IL-1 $\alpha$ ), tumor necrosis factor alpha (TNF- $\alpha$ ), and the complement component subunit 1q (C1q), which together are sufficient *in vitro* to induce A1 reactive astrocytes whose gene profiles closely mirror that of A1 reactive astrocytes *in vivo* (Liddel et al., 2017). The resulting cultures of pure A1 reactive astrocytes provide a powerful tool with which to investigate their functions. Using this model, we found that A1s have a striking loss of most major astrocyte functions: a decreased ability to induce synapse formation and function, diminished ability to phagocytose synapses, and a loss of ability to promote neuronal survival and growth. In an improvement to GFAP staining as a marker for reactivity, single-cell data showed that the complement component C3 was specifically upregulated in A1 reactive astrocytes (and not in resting or ischemic “A2” reactive astrocytes). This marker now provides a way to distinguish among different activation states of reactive astrocytes in both rodent and human tissue. Surprisingly, the A1 reactive astrocytes also exhibited a new function in which they secreted a yet to be identified neurotoxin that induced apoptosis of neurons and oligodendrocytes but no other CNS cell types. Important to note, when validating these findings *in vivo*, we found that A1 reactive astrocytes were rapidly induced after CNS injury and were responsible for the death of axotomized CNS neurons. When A1 formation was prevented genetically or pharmacologically, the death of the axotomized CNS neurons was entirely prevented. Interestingly, on their own, the activated microglia used for inducing A1s were insufficient to induce the death of neurons or oligodendrocytes.

This study highlights the importance of using the correct purification and culture system to model your disease, injury, or dysfunction of interest. If the model you are using does not recapitulate the human disease state of your cell of interest, it is not the best system to answer your question.

### Commercially available cell lines

Using commercially available cells is an easy way to acquire a range of cell types from patients with verified disease states. These cells also provide a quick way for laboratories that are new to cell separation techniques to gain access to cells and start experiments rapidly. Care should be taken, however, as many of these lines either are irreversibly activated, contain many precursor cell types, or are contaminated with other cell types. Additionally, like most cell culture methods, these cells are grown in serum-containing media, which as outlined above, is not a normal contributor to the tightly controlled CNS milieu (serum leakage into the brain is characteristic of ischemic injury).

Another caveat is that cell lines can change over time in culture even without any external contamination from cells or bacteria. As they grow generation after generation, chromosomal duplications and/or rearrangements, mutations, and epigenetic changes can alter their original phenotype. These changes often go undetected because cells from different sources can be morphologically similar. It unfortunately seems inevitable that cell-line alteration will occur (Lorsch et al., 2014), which is ultimately problematic. For these reasons, it is generally better for mechanistic studies of astrocytes to be performed in primary cells or for culture-line purity to be routinely tested.

### Induced pluripotent stem cells: monocultures and brain balls

Most recently, the proliferation of newer methods of producing astrocytes (or astrocyte-like cells) from human patient-derived samples has exploded. Multiple methods are now available that begin with different starting materials, be they embryonic stem cells or adult fibroblasts retro-engineered to induced pluripotent stem cell (iPSC) states that can then be enticed to differentiate into astrocytes (Krencik and Ullian, 2013; Santos et al., 2017). Each of these methods produces equally pure monolayered populations of astrocytes that have highlighted some key differences between rodent and human astrocytes, as well as providing new insights into the genetic differences in astrocytes between healthy and diseased individuals.

An alternative approach is to produce spheroids of either pure neurons or a mixture of glia and neurons (Paşca et al., 2015; Sloan et al., 2017). These systems provide patient-derived human cells with the added benefit of including multiple CNS cell types, being more akin to the *in vivo* setting, and allow for investigations of cell–cell interactions. For example, one can coculture nondiseased neurons with diseased astrocytes (or vice versa) to help ascertain the relative contributions that individual cell types make to disease. Of additional benefit is the fact that at the end of growing such spheres, other purification methods (e.g., IP, FACS) can be used to separate astrocytes for further culturing or sequencing analyses (Paşca et al., 2015; Sloan et al., 2017). Notably, recent advances in cortical neurospheres have shown that astrocytes in these organoids undergo maturation akin to that which occurs during normal human development (Sloan et al., 2017).

Like all methods, however, there are several pitfalls that must be considered (Fig. 1). The availability of originating human samples can be difficult at some institutions, and the length of time required (several months) for producing and maturing such spheroids can be both cost- and time-prohibitive for some researchers. In addition, the long culture times required can lead to increased instances of contamination if sterile culture protocols are not adhered to.

### What about our little friends, the microglia?

Purification and culture systems for microglia have largely lagged behind the successes of astrocyte culture systems. This has been a major impediment to further investigations into how they might interact with astrocytes in both physiological and reactive settings, whether this activation results from infection, disease, or trauma. In addition, the difficulty of producing appropriate transcriptome databases of resident microglia (as distinct from circulating peripheral immune cells) has meant that a “baseline” to aim for in the production of new culture methods has been difficult. Recent advances have shown that TMEM119 (transmembrane protein 119) can be used as an appropriate marker to delineate CNS and peripheral immune cells (Bennett et al., 2016). This baseline microglial transcriptome database has provided key validation of newer methods for studying these cells *in vitro*. It shows that TGF- $\beta$  signaling (Butovsky et al., 2014; Bohlen et al., 2017), in addition to IL-34 (colony-stimulating factor 1) and cholesterol (Bohlen et al., 2017), are required to mitigate the upregulation of

traditional microglial reactivity markers generally seen in previous microglia cultures. What has been surprising in these studies is that, although the reactivity can be minimized in serum-free media, a rapid and sustained downregulation of microglial signature genes still occurs when the cells are placed in culture (Bohlen et al., 2017; Gosselin et al., 2017). This suggests that improvements can be made to ensure that the transcripts that delineate microglia from peripheral immune cells are not lost when removing the cells from the CNS and placing them in culture.

### Things to keep in mind

It has been very difficult to distinguish the contributions of astrocytes from those of other CNS cells. This is particularly difficult with interactions between astrocytes and microglia because they usually become reactive in concert and are both involved in neuroinflammation. These delicate interactions are difficult to study in *in vivo* systems because many of the key proteins and genes are present or expressed by multiple cell types. As a result, it is generally better to use culture systems to complete such mechanistic investigations. But how does one address such questions, given the multitude of methods available to purify and culture these cells? Each method has pros and cons that need to be taken into account when choosing the most appropriate methods for your investigation (Fig. 1).

For instance, there is evidence that growing astrocytes on a three-dimensional polymer matrix might be even more appropriate than methods outlined above. These astrocytes show less upregulation of *Gfap* than cells grown in a two-dimensional monolayer, and their many branching processes make them morphologically complex (Puschmann et al., 2014). However, even these astrocytes are prepared according to the original MD-serum-containing methods of the 1980s, and as such, they are probably transcriptomically different from astrocytes present in the normal healthy CNS. The variety of purification and growth paradigms suggests that perfect culture systems for modeling a “normal” *in vivo* astrocyte are likely to require a combination of features, including specific trophic support, the correct substrate, and possibly other unknown factors.

### Final Remarks

Improved methods for producing highly purified astrocytes and microglia will allow their relative contributions and highly coordinated interactions to be better dissected and understood. In addition, the validation of available animal models of

neurodegenerative disease will be essential. Most of these models were produced to model particular aspects of neuronal dysfunction in disease. If these models are to be used to investigate immune–glial interactions in these diseases, we must ensure that they correctly recapitulate the glial dysfunction seen in human patients.

## Acknowledgement

This chapter is adapted from a previously published article: Liddelow SA, Barres BA (2017) Reactive astrocytes: production, function, and therapeutic potential. *Immunity* 46:957–967. Copyright 2017, Elsevier.

## References

- Anderson MA, Burda JE, Ren Y, Ao Y, O'Shea TM, Kawaguchi R, Coppola G, Khakh BS, Deming TJ, Sofroniew MV (2016) Astrocyte scar formation aids central nervous system axon regeneration. *Nature* 532:195–200.
- Barres BA, Silverstein BE, Corey DP, Chun LL (1988) Immunological, morphological, and electrophysiological variation among retinal ganglion cells purified by panning. *Neuron* 1:791–803.
- Barres BA (2014) Designing and troubleshooting immunopanning protocols for purifying neural cells. *Cold Spring Harb Protoc* 2014:1342–1347.
- Bennett ML, Bennett FC, Liddelow SA, Ajami B, Zamanian JL, Fernhoff NB, Mulinyawe SB, Bohlen CJ, Adil A, Tucker A, Weissman IL, Chang EF, Li G, Grant GA, Hayden Gephart MG, Barres BA (2016) New tools for studying microglia in the mouse and human CNS. *Proc Natl Acad Sci USA* 113:E1738–1746.
- Bohlen CJ, Bennett FC, Tucker AF, Collins HY, Mulinyawe SB, Barres BA (2017) Diverse requirements for microglial survival, specification, and function revealed by defined-medium cultures. *Neuron* 94:759–773.
- Butovsky O, Jedrychowski MP, Moore CS, Cialic R, Lanser AJ, Gabriely G, Koeglsperger T, Dake B, Wu PM, Doykan CE, Fanek Z, Liu L, Chen Z, Rothstein JD, Ransohoff RM, Gygi SP, Antel JP, Weiner HL (2014) Identification of a unique TGF- $\beta$ -dependent molecular and functional signature in microglia. *Nat Neurosci* 17:131–143.
- Cahoy JD, Emery B, Kaushal A, Foo LC, Zamanian JL, Christopherson KS, Xing Y, Lubischer JL, Krieg PA, Krupenko SA, Thompson WJ, Barres BA (2008) A transcriptome database for astrocytes, neurons, and oligodendrocytes: a new resource for understanding brain development and function. *J Neurosci* 28:264–278.
- Chai H, Diaz-Castro B, Shigetomi E, Monte E, Octeau JC, Yu X, Cohn W, Rajendran PS, Vondriska TM, Whitelegge JP, Coppola G, Khakh BS (2017) Neural circuit-specialized astrocytes: genomic, proteomic, morphological, and functional evidence. *Neuron* 95:531–549.
- Crotti A, Ransohoff RM (2016) Microglial physiology and pathophysiology: insights from genome-wide transcriptional profiling. *Immunity* 44:505–515.
- Foo LC, Allen NJ, Bushong EA, Ventura PB, Chung WS, Zhou L, Cahoy JD, Daneman R, Zong H, Ellisman MH, Barres BA (2011) Development of a method for the purification and culture of rodent astrocytes. *Neuron* 71:799–811.
- Foo LC (2013) Purification of rat and mouse astrocytes by immunopanning. *Cold Spring Harb Protoc* 2013:421–432.
- Gosselin D, Skola D, Coufal NG, Holtman IR, Schlachetzki JCM, Sajti E, Jaeger BN, O'Connor C, Fitzpatrick C, Pasillas MP, Pena M, Adair A, Gonda DD, Levy ML, Ransohoff RM, Gage FH, Glass CK (2017) An environmental-dependent transcriptional network specifies human microglia identity. *Science* 356:eaal3222.
- Krencik R, Ullian EM (2013) A cellular star atlas: using astrocytes from human pluripotent stem cells for disease studies. *Front Cell Neurosci* 7:25.
- Liddelow SA, Barres BA (2017) Reactive astrocytes: production, function, and therapeutic potential. *Immunity* 46:957–967.
- Liddelow SA, Guttenplan KA, Clarke LE, Bennett FC, Bohlen CJ, Schirmer L, Bennett ML, Münch AE, Chung WS, Peterson TC, Wilton DK, Frouin A, Napier BA, Panicker N, Kumar M, Buckwalter MS, Rowitch DH, Dawson VL, Dawson TM, Stevens B, et al. (2017) Neurotoxic reactive astrocytes are induced by activated microglia. *Nature* 541:481–487.

- Lorsch JR, Collins FS, Lippincott-Schwartz J (2014) Cell biology. Fixing problems with cell lines. *Science* 346:1452–1453.
- McCarthy KD, de Vellis J (1980) Preparation of separate astroglial and oligodendroglial cell cultures from rat cerebral tissue. *J Cell Biol* 85:890–902.
- Morita M, Higuchi C, Moto T, Kozuka N, Susuki J, Itofusa R, Yamashita J, Kudo Y (2003) Dual regulation of calcium oscillation in astrocytes by growth factors and pro-inflammatory cytokines via the mitogen-activated protein kinase cascade. *J Neurosci* 23:10944–10952.
- Nett WJ, Oloff SH, McCarthy KD (2002) Hippocampal astrocytes *in situ* exhibit calcium oscillations that occur independent of neuronal activity. *J Neurophysiol* 87(1):528–537.
- Paşca AM, Sloan SA, Clarke LE, Tian Y, Makinson CD, Huber N, Kim CH, Park JY, O'Rourke NA, Nguyen KD, Smith SJ, Huguenard JR, Geschwind DH, Barres BA, Paşca SP (2015) Functional cortical neurons and astrocytes from human pluripotent stem cells in 3D culture. *Nat Methods* 12:671–678.
- Placone AL, McGuiggan PM, Bergles DE, Guerrero-Cazares H, Quiñones-Hinojosa A, Searson PC (2015) Human astrocytes develop physiological morphology and remain quiescent in a novel 3D matrix. *Biomaterials* 42:134–143.
- Puschmann TB, Zandén C, De Pablo Y, Kirchhoff F, Pekna M, Liu J, Pekny M (2013) Bioactive 3D cell culture system minimizes cellular stress and maintains the *in vivo*-like morphological complexity of astroglial cells. *Glia* 61:432–440.
- Puschmann TB, Zandén C, Lebkuechner I, Philippot C, de Pablo Y, Liu J, Pekny M (2014) HB-EGF affects astrocyte morphology, proliferation, differentiation, and the expression of intermediate filament proteins. *J Neurochem* 128:878–889.
- Santos R, Vadodaria KC, Jaeger BN, Mei A, Lefcochilos-Fogelquist S, Mendes APD, Erikson G, Shokhirev M, Randolph-Moore L, Fredlender C, Dave S, Oefner R, Fitzpatrick C, Pena M, Barron JJ, Ku M, Denli AM, Kerman BE, Charnay P, Kelsoe JR, et al. (2017) Differentiation of inflammation-responsive astrocytes from glial progenitors generated from human induced pluripotent stem cells. *Stem Cell Reports* 8:1757–1769.
- Sloan SA, Darmanis S, Huber N, Khan TA, Birey F, Caneda C, Reimer R, Quake SR, Barres BA, Paşca SP (2017) Human astrocyte maturation captured in 3D cerebral spheroids derived from pluripotent stem cells. *Neuron* 95:779–790.
- Sofroniew MV (2015) Astrocyte barriers to neurotoxic inflammation. *Nat Rev Neurosci* 16:249–263.
- Tsugane M, Nagai Y, Kimura Y, Oka J, Kimura H (2007) Differentiated astrocytes acquire sensitivity to hydrogen sulfide that is diminished by the transformation into reactive astrocytes. *Antioxid Redox Signal* 9:257–269.
- Wolfes AC, Ahmed S, Awasthi A, Stahlberg MA, Rajput A, Magruder DS, Bonn S, Dean C (2016) A novel method for culturing stellate astrocytes reveals spatially distinct Ca<sup>2+</sup> signaling and vesicle recycling in astrocytic processes. *J Gen Physiol* 149:149–170.
- Zamanian JL, Xu L, Foo LC, Nouri N, Zhou L, Giffard RG, Barres BA (2012) Genomic analysis of reactive astrogliosis. *J Neurosci* 32:6391–6410.
- Zhang Y, Sloan SA, Clarke LE, Caneda C, Plaza CA, Blumenthal PD, Vogel H, Steinberg GK, Edwards MS, Li G, Duncan JA 3rd, Cheshier SH, Shuer LM, Chang EF, Grant GA, Gephart MG, Barres BA (2016) Purification and characterization of progenitor and mature human astrocytes reveals transcriptional and functional differences with mouse. *Neuron* 89:37–53.

# The Glymphatic System

Nadia Aalling, MSc,<sup>1</sup> Anne Sofie Finmann Munk, BSc,<sup>2</sup>  
Iben Lundgaard, PhD,<sup>3</sup> and Maiken Nedergaard, MD, DMSc<sup>1,3</sup>

---

<sup>1</sup>Center for Basic and Translational Neuroscience  
Faculty of Health and Medical Sciences  
University of Copenhagen  
Copenhagen N, Denmark

<sup>2</sup>Master of Science (MSc) in Human Biology Program  
Faculty of Health and Medical Sciences  
University of Copenhagen  
Copenhagen N, Denmark

<sup>3</sup>Center for Translational Neuromedicine  
University of Rochester Medical Center  
Rochester, New York

## Introduction

The glymphatic system is a recently discovered macroscopic waste clearance network that uses a unique complex of perivascular tunnels, formed by astroglial cells, to promote efficient elimination of soluble proteins and metabolites from the CNS. Besides waste elimination, the glymphatic system may also function to help distribute nonwaste compounds, such as glucose, lipids, amino acids, and neurotransmitters related to volume transmission, in the brain. Intriguingly, the glymphatic system functions mainly during sleep and is largely disengaged during wakefulness. The biological need for sleep across all species may therefore reflect that the brain must enter a state of activity that enables the elimination of potentially neurotoxic waste products, including amyloid-beta ( $A\beta$ ). The concept of the glymphatic system is relatively new, and this syllabus chapter reviews its basic structural elements, organization, regulation, and functions. We will discuss recent studies indicating that glymphatic function is suppressed in various diseases and that failure of glymphatic function, in turn, might contribute to pathology in neurodegenerative disorders, traumatic brain injury, and stroke. This chapter also addresses recent findings and discusses them within the broader context of what is known about immune function and waste elimination from the CNS.

## The Glymphatic Pathway

Clearance of excess fluid and interstitial solutes is critical for tissue homeostasis. In the peripheral tissues, soluble material, proteins, and fluid from the interstitial space are returned to the general circulation by the lymphatic system (Liao and Padera, 2013). The lymphatic network extends throughout all parts of the peripheral tissues, and the density of lymph vessels correlates with the rate of tissue metabolism. Although the brain and spinal cord are characterized by a disproportionally high metabolic rate (Wang et al., 2012), and synaptic transmission is exquisitely sensitive to changes in the environment, the CNS lacks conventional lymphatic vessels. Recently, lymphatic vessels have been identified in the fibrous membranes, meninges, and dura lining the subarachnoid space. These vessels express all the classical lymphatic endothelial cell markers and carry leukocytes, including T-lymphocytes (Aspelund et al., 2015; Louveau et al., 2015). CSF drains into these lymph vessels, which thereby act as a waste clearance path for the glymphatic system.

CSF and interstitial fluid (ISF) continuously interchange. From the subarachnoid space, CSF is driven into the perivascular space (also known as the

Virchow–Robin space) by a combination of arterial pulsatility, respiration, and CSF pressure gradients. Thus, the loose fibrous matrix of the perivascular space can be viewed as a low-resistance highway for CSF influx. In addition to being a pathway for the influx of CSF, the perivascular spaces are important sites for delivering energy substrate and regulating blood flow. In pathological conditions, such as multiple sclerosis and stroke, the innate inflammatory response and edema formation are initiated in the perivascular spaces (Ge et al., 2005; del Zoppo et al., 2016). The transport of CSF into the dense and complex brain parenchyma from the perivascular space occurs in part through aquaporin 4 (AQP4) water channels expressed in a highly polarized manner in astrocytic endfeet that ensheath the brain vasculature (Fig. 1). (Iliff et al., 2012; Iliff and Nedergaard, 2013). CSF interchanges with ISF within the brain parenchyma and facilitates a flow of CSF–ISF fluid, along with metabolites and waste solutes from the brain, to the lymphatic system via CSF drainage sites. These sites include the arachnoid villi, cranial and peripheral nerves, perivascular routes, and the newly discovered meningeal lymphatic vessels (Szentistványi et al., 1984; Johnston et al., 2004; Iliff et al., 2012, 2013b; Louveau et al., 2015; Morris et al., 2016). Whether the exit route from the parenchyma follows along veins (Iliff et al., 2012, 2013b) or along arteries (Morris et al., 2016) is still debated (Bakker et al., 2016).

This highly polarized macroscopic system of convective fluid fluxes with rapid interchange of CSF and ISF was described by Rennels and colleagues more than 30 years ago (Rennels et al., 1985). However, it was entitled the “glymphatic system” only in 2012, when the dynamics of CSF influx and clearance were characterized for the first time *in vivo* using two-photon microscopy in mice (Iliff et al., 2012). The name the “glymphatic system” was based on its similarity to the lymphatic system in the peripheral tissue in function, and on the important role of glial AQP4 channels in convective fluid transport.

## Drivers of Glymphatic Influx and Clearance

Glymphatic transport is driven by multiple mechanisms. Entry of CSF along the perivascular space is an energy-requiring process crucial for facilitating CSF–ISF exchange and clearance function. The initial proposal that arterial pulsation is the driving force of the convective CSF movement through the parenchyma (Iliff et al., 2012) was recently challenged (Jin et al., 2016) and elaborated on. The most recent computational modeling reports suggest that although arterial pulsation cannot generate enough force to

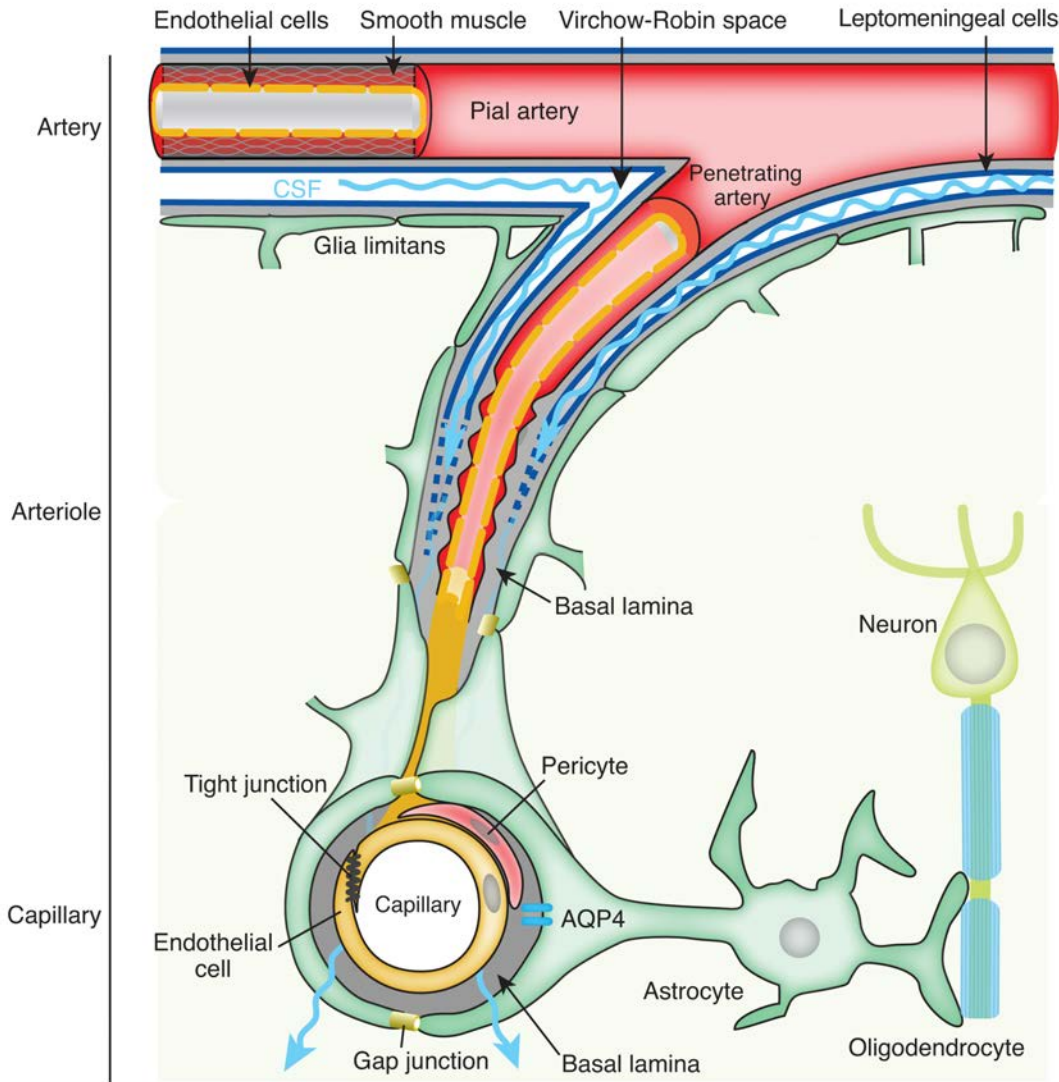


**Figure 1.** The neurovascular unit. The structure and function of the neurovascular unit allow bidirectional communication between the microvasculature and neurons, with astrocytes playing intermediary roles. Pia l arteries in the subarachnoid space bathed in CSF become penetrating arteries upon diving into the brain parenchyma. The perivascular space around penetrating arteries is termed the Virchow–Robin space. As the penetrating arteries branch into arterioles and capillaries, the CSF-containing Virchow–Robin spaces narrow and finally disappear. However, the perivascular space extends to arterioles and capillaries to venules, where it is made up by the basal lamina’s ECM that provides a continuity of the fluid space between arterioles and venules. Astrocytic vascular endfeet expressing *AQP4* surround the entire vasculature and form the boundary of the perivascular spaces. Reprinted with permission from Jessen NA et al. (2015), Fig. 3. Copyright 2015, Springer US.

drive convective bulk flow, it can still propagate fast solute transport in the periarterial space through a combined effect of mixing and diffusion (Asgari et al., 2015, 2016). Thus, arterial pulsation, respiration, and the pressure generated through a constant production of CSF by the choroid plexus all drive glymphatic fluid transport, in combination with intracellular astrocytic water flow through *AQP4* channels and a yet unidentified force. The molecular mechanism of CSF flow across astrocytic endfeet is poorly understood. Insight into the role of the connexins (43 and 30) and

sodium transporters expressed at the endfeet could provide further knowledge of the ionic and molecular basis of solute movement across the endfeet (Simon et al., 2017).

Similar to the glymphatic flow in the brain parenchyma, a glymphatic system of the eye has recently been proposed. CSF surrounds the optic nerve, and studies have reported some level of exchange between the CSF and ISF of the optic nerve in the anterior part (Denniston and Keane, 2015; Wostyn et al., 2016).

Further exploration of this pathway during various physiological and pathological conditions might help us to understand the implications of several ocular diseases, including glaucoma (Wostyn et al., 2017) and papilloedema secondary to raised intracranial pressure (Denniston et al., 2017).

## The Glymphatic System Is Turned On During Sleep and After Exercise

In rodents, glymphatic activity is dramatically enhanced during sleep and suppressed during wakefulness. Using *in vivo* two-photon imaging, it was shown that the CSF influx in mice in the awake state was reduced by 90% compared with sleeping and anesthetized mice (Xie et al., 2013). The sleep–wake difference in glymphatic influx correlated with the volume fraction of interstitial space that was 13–15% in the awake state and expanded to 22–24% in both sleeping and anesthetized mice. Thus, the increase in interstitial space volume in the sleep state reduces tissue resistance to convective flow, permitting CSF–ISF exchange and clearance of metabolites. In contrast, applying norepinephrine significantly suppressed the glymphatic influx and decreased the interstitial volume fraction. This suggests that the burst release of norepinephrine during arousal increases the cellular volume fraction, resulting in a decrease in the interstitial space (O'Donnell et al., 2012). The concerted effect of norepinephrine thus acts via different mechanisms on both fluid availability and convective fluxes to suppress glymphatic function; therefore, norepinephrine can be considered a key regulator of both the switch between the sleep and wakeful state and solute clearance from the brain.

The suppressing effects of wakefulness on glymphatic clearance of metabolites are further enhanced by sleep deprivation (Plog et al., 2015), which correlates with abolishment of AQP4 polarization at the astrocytic endfeet parallel to the vasculature (Liu et al., 2017). AQP4 and its polarization to astrocytic endfeet are important for maintaining fluid and ion homeostasis and crucial to glymphatic influx and clearance in the young mouse brain. The genetic deletion of *Aqp4* was previously shown to impair CSF–ISF exchange by approximately 65% (Iliff et al., 2012), and loss of polarization occurs in parallel with reactive astrogliosis during pathology and aging (Kress et al., 2014; Plog et al., 2015; Gleiser et al., 2016). Interestingly, a recent report showed that aged mice (14–16 months old) that had been running voluntarily for 6 weeks did not have suppressed glymphatic influx or loss of AQP4 polarization as

their age-matched littermates did (He et al., 2017). The molecular mechanisms behind the beneficial effects of exercise on brain cognition are still poorly defined, but this finding reveals a favorable role for exercise in maintaining AQP4 polarization and glymphatic activity during aging.

## Convective CSF Fluxes in Aging and Pathology

### Glymphatic activity decreases sharply during aging

Assessment of glymphatic function in old versus young mice showed a dramatic ~80–90% reduction in aged compared with young mice (Figs. 2A,B) (Kress et al., 2014). The suppression of glymphatic activity included both reduced influx of CSF tracers and reduced clearance of radiolabeled A $\beta$  and inulin. As mentioned above, the decreased glymphatic activity during aging could be attributed to increased reactive gliosis. Gliosis is defined by hypertrophy of GFAP-positive astrocyte processes (Sabbatini et al., 1999), which appears in parallel with loss of AQP4 polarization. Other factors perhaps contributing to the reduction of glymphatic activity due to aging are the declines in CSF production by 66% and CSF pressure by 27% (Chen et al., 2009; Fleischman et al., 2012; Iliff et al., 2013b). Aging is also accompanied by stiffening of the arterial wall, leading to a reduction in arterial pulsatility—one of the drivers of glymphatic influx (Iliff et al., 2013b). The observation of age-related decline in glymphatic activity is important because the greatest risk factor identified for neurodegenerative diseases is aging.

### Glymphatic flow is reduced before A $\beta$ aggregation

The failure of the glymphatic system in aging might thus contribute to the accumulation of misfolded and hyperphosphorylated proteins. In this way, it renders the brain more vulnerable to developing a neurodegenerative pathology or perhaps escalates the progression of cognitive dysfunction. Indeed, all prevalent neurodegenerative diseases are characterized by accumulation of aggregated proteins (Ross and Poirier, 2004). A macroscopic clearance mechanism of brain interstitial solutes may be of particular importance for clearing proteins from the ISF to prevent aggregate formation in neurodegenerative diseases including Alzheimer's disease (AD) (Weller, 1998). Several studies in rodents have reported that A $\beta$  is rapidly cleared from the mouse brain along the glymphatic pathway and that this clearance is enhanced during anesthesia and sleep and suppressed by sleep deprivation (Iliff et al., 2012; Xie et al., 2013; He et al., 2017). Also,

apolipoprotein E is transported via the glymphatic system from the choroid plexus CSF to neurons (Achariyar et al., 2017). Together with the recent finding of a significant reduction in glymphatic transport before deposition of A $\beta$  in the *APP/PS1* mouse model of AD (Peng et al., 2016), this suggests that AD onset might be postponed by early restoration of glymphatic flow.

Reduced glymphatic clearance of A $\beta$  in animal models (Fig. 2C) (Peng et al., 2016) correlates with abnormally enlarged perivascular space volume, which is also observed in the brains of AD patients compared with aged-matched control subjects (Shinkai et al., 1995; Roher et al., 2003). Recent approaches to investigate the perivascular space volume and CSF flow in humans using magnetic resonance imaging

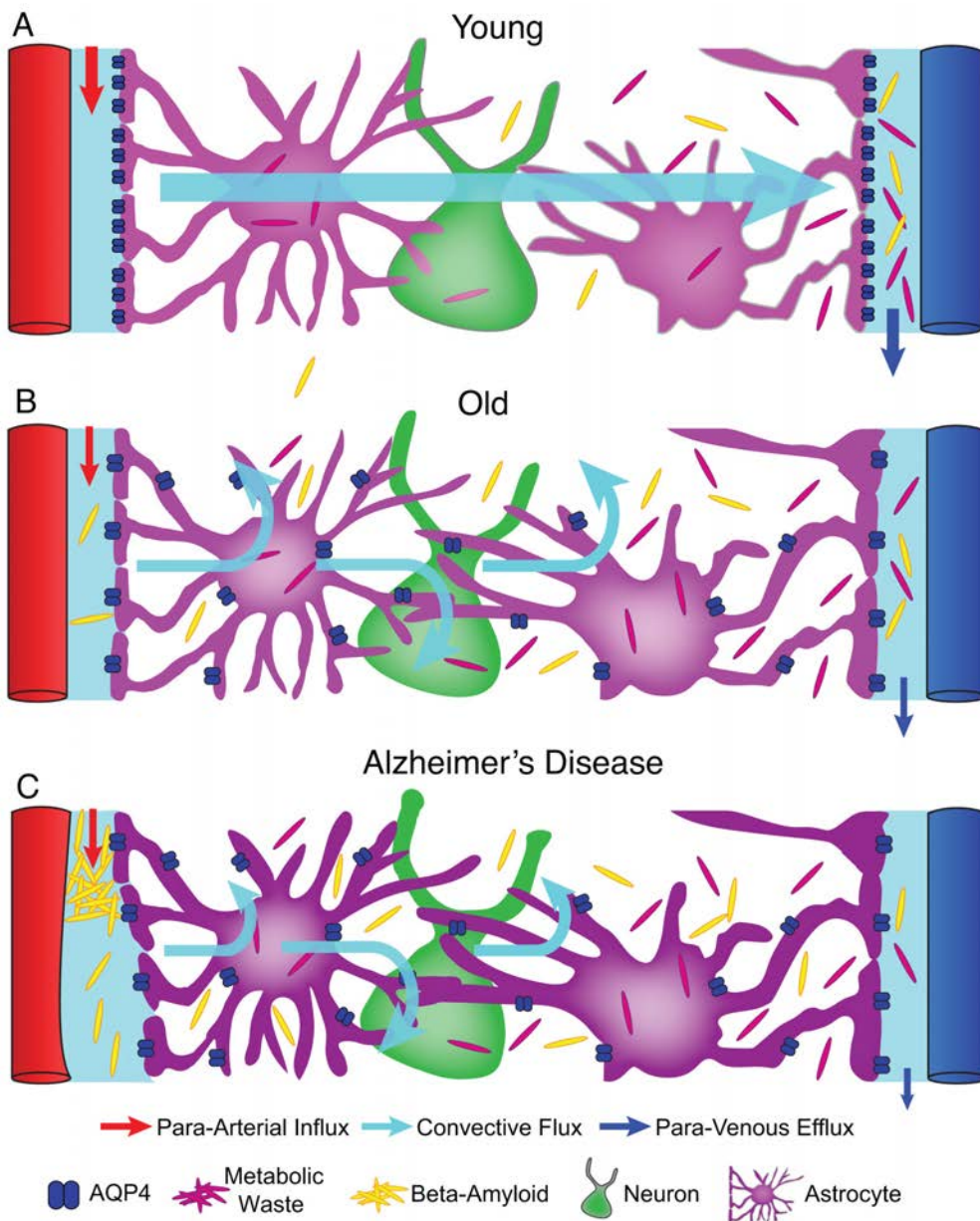


**Figure 2.** Model of glymphatic function in the young, old, and AD brain. **A**, In young and healthy people, CSF enters the brain parenchyma via periarterial pathways, washes out solutes from the interstitial space, and empties along the veins. **B**, With aging, glymphatic function is reduced, possibly owing to astrocytes becoming reactive and *AQP4* depolarized from the vascular endfeet to parenchymal processes. **C**, In AD, the perivascular space of penetrating arteries is subject to accumulation of A $\beta$  peptides. We hypothesize that accumulation of A $\beta$  might be caused by impairment of the glymphatic system and that the perivascular pathways are further blocked by protein aggregates such as A $\beta$ . In this model, the resulting changes in the perivascular environment lead to abnormal enlargement of perivascular space downstream, which further decreases glymphatic clearance. Reprinted with permission from Jessen NA et al. (2015), Fig. 5. Copyright 2015, Springer US.

(MRI) and diffusion tensor image analysis likewise reported dilated Virchow–Robin spaces, especially in the white matter (Chen et al., 2011; Ramirez et al., 2016) and decreased diffusivity along the perivascular space (Taoka et al., 2017) in the brain of human AD patients. Decreased diffusivity likely reflects decreased influx of CSF along the arteries and therefore a decrease in glymphatic flux. In relation to the increased glymphatic activity during sleep, work from Holtzman and colleagues documented that the concentration of A $\beta$  in CSF follows the sleep–wake cycle in healthy human subjects; however, this fluctuation is disrupted in AD families with increased fibrillar A $\beta$  deposits caused by autosomal dominant inheritance of the *PSEN1 E280A* mutation (Roh et al., 2012). It is known that quality of sleep is lower in AD patients (Ju et al., 2013), and a recent study estimated a negative correlation between quality of sleep and the Virchow–Robin space volume in patients evaluated for cerebrovascular disease (Berezuk et al., 2015). Thus, we speculate that reduced quality of sleep in AD patients might be the result of dilated perivascular space that is likely caused by accumulating A $\beta$  deposits (Roher et al., 2003) and perivascular macrophages (Hawkes and McLaurin, 2009) clogging the glymphatic pathway.

Decreased glymphatic influx was also recently identified in a mouse model of type 2 diabetes (Jiang et al., 2017). Patients with diabetes have been reported to have accumulated amylin oligomers and plaques in the perivascular spaces of the brain parenchyma (Jackson et al., 2013). In rats overexpressing human amylin in the pancreas, the perivascular amylin accumulation in the brain has been found to induce an inflammatory response with activation of microglia and astrocytes (Srodulski et al., 2014). This finding could suggest that the glymphatic impairment in the diabetic mouse model is caused by the same mechanism as in AD but that amylin instead of A $\beta$  accumulates and clogs the perivascular CSF influx pathway.

### Glymphatic influx is impeded in conditions of adaptive immune cell infiltration

Dilated perivascular spaces are evident not only in neurodegenerative diseases but also in small-vessel disease (Doubal et al., 2010) and diseases of the CNS associated with a neuroinflammatory response, such as traumatic brain injury (Inglese et al., 2005), multiple sclerosis (Wuerfel et al., 2008), and subarachnoid hemorrhage (Gaberel et al., 2014; Luo et al., 2016; Golanov et al., 2017; Goulay et al., 2017). In these conditions, the Virchow–Robin

space turns into an immunological space that expands as the blood–brain barrier is disrupted, and the Virchow–Robin space becomes infiltrated with hematopoietic cells of the adaptive immune system (Esiri and Gay, 1990; Prinz and Priller, 2017). Recent reports have evaluated the glymphatic perivascular flow after traumatic brain injury in mice (Plog et al., 2015) and after subarachnoid hemorrhage in mice (Golanov et al., 2017), nonhuman primates (Goulay et al., 2017), and humans (Gaberel et al., 2014); they found reduced glymphatic influx in all cases.

### Glymphatic flow is reduced after cortical spreading depression: a possible new mechanism

The perivascular space can be restricted by factors other than deposition of aggregated proteins and infiltration of immune cells, influencing the glymphatic flow. Following cortical spreading depression (or spreading depolarization), the perivascular space of pial and penetrating arteries and veins was recently found to rapidly and substantially decrease in volume. The restriction lasted several minutes and recovered gradually over 30 min (Schain et al., 2017). During propagation of the depolarizing waves, extracellular K<sup>+</sup> increases and the extracellular space volume is reduced. The increase in extracellular K<sup>+</sup> during spreading depression is slowed in *Aqp4* knock-out animals, probably owing to a larger basal extracellular space volume in these animals, which limits the swelling rate and wave propagation velocity (Yao et al., 2015). Thus, the decrease in perivascular space volume and glymphatic clearance after spreading depression is likely mediated by a reduction in extracellular space volume. Cortical spreading depression is associated with migraine, as well as traumatic brain injury and stroke. An understanding of how the glymphatic system is impaired in these conditions could provide the means for preventing, intervening, or treating the headache that is often a long-term consequence of this condition.

### Future Directions

#### Preventive treatment

Evidence from animals and the few clinical studies performed so far suggest that lessened CSF flow through perivascular Virchow–Robin spaces is associated with reduced function of the glymphatic system. In a mouse model of AD, it was recently found that the glymphatic system was reduced at an early stage before major aggregations of A $\beta$  could be detected (Peng et al., 2016). The order of events is important because it indicates that early intervention by improving glymphatic flow could delay onset

of AD or slow down AD progression. Impaired glymphatic flow leads to reduced clearance of waste metabolites (e.g., A $\beta$ ); it also leads to impaired distribution of lipids (Rangroo Thrane et al., 2013), glucose (Lundgaard et al., 2015), and probably electrolytes, macromolecules, and other larger compounds important for homeostasis that enter the brain predominantly via the blood–CSF barrier at the choroid plexus. Loss of AQP4 polarization at astrocytic endfeet is an early event in the aging brain; however, it was recently found not to occur in physically active animals (He et al., 2017), pointing toward one way in which the glymphatic system can be maintained. Further research into the molecular mechanisms behind the beneficial effect of exercise on glymphatic flow maintenance might lead to the development of new, preventive treatment options in the future. Therefore, diagnosis of early disease states is increasingly necessary.

### Clinical assessment of glymphatic flow

Clinical assessment of abnormal glymphatic flow could be the key to making early diagnostic tests. Studies using contrast-enhanced MRI provide the experimental groundwork for evaluating glymphatic pathway function in the human brain, and in future, could assess whether failure of CSF fluxes contributes to disease progression. Benveniste's group has made headway toward developing a glymphatic diagnostic test based on MRI scans. By delivering contrast agent into the cisterna magna, the movement of CSF can be followed in real time across the entire brain (Iliff et al., 2013a; Lee et al., 2017). Subsequent studies showed that intrathecal lumbar injections with MRI gadolinium contrast, which are routinely used in clinical myelographic studies, provide a viable alternative route to assess the basic parameters of glymphatic function (Yang et al., 2013; Eide and Ringstad, 2015). However, development of a safe and minimally invasive imaging approach to visualize glymphatic function is necessary for future translational efforts.

Recent work using less invasive positron emission tomography scanning with a tracer for tau pathology, <sup>18</sup>F-THK5117, used CSF time activity as a biomarker for CSF clearance. With this approach, researchers were able to see that CSF clearance was reduced in patients with AD and that clearance was inversely associated with A $\beta$  deposition. Even less invasive is MRI without the use of contrast agent. By using a magnetic resonance encephalography (MREG) sequence, Kviviniemi and colleagues (2015) were able to detect cardiac, respiratory, and low-frequency pulsations—three mechanisms affecting CSF pulsations. Implementing MREG for diagnostics could offer a less invasive, novel

approach for early detection of fluid dynamics and, thus, glymphatic fluxes.

### New roles for the glymphatic system

Future studies that focus on the glymphatic system are expected to identify functions of convective CSF fluxes beyond the removal of metabolic waste products. We speculate that the glymphatic system might serve as a pathway for delivery and distribution of drugs, including cancer drugs, within the brain (Hadaczek et al., 2006). Further, we expect that growth factors produced by the choroid plexus, as well as neuromodulators released by several brain stem nuclei positioned close to the ventricular system, are distributed widely across the CNS by the glymphatic system. Thus, in addition to microscopic release of neuromodulators from local nerve terminals followed by local diffusion, volume transmission may involve circulation by macroscopic convective CSF fluxes via the glymphatic system.

### Acknowledgments

This chapter is an expanded and updated version of a previously published article: Jessen NA, et al. (2015) The glymphatic system—a beginner's guide. *Neurochem Res* 40:2583–2599. Copyright 2015, Springer US.

### References

- Achariyar TM, Li B, Peng W, Verghese PB, Shi Y, McConnell E, Benraiss A, Kasper T, Song W, Takano T, Holtzman DM, Nedergaard M, Deane R (2017) Erratum to: Glymphatic distribution of CSF-derived apoE into brain is isoform specific and suppressed during sleep deprivation. *Mol Neurodegener* 12:3.
- Asgari M, de Zélicourt D, Kurtcuoglu V (2015) How astrocyte networks may contribute to cerebral metabolite clearance. *Sci Rep* 5:15024.
- Asgari M, de Zélicourt D, Kurtcuoglu V (2016) Glymphatic solute transport does not require bulk flow. *Sci Rep* 6:38635.
- Aspelund A, Antila S, Proulx ST, Karlsen T V., Karaman S, Detmar M, Wiig H, Alitalo K (2015) A dural lymphatic vascular system that drains brain interstitial fluid and macromolecules. *J Exp Med* 212:991–999.
- Bakker EN, Bacskai BJ, Arbel-Ornath M, Aldea R, Bedussi B, Morris AWJ, Weller RO, Carare RO (2016) Lymphatic clearance of the brain: perivascular, paravascular and significance for neurodegenerative diseases. *Cell Mol Neurobiol* 36:181–194.

- Berezuk C, Ramirez J, Gao F, Scott CJM, Huroy M, Swartz RH, Murray BJ, Black SE, Boulos MI (2015) Virchow–Robin spaces: correlations with polysomnography-derived sleep parameters. *Sleep* 38:853–858.
- Chen RL, Kassem NA, Redzic ZB, Chen CP, Segal MB, Preston JE (2009) Age-related changes in choroid plexus and blood-cerebrospinal fluid barrier function in the sheep. *Exp Gerontol* 44:289–296.
- Chen W, Song X, Zhang Y; Alzheimer’s Disease Neuroimaging Initiative. (2011) Assessment of the Virchow–Robin spaces in Alzheimer disease, mild cognitive impairment, and normal aging, using high-field MR imaging. *AJNR Am J Neuroradiol* 32:1490–1495.
- del Zoppo GJ, Moskowitz M, Nedergaard M (2016) The neurovascular unit and responses to ischemia. In: *Stroke: pathophysiology, diagnosis, and management*, Ed 6 (Grotta J, Albers G, Broderick J, Kasner S, Lo E, Medelow A, Sacco R, Wong L, eds), pp 90–101. Amsterdam: Elsevier.
- Denniston AK, Keane PA (2015) Paravascular pathways in the eye: Is there an “ocular glymphatic system”? *Investig Ophthalmol Vis Sci* 56:3955–3956.
- Denniston AK, Keane PA, Aojula A, Sinclair AJ, Mollan SP (2017) The ocular glymphatic system and idiopathic intracranial hypertension: Author response to “hypodense holes and the ocular glymphatic system.” *Investig Ophthalmol Vis Sci* 58:1134–1136.
- Doubal FN, MacLulich AMJ, Ferguson KJ, Dennis MS, Wardlaw JM (2010) Enlarged perivascular spaces on MRI are a feature of cerebral small vessel disease. *Stroke* 41:450–454.
- Eide PK, Ringstad G (2015) MRI with intrathecal MRI gadolinium contrast medium administration: a possible method to assess glymphatic function in human brain. *Acta Radiol Open* 4:2058460115609635.
- Esiri MM, Gay D (1990) Immunological and neuropathological significance of the Virchow–Robin space. *J Neurol Sci* 100:3–8.
- Fleischman D, Berdahl JP, Zaydlarova J, Stinnett S, Fautsch MP, Allingham RR (2012) Cerebrospinal fluid pressure decreases with older age. *PLoS One* 7:e52664.
- Gaberel T, Gakuba C, Goulay R, Martinez De Lizarrondo S, Hanouz JL, Emery E, Touze E, Vivien D, Gauberti M (2014) Impaired glymphatic perfusion after strokes revealed by contrast-enhanced MRI: a new target for fibrinolysis? *Stroke* 45:3092–3096.
- Ge Y, Law M, Herbert J, Grossman RI (2005) Prominent perivenular spaces in multiple sclerosis as a sign of perivascular inflammation in primary demyelination. *AJNR Am J Neuroradiol* 26:2316–2319.
- Gleiser C, Wagner A, Fallier-Becker P, Wolburg H, Hirt B, Mack AF (2016) Aquaporin-4 in astroglial cells in the CNS and supporting cells of sensory organs—a comparative perspective. *Int J Mol Sci* 17:E1411.
- Golanov EV, Bovshik EI, Wong KK, Pautler RG, Foster CH, Federley RG, Zhang JY, Mancuso J, Wong ST, Britz GW (2017) Subarachnoid hemorrhage-induced block of cerebrospinal fluid flow: role of brain coagulation factor III (tissue factor). *J Cereb Blood Flow Metab* 0271678X1770115. [Epub ahead of print]
- Goulay R, Flament J, Gauberti M, Naveau M, Pasquet N, Gakuba C, Emery E, Hantraye P, Vivien D, Aron-Badin R, Gaberel T (2017) Subarachnoid hemorrhage severely impairs brain parenchymal cerebrospinal fluid circulation in nonhuman primate. *Stroke* 48:2301–2305.
- Hadaczek P, Yamashita Y, Mirek H, Tamas L, Bohn MC, Noble C, Park JW, Bankiewicz K (2006) The “perivascular pump” driven by arterial pulsation is a powerful mechanism for the distribution of therapeutic molecules within the brain. *Mol Ther* 14:69–78.
- Hawkes CA, McLaurin J (2009) Selective targeting of perivascular macrophages for clearance of beta-amyloid in cerebral amyloid angiopathy. *Proc Natl Acad Sci USA* 106:1261–1266.
- He X-F, Liu D-X, Zhang Q, Liang F-Y, Dai G-Y, Zeng J-S, Pei Z, Xu G-Q, Lan Y (2017) Voluntary exercise promotes glymphatic clearance of amyloid beta and reduces the activation of astrocytes and microglia in aged mice. *Front Mol Neurosci* 10:144.
- Iliff JJ, Wang M, Liao Y, Plogg BA, Peng W, Gundersen GA, Benveniste H, Vates GE, Deane R, Goldman SA, Nagelhus EA, Nedergaard M (2012) A paravascular pathway facilitates CSF flow through the brain parenchyma and the clearance of interstitial solutes, including amyloid  $\beta$ . *Sci Transl Med* 4:147ra111.
- Iliff JJ, Nedergaard M (2013) Is there a cerebral lymphatic system? *Stroke* 44(6 Suppl 1):S93–S95.
- Iliff JJ, Lee H, Yu M, Feng T, Logan J, Nedergaard M, Benveniste H (2013a) Brain-wide pathway for waste clearance captured by contrast-enhanced MRI. *J Clin Invest* 123:1299–1309.

- Illiff JJ, Wang M, Zeppenfeld DM, Venkataraman A, Plog BA, Liao Y, Deane R, Nedergaard M (2013b) Cerebral arterial pulsation drives paravascular CSF–interstitial fluid exchange in the murine brain. *J Neurosci* 33:18190–18199.
- Inglese M, Bomszyk E, Gonen O, Mannon LJ, Grossman RI, Rusinek H (2005) Dilated perivascular spaces: hallmarks of mild traumatic brain injury. *AJNR Am J Neuroradiol* 26:719–724.
- Jackson K, Barisone GA, Diaz E, Jin LW, DeCarli C, Despa F (2013) Amylin deposition in the brain: a second amyloid in Alzheimer disease? *Ann Neurol* 74:517–526.
- Jessen NA, Munk ASF, Lundgaard I, Nedergaard M (2015) The glymphatic system—a beginner’s guide. *Neurochem Res* 40:2583–2599.
- Jiang Q, Zhang L, Ding G, Davoodi-Bojd E, Li Q, Li L, Sadry N, Nedergaard M, Chopp M, Zhang Z (2017) Impairment of the glymphatic system after diabetes. *J Cereb Blood Flow Metab* 37:1326–1337.
- Jin BJ, Smith AJ, Verkman AS (2016) Spatial model of convective solute transport in brain extracellular space does not support a “glymphatic” mechanism. *J Gen Physiol* 148:489–501.
- Johnston M, Zakharov A, Papaiconomou C, Salmasi G, Armstrong D (2004) Evidence of connections between cerebrospinal fluid and nasal lymphatic vessels in humans, non-human primates and other mammalian species. *Cerebrospinal Fluid Res* 1:2.
- Ju Y-ES, McLeland JS, Toedebusch CD, Xiong C, Fagan AM, Duntley SP, Morris JC, Holtzman DM (2013) Sleep quality and preclinical Alzheimer disease. *JAMA Neurol* 70:587–593.
- Kress BT, Illiff JJ, Xia M, Wang M, Wei H, Zeppenfeld D, Xie L, Kang H, Xu Q, Liew J, Plog BA, Ding F, Deane R, Nedergaard M (2014) Impairment of paravascular clearance pathways in the aging brain. *Ann Neurol* 76:845–861.
- Lee H, Mortensen K, Sanggaard S, Koch P, Brunner H, Quistorff B, Nedergaard M, Benveniste H (2017) Quantitative Gd-DOTA uptake from cerebrospinal fluid into rat brain using 3D VFA-SPGR at 9.4T. *Magn Reson Med*. doi: 10.1002/mrm.26779. [Epub ahead of print]
- Liao S, Padera TP (2013) Lymphatic function and immune regulation in health and disease. *Lymphat Res Biol* 11:136–143.
- Liu DX, He X, Wu D, Zhang Q, Yang C, Liang FY, He XF, Dai GY, Pei Z, Lan Y, Xu GQ (2017) Continuous theta burst stimulation facilitates the clearance efficiency of the glymphatic pathway in a mouse model of sleep deprivation. *Neurosci Lett* 653:189–194.
- Louveau A, Smirnov I, Keyes TJ, Eccles JD, Rouhani SJ, Peske JD, Derecki NC, Castle D, Mandell JW, Lee KS, Harris TH, Kipnis J (2015) Structural and functional features of central nervous system lymphatic vessels. *Nature* 523:337–341.
- Lundgaard I, Li B, Xie L, Kang H, Sanggaard S, Haswell JDR, Sun W, Goldman S, Blekot S, Nielsen M, Takano T, Deane R, Nedergaard M (2015) Direct neuronal glucose uptake heralds activity-dependent increases in cerebral metabolism. *Nat Commun* 6:6807.
- Luo C, Yao X, Li J, He B, Liu Q, Ren H, Liang F, Li M, Lin H, Peng J, Yuan TF, Pei Z, Su H (2016) Paravascular pathways contribute to vasculitis and neuroinflammation after subarachnoid hemorrhage independently of glymphatic control. *Cell Death Dis* 7:e2160.
- Morris AWJ, Sharp MMG, Albargothy NJ, Fernandes R, Hawkes CA, Verma A, Weller RO, Carare RO (2016) Vascular basement membranes as pathways for the passage of fluid into and out of the brain. *Acta Neuropathol* 131:725–736.
- O’Donnell J, Zeppenfeld D, McConnell E, Pena S, Nedergaard M (2012) Norepinephrine: a neuromodulator that boosts the function of multiple cell types to optimize CNS performance. *Neurochem Res* 37:2496–2512.
- Peng W, Achariyar TM, Li B, Liao Y, Mestre H, Hitomi E, Regan S, Kasper T, Peng S, Ding F, Benveniste H, Nedergaard M, Deane R (2016) Suppression of glymphatic fluid transport in a mouse model of Alzheimer’s disease. *Neurobiol Dis* 93:215–225.
- Plog BA, Dashnaw ML, Hitomi E, Peng W, Liao Y, Lou N, Deane R, Nedergaard M (2015) Biomarkers of traumatic injury are transported from brain to blood via the glymphatic system. *J Neurosci* 35:518–526.
- Prinz M, Priller J (2017) The role of peripheral immune cells in the CNS in steady state and disease. *Nat Neurosci* 20:136–144.

- Ramirez J, Berezuk C, McNeely AA, Gao F, McLaurin J, Black SE (2016) Imaging the perivascular space as a potential biomarker of neurovascular and neurodegenerative diseases. *Cell Mol Neurobiol* 36:289–299.
- Rangroo Thrane V, Thrane AS, Plog BA, Thiyagarajan M, Iliff JJ, Deane R, Nagelhus EA, Nedergaard M (2013) Paravascular microcirculation facilitates rapid lipid transport and astrocyte signaling in the brain. *Sci Rep* 3:2582.
- Rennels ML, Gregory TF, Blaumanis OR, Fujimoto K, Grady PA (1985) Evidence for a “paravascular” fluid circulation in the mammalian central nervous system, provided by the rapid distribution of tracer protein throughout the brain from the subarachnoid space. *Brain Res* 326:47–63.
- Roh JH, Huang Y, Bero AW, Kasten T, Stewart FR, Bateman RJ, Holtzman DM (2012) Disruption of the sleep-wake cycle and diurnal fluctuation of  $\beta$ -amyloid in mice with Alzheimer’s disease pathology. *Sci Transl Med* 4:150ra122.
- Roher AE, Kuo Y-M, Esh C, Knebel C, Weiss N, Kalback W, Luehrs DC, Childress JL, Beach TG, Weller RO, Kokjohn TA (2003) Cortical and leptomeningeal cerebrovascular amyloid and white matter pathology in Alzheimer’s disease. *Mol Med* 9:112–122.
- Ross CA, Poirier MA (2004) Protein aggregation and neurodegenerative disease. *Nat Med* 10(Suppl):S10–S17.
- Sabbatini M, Barili P, Bronzetti E, Zaccheo D, Amenta F (1999) Age-related changes of glial fibrillary acidic protein immunoreactive astrocytes in the rat cerebellar cortex. *Mech Ageing Dev* 108:165–172.
- Schain AJ, Melo-Carrillo A, Strassman AM, Burstein R (2017) Cortical spreading depression closes paravascular space and impairs glymphatic flow: implications for migraine headache. *J Neurosci* 37:2904–2915.
- Shinkai Y, Yoshimura M, Ito Y, Odaka A, Suzuki N, Yanagisawa K, Ihara Y (1995) Amyloid  $\beta$ -proteins 1–40 and 1–42(43) in the soluble fraction of extra and intracranial blood vessels. *Ann Neurol* 38:421–428.
- Simon MJ, Murchison C, Iliff JJ (2017) A transcriptome-based assessment of the astrocytic dystrophin-associated complex in the developing human brain. *J Neurosci Res*. doi: 10.1002/jnr.24082 [Epub ahead of print].
- Srodulski S, Sharma S, Bachstetter AB, Brelsfoard JM, Pascual C, Xie XS, Saatman KE, Van Eldik LJ, Despa F (2014) Neuroinflammation and neurologic deficits in diabetes linked to brain accumulation of amylin. *Mol Neurodegener* 9:30.
- Szentistványi I, Patlak CS, Ellis RA, Cserr HF (1984) Drainage of interstitial fluid from different regions of rat brain. *Am J Physiol* 246(6 Pt 2):F835–F844.
- Taoka T, Masutani Y, Kawai H, Nakane T, Matsuoka K, Yasuno F, Kishimoto T, Naganawa S (2017) Evaluation of glymphatic system activity with the diffusion MR technique: diffusion tensor image analysis along the perivascular space (DTI-ALPS) in Alzheimer’s disease cases. *Jpn J Radiol* 35:172–178.
- Wang Z, Ying Z, Bosy-Westphal A, Zhang J, Heller M, Later W, Heymsfield SB, Müller MJ (2012) Evaluation of specific metabolic rates of major organs and tissues: comparison between nonobese and obese women. *Obesity (Silver Spring)* 20:95–100.
- Weller RO (1998) Pathology of cerebrospinal fluid and interstitial fluid of the CNS: significance for Alzheimer disease, prion disorders and multiple sclerosis. *J Neuropathol Exp Neurol* 57:885–894.
- Wostyn P, de Groot V, van Dam D, Audenaert K, de Deyn PP, Killer HE (2016) The glymphatic system: a new player in ocular diseases? *Investig Ophthalmol Vis Sci* 57:5426–5427.
- Wostyn P, De Groot V, Van Dam D, Audenaert K, De Deyn PP, Killer HE (2017) “Hypodense holes” and the ocular glymphatic system: Author response: “Black holes” and the ocular glymphatic system. *Invest Ophthalmol Vis Sci* 58:1132–1133.
- Wuerfel J, Haertle M, Waiczies H, Tysiak E, Bechmann I, Wernecke KD, Zipp F, Paul F (2008) Perivascular spaces—MRI marker of inflammatory activity in the brain? *Brain* 131(Pt 9):2332–2340.
- Xie L, Kang H, Xu Q, Chen MJ, Liao Y, Thiyagarajan M, O’Donnell J, Christensen DJ, Nicholson C, Iliff JJ, Takano T, Deane R, Nedergaard M (2013) Sleep drives metabolite clearance from the adult brain. *Science* 342:373–377.
- Yang L, Kress BT, Weber HJ, Thiyagarajan M, Wang B, Deane R, Benveniste H, Iliff JJ, Nedergaard M (2013) Evaluating glymphatic pathway function utilizing clinically relevant intrathecal infusion of CSF tracer. *J Transl Med* 11:107.
- Yao X, Smith AJ, Jin BJ, Zador Z, Manley GT, Verkman AS (2015) Aquaporin-4 regulates the velocity and frequency of cortical spreading depression in mice. *Glia* 63:1860–1869.

# The Maternal Interleukin-17a Pathway in Mice Promotes Autism-Like Phenotypes in Offspring

Gloria B. Choi, PhD,<sup>1</sup> Yeong S. Yim, PhD,<sup>1</sup>  
Helen Wong, PhD,<sup>2,3</sup> Sangdoon Kim, PhD,<sup>4</sup>  
Hyun Ju Kim, PhD,<sup>4</sup> Sangwon V. Kim, PhD,<sup>5</sup>  
Charles A. Hoeffler, PhD,<sup>2,3</sup> Jun R. Huh, PhD,<sup>4,5</sup>  
and Dan R. Littman, MD, PhD<sup>5,6</sup>

---

<sup>1</sup>The McGovern Institute for Brain Research  
Department of Brain and Cognitive Sciences  
Massachusetts Institute of Technology  
Cambridge, Massachusetts

<sup>2</sup>Center for Neural Science  
New York University  
New York, New York

<sup>3</sup>Department of Integrated Physiology  
Institute for Behavioral Genetics  
University of Colorado  
Boulder, Colorado

<sup>4</sup>Division of Infectious Diseases and Immunology  
Department of Medicine  
University of Massachusetts Medical School  
Worcester, Massachusetts

<sup>5</sup>The Kimmel Center for Biology and Medicine  
Skirball Institute of Biomolecular Medicine  
New York University School of Medicine  
New York, New York

<sup>6</sup>Howard Hughes Medical Institute  
New York, New York

## Introduction

Viral infection during pregnancy has been correlated with increased frequency of autism spectrum disorder (ASD) in offspring. This observation has been modeled in rodents subjected to maternal immune activation (MIA). The immune cell populations critical in the MIA model have not been identified. Using both genetic mutants and blocking antibodies in mice, we show that both ROR $\gamma$ t (retinoic acid receptor–related orphan nuclear receptor gamma-t)–dependent effector T-lymphocytes (e.g., Th17 cells) and the effector cytokine interleukin-17a (IL-17a) are required in mothers for MIA-induced behavioral abnormalities in offspring. We find that MIA induces an abnormal cortical phenotype, which is also dependent on maternal IL-17a, in the fetal brain. Our data suggest that therapeutic targeting of Th17 cells in susceptible pregnant mothers may reduce the likelihood of bearing children with inflammation-induced ASD-like phenotypes.

Several studies have suggested that viral infection of women during pregnancy correlates with an increased frequency of ASD in the offspring (Ashwood et al., 2006; Atladottir et al., 2009, 2010; Patterson, 2009; Brown et al., 2014; Lee et al., 2015). In the rodent maternal immune activation model of this phenomenon (Smith et al., 2007), offspring from pregnant mice infected with virus or injected intraperitoneally with synthetic double-stranded RNA (poly(I:C)), a mimic of viral infection, exhibit behavioral symptoms reminiscent of ASD: social deficits, abnormal communication, and repetitive behaviors (Malkova et al., 2012). Th17 cells are responsible for immune responses against extracellular bacteria and fungi, and their dysregulation is thought to underlie numerous inflammatory and autoimmune diseases (Wilke et al., 2011), such as asthma, rheumatoid arthritis, psoriasis, inflammatory bowel disease, and multiple sclerosis. The transcription factor ROR $\gamma$ t is expressed in several cell types in the immune system. It is a key transcriptional regulator for the development of Th17 cells, as well as  $\gamma\delta$  T-cells and innate lymphoid cells (e.g., ILC3) that express Th17 cell–like cytokines, in both humans and mice (Ivanov et al., 2006; Lochner et al., 2008; Manel et al., 2008; Spits and Di Santo, 2011).

Th17 cells and their cytokine mediators have been suggested to have a role in ASD. For example, elevated levels of IL-17a, the predominant Th17 cytokine, have been detected in the serum of a subset of autistic children (Suzuki et al., 2011; Al-Ayadhi and Mostafa, 2012). A genome-wide copy number variant (CNV) analysis identified *IL17A* as one of many genes enriched in autistic patients (van der

Zwaag et al., 2009). Similarly, in the MIA mouse model, CD4<sup>+</sup> T-lymphocytes from affected offspring produced higher levels of IL-17a upon *in vitro* activation (Mandal et al., 2010; Hsiao et al., 2012). Although these data suggest that Th17 cells may be involved in ASD patients, whether Th17 cells are the specific immune cell population that is necessary for MIA phenotypes is unknown. Here we show that maternal ROR $\gamma$ t-expressing pro-inflammatory T-cells, a major source of IL-17a, are required in the MIA model for induction of ASD-like phenotypes in offspring. Consistent with this notion, antibody blockade of IL-17a activity in pregnant mice protected against the development of MIA-induced behavioral abnormalities in the offspring. Notably, we also found atypical cortical development in affected offspring, and this abnormality was rescued by inhibition of maternal Th17/IL-17a pathways.

## Elevated Fetal Brain IL-17Ra mRNA Follows Increased Maternal IL-17a in MIA

Pregnant mothers injected with poly(I:C) on embryonic day 12.5 (E12.5) had strong induction of serum cytokines IL-6, tumor necrosis factor-alpha (TNF-alpha), interferon-beta (IFN- $\beta$ ) and IL-1 $\beta$  at 3 h, compared with PBS-injected control dams (Figs. 1A, S1A–C) (supplementary figures are available at <https://www.ncbi.nlm.nih.gov/pmc/articles/PMC4782964>). Additionally, poly(I:C) injection resulted in a strong increase of serum IL-17a at E14.5 (Fig. 1B). In contrast, poly(I:C) did not affect the levels of the anti-inflammatory cytokine IL-10 in the serum nor in placenta and decidua extracts (Fig. S1D). It was previously shown that the pro-inflammatory effector cytokine IL-6, a key factor for Th17 cell differentiation (Kuchroo and Awasthi, 2012), is required in pregnant mothers for MIA to produce ASD-like phenotypes in the offspring (Smith et al., 2007). We found that poly(I:C) injection into pregnant dams lacking IL-6 (IL-6 knock-out [KO]) failed to increase the serum levels of IL-17a at E14.5, consistent with IL-6 acting upstream of IL-17a. Conversely, recombinant IL-6 injections into wild-type (WT) mothers were sufficient to induce IL-17a levels comparable with those of poly(I:C)–injected WT mothers (Fig. S1E). Placenta- and decidua-associated mononuclear cells, isolated from poly(I:C)-treated animals at E14.5 and cultured for 24 h, expressed similar amounts of IL-6 mRNA compared with PBS-injected controls (Fig. 1C). In contrast, IL-17a mRNA expression in these cells was strongly upregulated by poly(I:C) injection (Fig. 1D). This increase in mRNA expression was correlated with enhanced secretion of IL-17a by placenta- and decidua-associated mononuclear cells

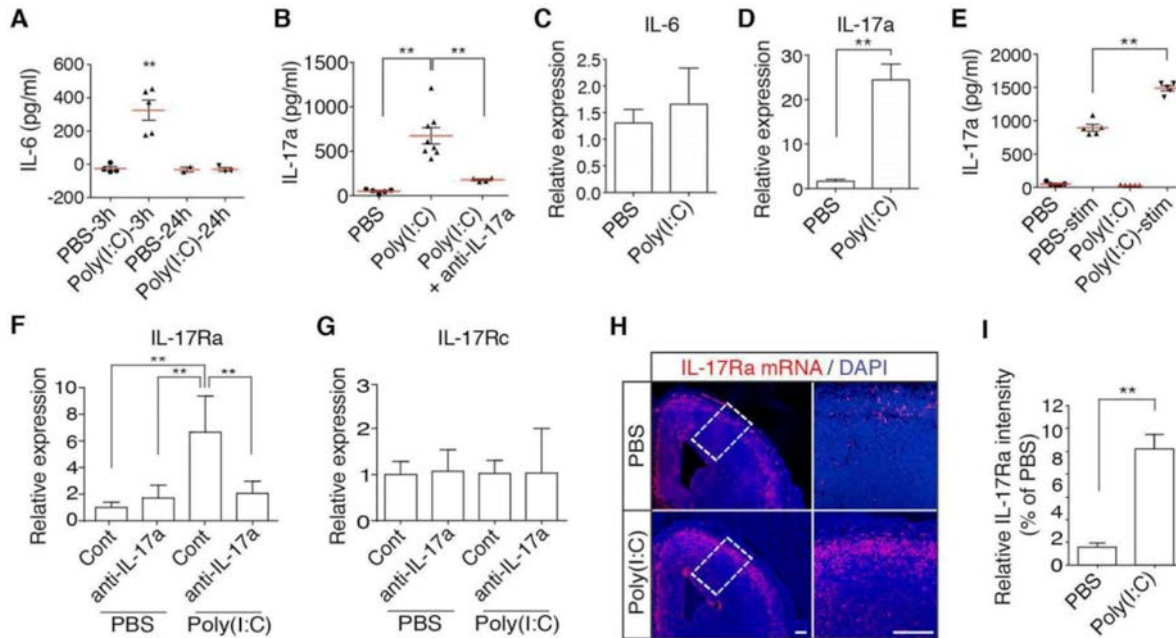


**Figure 1.** IL-17a increase in mothers subjected to MIA leads to elevated IL-17Ra mRNA expression in the offspring. **A**, Serum concentrations of IL-6 ( $n = 3\text{--}5$  mice per group; 2 independent experiments) at 3 h or 24 h after PBS or poly(I:C) injection into pregnant dams at E12.5. **B**, Serum concentrations of maternal IL-17a ( $n = 4\text{--}8$  mice per group; 2 independent experiments) at E14.5 in PBS- or poly(I:C)-injected mothers, pretreated with or without IL-17a-blocking antibodies. **C**, **D**, Relative IL-6 (**C**) and IL-17a (**D**) mRNA expression in cells isolated from placenta/decidua of PBS- or poly(I:C)-treated mothers at E14.5 and cultured *in vitro* for 24 h. The results are representative of three independent experiments. For each probe set, relative mRNA expression of one biological replicate from PBS-treated dams was set at 1. Real-time PCR analysis of the relative expression of indicated genes compared with the level of *Gapdh* in cells from PBS-treated dams. **E**, Supernatant concentrations of IL-17a from *ex vivo* cultured mononuclear cells, isolated from placenta/decidua of PBS- or poly(I:C)-treated pregnant dams. Stim refers to PMA and ionomycin stimulation. **F**, **G**, Relative IL-17Ra (**F**) and IL-17Rc (**G**) mRNA levels in E14.5 male fetal brain, derived from PBS- or poly(I:C)-injected mothers pretreated with IgG isotype control (Cont) or IL-17a-blocking antibodies (anti-IL-17a). The relative mRNA fold change, compared with the PBS- and Cont-treated group, is plotted on the y-axis ( $n = 7$  [PBS, Cont],  $n = 7$  [PBS, anti-IL-17a],  $n = 7$  [poly(I:C), Cont], and  $n = 7$  [poly(I:C), anti-IL-17a]; 2–3 independent experiments). **H**, *In situ* hybridization with an IL-17Ra RNA probe in E14.5 male fetal brains derived from PBS- or poly(I:C)-injected mothers. Images are representative of four independent experiments. **I**, Relative signal intensity for images shown in **H**. Scale bar, 100  $\mu\text{m}$ . **A**, **B**, **E**, **F**, **G**, One-way ANOVA with Tukey *post hoc* tests; **C**, **D**, **I**, Student's *t*-test.  $**p < 0.01$ . Graphs show mean  $\pm$  SEM. : Reprinted with permission from Choi GB et al. (2016), Figure 1. Copyright 2016, American Association for the Advancement of Science.

from poly(I:C)-treated dams (Fig. 1E), upon *ex vivo* stimulation with PMA and ionomycin that mimics T-cell receptor activation. IL-17a induction was specific to the placenta and decidua, as small intestine mononuclear cells from poly(I:C)-treated pregnant dams did not secrete more IL-17a than those from PBS-treated controls (Fig. S1F).

We also observed that expression of the IL-17a receptor subunit A (IL-17Ra), but not subunit C (IL-17Rc), mRNA was strongly augmented in the fetal brain upon induction of MIA (Figs. 1F,G). Using *in situ* hybridization, IL-17Ra mRNA was detected in the mouse cortex, and its expression was strongly upregulated in E14.5 fetal brains following poly(I:C) injection of pregnant dams (Figs. 1H,I). The *in situ*

probe detecting endogenous expression of IL-17Ra was specific, as it did not produce detectable signal in E14.5 fetal brain that lacks IL-17Ra (Fig. S2).

## Maternal IL-17a Promotes Abnormal Cortical Development in Offspring

We next investigated whether pathological activation of the IL-17 pathway in pregnant mothers affects fetal brain development and subsequently contributes to the ASD-like behavioral phenotypes in offspring. To test this hypothesis, we pretreated pregnant mothers with IgG isotype control or IL-17a-blocking antibodies before injecting them with PBS or poly(I:C) (Fig. S3). We then examined

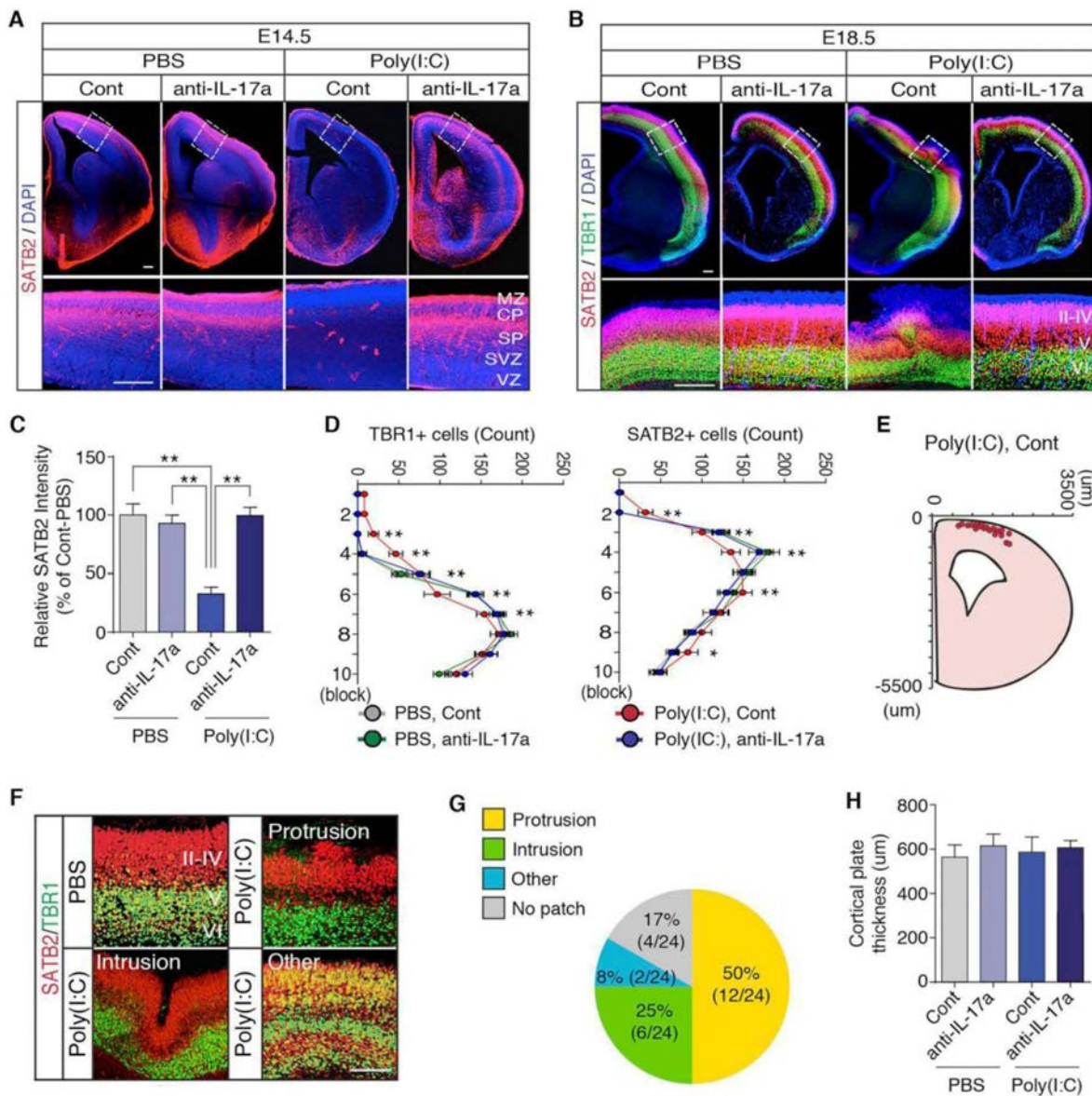


**Figure 2.** The IL-17a pathway promotes abnormal cortical development in the offspring of pregnant dams following MIA. **A**, Immunofluorescence staining of SATB2 (a marker of postmitotic neurons in superficial cortical layers) in E14.5 male fetal brain, derived from PBS- or poly(I:C)-injected mothers, pretreated with IgG isotype control (Cont) or IL-17a blocking antibodies (anti-IL-17a). MZ, marginal zone; CP, cortical plate; SP, subplate; SVZ, subventricular zone; VZ, ventricular zone. **B**, Staining of SATB2 and TBR1 in E18.5 male fetal brains from animals treated as in **A**. II-IV, V, and VI refer to different cortical layers. **C**, Quantification of SATB2 intensity in the cortical plate of E14.5 fetal brains (n = 8 [PBS, Cont], n = 8 [PBS, anti-IL-17a], n = 8 [poly(I:C), Cont], and n = 8 [poly(I:C), anti-IL-17a]; 3 independent experiments). **D**, Quantification of TBR1- and SATB2-positive cells in a 300 × 300 μm<sup>2</sup> region of interest centered on the malformation in the cortical plate of E18.5 fetal brains (n = 20 [PBS, Cont], n = 20 [PBS, anti-IL-17a], n = 24 [poly(I:C), Cont], and n = 20 [poly(I:C), anti-IL-17a]; 5 independent experiments). **E**, The spatial location of the cortical patch in E18.5 male fetal brains from poly(I:C)-injected mothers pretreated with control antibodies (n = 20 [poly(I:C), Cont]). **F**, The disorganized patches of cortex observed in fetuses from poly(I:C)-injected mothers were categorized into groups based on morphology: Protrusions, intrusions, or other abnormal patterns and their representative images are shown. II-IV, V, and VI refer to different cortical layers. **G**, Percentage of the cortical patches in each category (n = 24 [poly(I:C), Cont]). **H**, Thickness of the cortical plate in E18.5 fetal brains, derived from PBS- or poly(I:C)-injected mothers, pretreated with IgG isotype control or IL-17a-blocking antibodies (n = 20 [PBS, Cont], n = 20 [PBS, anti-IL-17a], n = 20 [poly(I:C), Cont], and n = 20 [poly(I:C), anti-IL-17a]; 5 independent experiments). Scale bars: **A**, **B**, **F**, 100 μm. **C**, **H**, One-way ANOVA; **D**, Two-way ANOVA with Tukey *post hoc* tests. \*\*p < 0.01 and \*p < 0.05. Graphs show mean ± SEM. Reprinted with permission from Choi GB et al. (2016), Figure 2. Copyright 2016, American Association for the Advancement of Science.

cortical development in the fetus for the following reasons:

1. Poly(I:C) injection of mothers increases IL-17Ra expression in the cortex of the fetal brain (Figs. 1H,I);
2. Cortical development starts at ~E11 (Dehay and Kennedy, 2007), which aligns well with the time points of potential fetal exposure to MIA (Smith et al., 2007);
3. Disorganized cortex and focal patches of abnormal laminar cytoarchitecture have been found in the brains of ASD patients (Casanova et al., 2013; Stoner et al., 2014); and
4. MIA has been shown to affect cortical development (De Miranda et al., 2010; Smith et al., 2012).

We analyzed cortical lamination (an orderly layered structure of the developing cortex) in fetal brains at E14.5 and E18.5 as well as in the adult brain using antibodies specific for the following proteins expressed in the cortex in a layer-specific manner (Molyneux et al., 2007): special AT-rich sequence-binding protein 2 (SATB2) (Alcamo et al., 2008), T-brain-1 (TBR1, a marker restricted to deeper cortical layers) (Englund et al., 2005), and COUP-TF (chicken ovalbumin upstream promoter transcription factor–interacting protein 2 [CTIP2]) (Leid et al., 2004). MIA led to delayed expression of SATB2 (a marker of postmitotic neurons in superficial cortical layers) at E14.5 compared with fetuses of control animals (Figs. 2A,C). At E18.5, MIA resulted in a patch of disorganized cortical cytoarchitecture (Figs. 2B,D–G) but did not affect cortical thickness of the fetal brains (Fig. 2H). This singular patch of disorganized cortex occurred at a similar medial-lateral position in a majority of E18.5 fetal brains (Figs. 2E,G) derived from mothers injected with poly(I:C), but not PBS. The abnormal expression patterns of SATB2, TBR1, and CTIP2 were maintained in adult MIA offspring (Fig. S4). Significantly, normal expression of these cortical layer-specific markers, as well as laminar cortical organization, were largely preserved in the offspring of poly(I:C)-injected mothers pretreated with IL-17a-blocking antibody (Figs. 2A–D, S4).

Pretreatment with IL-17a-blocking antibody also suppressed the MIA-mediated increase in IL-17Ra mRNA expression in fetal brain at E14.5 (Fig. 1F). This suppression was accompanied by a reduction in maternal serum IL-17a (Fig. 1B), indicating that

the upregulation of IL-17Ra mRNA in fetal brains requires maternal IL-17a signaling. Of note, IL-17a antibody blockade of the IL-17a/IL-17Ra signaling pathway did not result in a concomitant increase of the serum IL-10 levels, and IL-17a mRNA expression was not detected in fetal brain at E14.5, regardless of poly(I:C) injection. Together, these data demonstrate that the maternal IL-17a-dependent pathway mediates disorganized cortical phenotypes in offspring following *in utero* MIA and suggest that this may be due to exposure of the fetus and its brain to increased levels of IL-17a.

### Maternal IL-17a Promotes ASD-Like Behavioral Abnormalities in Offspring

We next tested the functional relevance of the maternal IL-17a pathway for MIA-induced ASD-like behavioral abnormalities in offspring (Fig. S3). We first assessed MIA offspring for abnormal communication by measuring pup ultrasonic vocalization (USV) responses (Schwartz et al., 2013). Following separation from mothers, pups from poly(I:C)-injected mothers pretreated with IgG isotype control antibody emitted more USV calls than those from PBS-injected mothers (Fig. 3A), in agreement with previous studies (Yee et al., 2012; Schwartz et al., 2013). Some studies have reported reduced USV calls upon MIA (Malkova et al., 2012; Hsiao et al., 2013), but these opposite effects may reflect differences in methodological approaches, including dose and number of exposures to poly(I:C) as well as timing of poly(I:C) administration. Altogether, these results indicate that MIA induces abnormal USV in offspring. Pretreating poly(I:C)-injected mothers with IL-17a-blocking antibody resulted in offspring that emitted a similar number of USV calls as the pups from PBS-injected control mothers (Fig. 3A), demonstrating that IL-17a-mediated signaling events are necessary for the MIA-induced abnormal USV phenotype. As previously reported (Smith et al., 2007; Malkova et al., 2012), we found that prenatal exposure to MIA also caused social interaction deficits in adult offspring (Fig. 3B). This defect was fully rescued in offspring from poly(I:C)-injected mothers pretreated with IL-17a-blocking antibody (Fig. 3B). Repetitive/perseverative behaviors are another core feature in ASD that we tested next in our experimental mice using the marble burying assay (Hoeffler et al., 2008). Offspring from poly(I:C)-injected mothers displayed enhanced marble burying compared with offspring from PBS-injected mothers (Fig. 3C), consistent with previous studies (Smith et al., 2007; Schwartz et al., 2013). Pretreatment with IL-17a-blocking

## NOTES

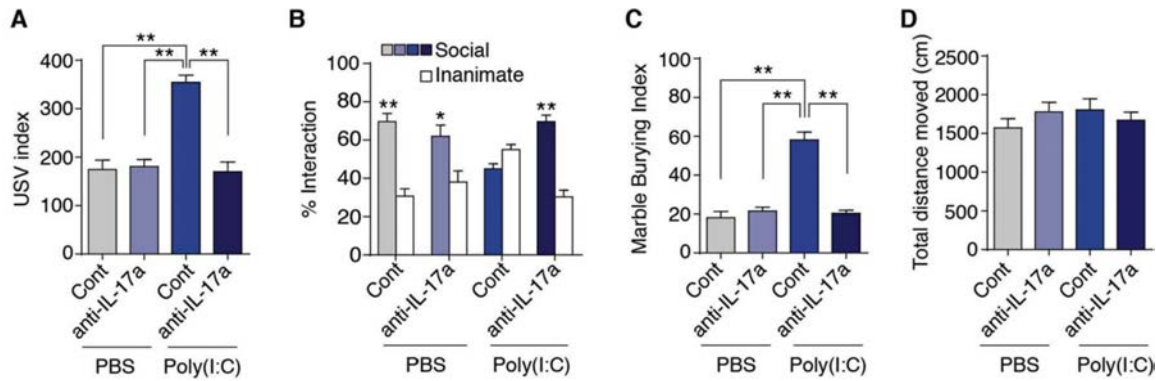


**Figure 3.** The IL-17a pathway promotes ASD-like phenotypes in the MIA offspring. **A**, USV assay. At postnatal day 9 (P9), pups from the indicated experimental groups were separated from their mothers to elicit USV calls. The number of pup calls is plotted on the y-axis ( $n = 25$  [PBS, Cont],  $n = 28$  [PBS, anti-IL-17a],  $n = 38$  [poly(I:C), Cont], and  $n = 34$  [poly(I:C), anti-IL-17a]; 6–7 independent experiments). **B**, Social approach behavior. Graphed as a social preference index (% time spent investigating social or inanimate stimulus out of total object investigation time) ( $n = 15$  [PBS, Cont],  $n = 15$  [PBS, anti-IL-17a],  $n = 16$  [poly(I:C), Cont], and  $n = 20$  [poly(I:C), anti-IL-17a]; 6–7 independent experiments). **C**, Marble burying behavior. Percentage of the number of buried marbles is plotted on the y-axis ( $n = 15$  [PBS, Cont],  $n = 15$  [PBS, anti-IL-17a],  $n = 15$  [poly(I:C), Cont], and  $n = 20$  [poly(I:C), anti-IL-17a]; 6–7 independent experiments). **D**, Total distance traveled during social approach behavior. **A**, **C**, **D**, One-way ANOVA with Tukey *post hoc* tests; **B**, Two-way ANOVA with Tukey *post hoc* tests.  $**p < 0.01$  and  $*p < 0.05$ . Graphs show mean  $\pm$  SEM. Reprinted with permission from Choi GB et al. (2016), Figure 3. Copyright 2016, American Association for the Advancement of Science.

antibody of poly(I:C)-injected mothers rescued marble burying behavior in the offspring (Fig. 3C). Notably, distinct behavioral phenotypes observed among different treatment groups did not result from differences in activity or arousal, as total distances moved during the sociability or marble burying tests were indistinguishable (Fig. 3D). Moreover, different treatment groups displayed comparable sex ratios, litter sizes, and weights (Fig. S5). Taken together, these data indicate that the IL-17a pathway in pregnant mice is crucial for mediating the MIA-induced behavioral phenotypes in offspring.

### ROR $\gamma$ t Expression in Maternal T-Cells Is Required for ASD-Like Phenotypes in the MIA Offspring

Because ROR $\gamma$ t is a critical regulator of the IL-17a pathway (Ivanov et al., 2006), we next investigated the role of maternal ROR $\gamma$ t in MIA-induced behavioral phenotypes in offspring. Significantly, Th17 cells and IL-17a have been detected in the decidua as well as in the serum during pregnancy in humans (Nakashima et al., 2010; Martinez-Garcia et al., 2011; Wu et al., 2014). CD45<sup>+</sup> mononuclear cells, including CD4<sup>+</sup> T-cells, isolated from placenta and decidua of immune-activated WT mothers, but not from immune-activated mothers lacking both ROR $\gamma$ t and the closely related ROR $\gamma$  isoform (ROR $\gamma$  KO), produced IL-17a upon *ex vivo* activation with

PMA and ionomycin (Figs. S6A,B). Cells isolated from WT and ROR $\gamma$  KO mice secreted similar amounts of IFN- $\gamma$ , consistent with the specific effect of ROR $\gamma$ t on IL-17a expression (Fig. S6C). In line with this observation, poly(I:C) treatment increased placenta/decidua-associated Th17 but not regulatory T (Treg) cells in pregnant dams, compared with PBS treatment (Figs. S6D,E). ROR $\gamma$  KO mice lack ROR $\gamma$ / $\gamma$ t expression not only in CD4<sup>+</sup> T-cells but also in other lymphoid and non-immune system cells, and they have defective development of secondary and tertiary lymphoid organs (Sun et al., 2000; Eberl and Littman, 2004).

To determine whether ROR $\gamma$ t function specifically in T-cells mediates MIA-induced phenotypes, we bred ROR $\gamma$ t<sup>fl</sup> animals (Fig. S7) to *Cd4-Cre* mice to selectively inactivate *rorc(t)* in the T-cells of pregnant mothers (ROR $\gamma$ t T-cell-specific knock-out [TKO]) (Huh et al., 2011). In these animals, the functions of Th17 cells (CD4<sup>+</sup>ROR $\gamma$ t<sup>+</sup> cells) and other ROR $\gamma$ t-expressing  $\alpha\beta$  T-cells are inhibited, but there is no effect in ROR $\gamma$ t-expressing innate (or innate-like) immune cells, including  $\gamma\delta$ T, lymphoid tissue-inducer cells, and ILC3 (Lochner et al., 2008; Spits and Di Santo, 2011), as well as in ROR $\gamma$ -expressing nonlymphoid cells. We found that ROR $\gamma$ t TKO mothers failed to produce IL-17a even after poly(I:C) injection (Fig. S6F). Important to note, poly(I:C)-induced malformation of the cortex was prevented

in offspring from ROR $\gamma$ t TKO mothers (Figs. 4A,B), similar to anti-IL-17a treatment (Figs. 2B,D). Moreover, we found that prenatal exposure to MIA increased USV calls in pups derived from WT or ROR $\gamma$ t heterozygous (HET) mothers, but offspring of ROR $\gamma$ t TKO mothers had normal USV behavior (Fig. 4C). T-cell-specific deletion of maternal ROR $\gamma$ t also abrogated the MIA-induced social interaction deficit and excessive marble burying in offspring (Figs. 4D,E). These results were not caused by general activity defects in the offspring of WT, ROR $\gamma$ t HET, or TKO mothers (Fig. 4F). Because these offspring were derived from mating ROR $\gamma$ t WT/HET/TKO female mice with WT male mice, they all carried at least one copy of functional ROR $\gamma$ t. Therefore, the rescue of MIA-induced phenotypes observed in the offspring of ROR $\gamma$ t TKO mothers was not likely the result of lack of Th17 cells in the offspring. Taken

together, these data indicate that maternal CD4<sup>+</sup> T-lymphocytes expressing ROR $\gamma$ t (i.e., Th17 cells) are necessary for the MIA-mediated expression of cortical abnormalities and three ASD-like behaviors modeled in mouse offspring.

## IL-17a Administration to the Fetal Brain Promotes Abnormal Cortical Development and ASD-Like Behavioral Phenotypes

To determine whether IL-17a acts on receptors in the mother or the fetus to induce the MIA phenotype, we injected poly(I:C) into IL-17Ra WT, HET, or KO mothers that had been bred to IL-17Ra WT or HET males (Iwakura et al., 2011). Removing one or both copies of *il17ra* in the mother was sufficient to rescue the MIA-induced sociability deficit in offspring regardless

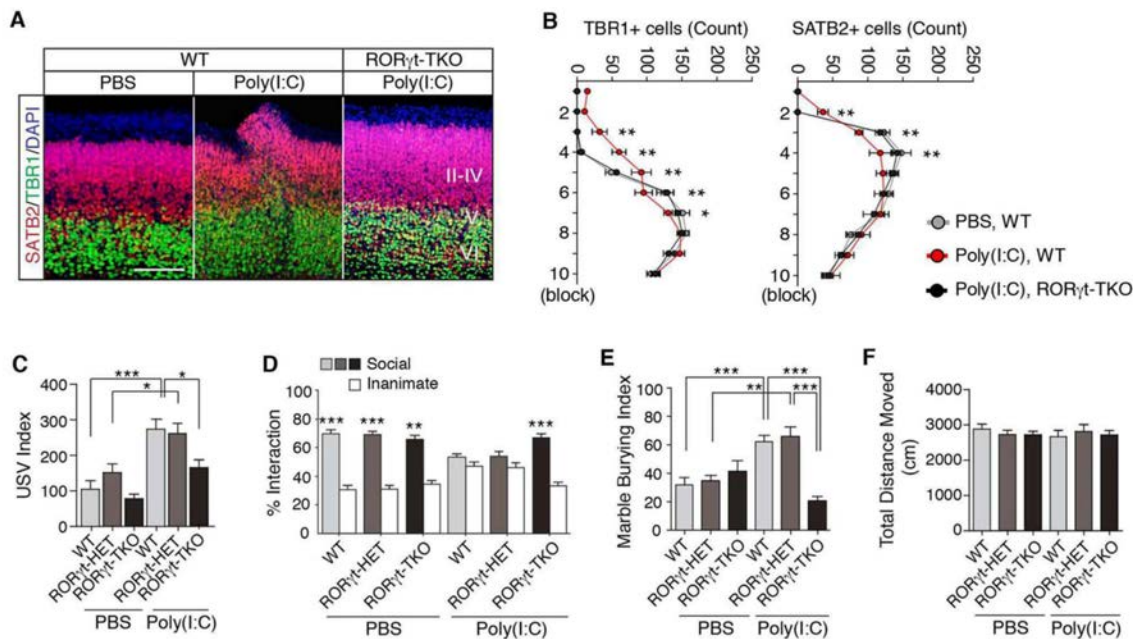


**Figure 4.** ROR $\gamma$ t expression in maternal T-cells is required for manifestation of ASD-like phenotypes in the MIA model. **A**, SATB2 and TBR1 staining in the cortex of E18.5 fetal brains following MIA induction with poly(I:C) in mothers with the indicated genotypes. II-IV, V, and VI refer to different cortical layers. Images are representative of three independent experiments. Scale bar, 100  $\mu$ m. **B**, Quantification of TBR1- and SATB2-positive cells in a 300  $\times$  300  $\mu$ m<sup>2</sup> region of interest centered on the malformation in the cortical plate of E18.5 male fetal brains ( $n = 6$  [PBS, WT],  $n = 6$  [poly(I:C), WT], and  $n = 6$  [poly(I:C), ROR $\gamma$ t-TKO]). **C**, Number of USVs emitted by P9 pups. Total USVs emitted during test period (3 min) are plotted on the y-axis ( $n = 16$ , 18, and 15 offspring from PBS-treated WT, ROR $\gamma$ t HET, and ROR $\gamma$ t TKO mothers;  $n = 15$ , 11, and 28 from poly(I:C)-treated WT, ROR $\gamma$ t HET, and ROR $\gamma$ t TKO mothers); data from 4–7 independent dams. **D**, Social approach behavior is graphed as a social preference index (% time spent investigating social or inanimate stimulus/total exploration time for both objects) ( $n = 21$ , 15, and 15 adult offspring from PBS-treated WT, ROR $\gamma$ t HET, and ROR $\gamma$ t TKO mothers;  $n = 36$ , 15, and 21 from poly(I:C)-treated WT, ROR $\gamma$ t HET, and ROR $\gamma$ t TKO mothers); data from 4–7 independent dams. **E**, Marble burying behavior is graphed as the percentage of buried marbles. ( $n = 14$ , 19, and 15 adult offspring from PBS-treated WT, ROR $\gamma$ t HET, and ROR $\gamma$ t TKO mothers;  $n = 32$ , 15, and 25 from poly(I:C)-treated WT, ROR $\gamma$ t HET, and ROR $\gamma$ t TKO mice per group); data from 4–7 independent dams. **F**, Total distance moved by offspring tested for social behavior and marble burying. ROR $\gamma$ t HET refers to ROR $\gamma$ <sup>Neo/+</sup>; CD4-Cre/+, and ROR $\gamma$ t TKO refers to ROR $\gamma$ <sup>FL/ROR $\gamma$ <sup>Neo</sup></sup>; CD4-Cre/+. **C**, One-way ANOVA with Holm–Sidak post hoc tests. **B**, **D**, Two-way ANOVA with Tukey post hoc tests. **E**, **F**, One-way ANOVA with Tukey post hoc tests. \*\*\* $p < 0.001$ , \*\* $p < 0.01$ , and \* $p < 0.05$ . Graphs show mean  $\pm$  SEM. Reprinted with permission from Choi GB et al. (2016), Figure 4. Copyright 2016, American Association for the Advancement of Science.

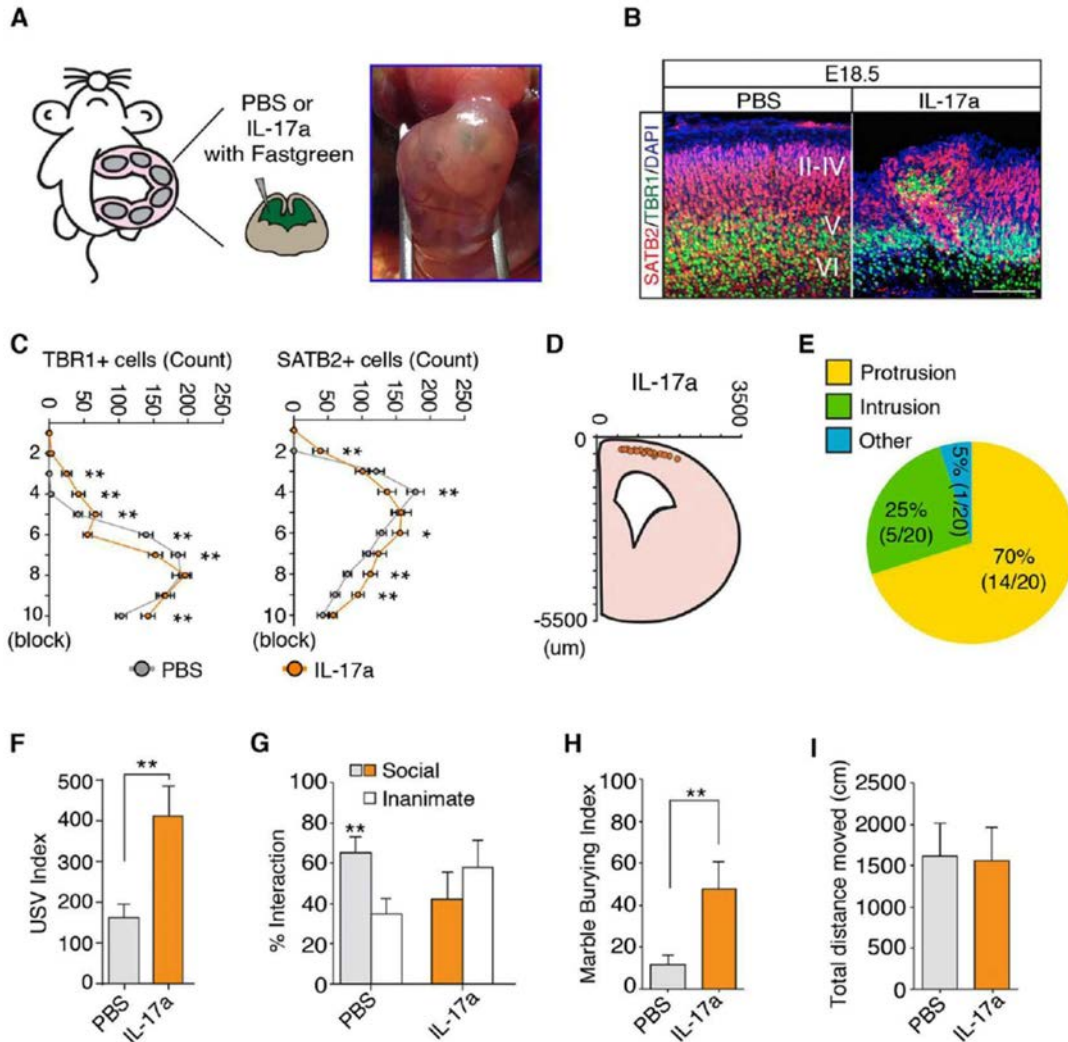


**Figure 5.** IL-17a administration to the fetus promotes abnormal cortical development and ASD-like behavioral phenotypes. **A**, Schematic diagram of the experimental method. Each embryo was injected intraventricularly at E14.5 with PBS or recombinant IL-17a protein mixed with Fastgreen dye (Sigma-Aldrich, St. Louis, MO). **B**, SATB2 and TBR1 staining in the cortex of E18.5 male fetal brains treated as in **A**. II-IV, V, and VI refer to different cortical layers. Images are representative of five independent experiments. Scale bar, 100  $\mu\text{m}$ . **C**, Quantification of TBR1- and SATB2-positive cells in a  $300 \times 300 \mu\text{m}^2$  region of interest corresponding to the region of the cortical plate containing the malformation in E18.5 male fetal brain ( $n = 20$  [PBS],  $n = 20$  [IL-17a]). **D**, The spatial location of the disorganized cortical patch in E18.5 fetal brain ( $n = 20$  [IL-17a]). **E**, Percentage of the cortical patches in each category ( $n = 20$  [IL-17a]). **F**, USV assay. The number of pup calls is plotted on the y-axis ( $n = 15$  [PBS],  $n = 17$  [IL-17a]; 5–6 independent dams per treatment). **G**, Social approach behavior. Graphed as a social preference index (% time spent investigating social or inanimate stimulus out of total object investigation time) ( $n = 12$  [PBS],  $n = 18$  [IL-17a]; 5–6 independent experiments). **H**, Marble burying behavior. Percentage of the number of buried marbles is plotted on the y-axis ( $n = 12$  [PBS],  $n = 18$  [IL-17a]; 5–6 independent experiments). **I**, Total distance traveled during social approach test. **C**, Two-way ANOVA with Tukey *post hoc* tests. **F**, **H**, **I**, Student's *t*-tests. **G**, One-way ANOVA with Tukey *post hoc* test.  $**p < 0.01$ ,  $*p < 0.05$ . Graphs show mean  $\pm$  SEM. Reprinted with permission from Choi GB et al. (2016), Figure 5. Copyright 2016, American Association for the Advancement of Science.

of their genotypes (Fig. S8A). Moreover, we found that reduced expression of maternal IL-17Ra in *il17ra* HET mothers led to reduced serum IL-17a in poly(I:C)-treated mothers (Fig. S8B). Thus, it is difficult, if not impossible, to test the functional significance of the IL-17Ra in offspring with a full germline *il17ra* KO without affecting maternal Th17 cell activity.

To circumvent this problem, we asked whether increasing IL-17Ra activity in the offspring, by introducing IL-17a directly into the fetal brain in the absence of maternal inflammation, would be sufficient to induce MIA phenotypes. Injection of recombinant IL-17a protein into the ventricles of the fetal brain at E14.5 in the absence of MIA (Fig. 5A) led to the

appearance of disorganized cortical patches in a similar location to those induced by MIA (Figs. 5B–E). Unlike poly(I:C) injection, however, intraventricular injection of IL-17a resulted in thinned cortical plates at the medial but not lateral part of the brain (Fig. S9). This effect may reflect differences in the levels or types of inflammation associated with poly(I:C) versus IL-17a injections or the time points at which poly(I:C) (E12.5) and IL-17a (E14.5) were administered. We also found that, compared with sham injection, IL-17a injections led to an enhanced USV phenotype, social approach deficit, and increased marble burying behavior all similar in magnitude to those observed in MIA-exposed offspring (Figs. 5F–H). These behavioral abnormalities did not derive from group differences in mobility (Fig. 5I). Significantly, neither cortical disorganization nor enhanced USV phenotypes were observed following IL-17a injections into the ventricles of IL-17Ra KO fetuses or upon IL-6 injections into WT fetal brains (Figs. S10A–C), suggesting that IL-17a, but not IL-6, acts directly in the fetal brain to induce these phenotypes. Of note, in agreement with previous reports (Smith et al., 2007; Hsiao and Patterson, 2011), IL-6 injection into

pregnant WT mothers was sufficient to produce MIA-associated behavioral (enhanced USV) and cortical phenotypes in the offspring (Figs. S10D–F). Important to note, pretreatment of pregnant mothers with anti-IL-17a–blocking antibody prevented the phenotypes induced by maternal IL-6 injection (Figs. S10D–F). Lastly, IL-17a injection into brains of fetuses from poly(I:C)–injected IL-6 KO mothers was sufficient to elicit increased pup USVs compared with PBS-injected controls (Fig. S10G). These data collectively demonstrate that activation of the IL-17Ra pathway in the fetal brain, induced by intraventricular injection of IL-17a into the fetus or by intraperitoneal injection of poly(I:C) or IL-6 into pregnant mothers, results in MIA-associated phenotypes in the offspring.

### Therapeutic Treatment with Anti-IL-17a Blocking Antibody in Pregnant Dams Ameliorates MIA-Associated Behavioral Abnormalities

Our results suggest that pathological activation of the Th17 cell/IL-17 pathway during gestation in mothers

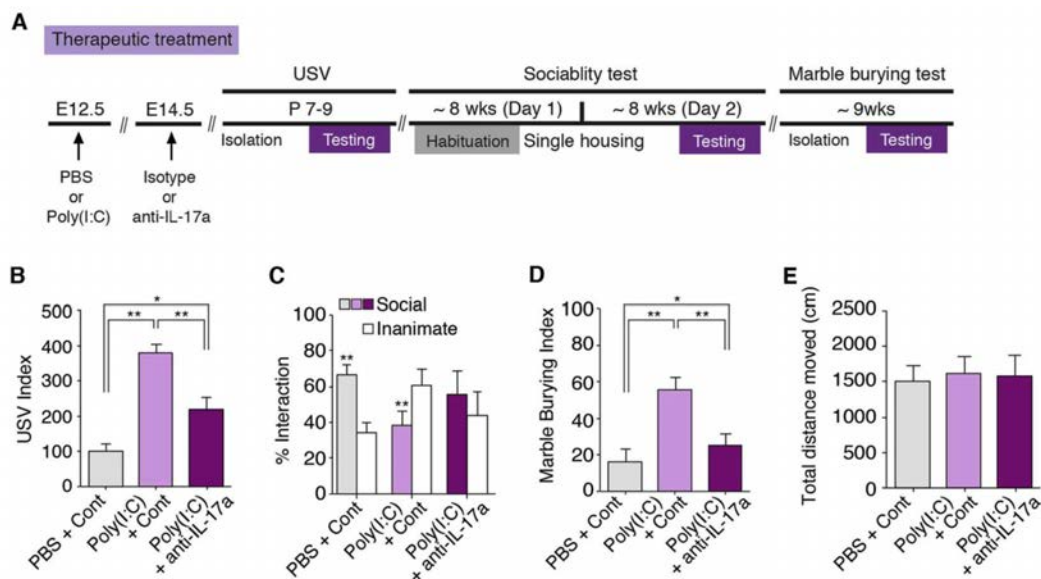


**Figure 6.** Therapeutic effects of blocking IL-17a signaling in pregnant dams. **A**, Schematic diagram of the experimental design. At E12.5, pregnant mothers were injected with PBS or poly(I:C) to induce MIA. Two days later (E14.5), the pregnant mothers were treated with IgG isotype or anti-IL-17a–blocking antibodies. At P7–P9, pups were separated from the mothers to measure USV calls. At ~8 weeks, male offspring were subjected to the social approach test and marble burying test. **B**, USV assay. The number of pup calls is plotted on the y-axis ( $n = 17$  [PBS + Cont],  $n = 17$  [poly(I:C) + Cont], and  $n = 27$  [poly(I:C) + anti-IL-17a]; 3–4 independent dams per treatment). **C**, Social approach behavior. Graphed as a social preference index (% time spent investigating social or inanimate stimulus out of total object investigation time) ( $n = 12$  [PBS + Cont],  $n = 10$  [poly(I:C) + Cont],  $n = 17$  [poly(I:C) + anti-IL-17a]; 3–4 independent dams per treatment). **D**, Marble burying behavior. Percentage of the number of buried marbles is plotted on the y-axis ( $n = 12$  [PBS + Cont],  $n = 10$  [poly(I:C) + Cont],  $n = 17$  [poly(I:C) + anti-IL-17a]; 3–4 independent dams per treatment). **E**, Total distance traveled during social approach behavior. **B**, **D**, **E**, One-way ANOVA with Tukey *post hoc* tests. **C**, Two-way ANOVA with Tukey *post hoc* test. \*\* $p < 0.01$  and \* $p < 0.05$ . Graphs show mean  $\pm$  SEM. Reprinted with permission from Choi GB et al. (2016), Figure 6. Copyright 2016, American Association for the Advancement of Science.

with some inflammatory conditions may alter fetal brain development and contribute to the ASD-like behavioral phenotypes in offspring (Fig. S11). Th17 cells require ROR $\gamma$ t for their differentiation and exert their functions by secreting multiple cytokines, including IL-17a. Abrogation of ROR $\gamma$ t expression in maternal  $\alpha\beta$  T-cells or blockade of the IL-17 pathway in pregnant dams resulted in the complete rescue of cortical developmental abnormalities and ASD-like behavioral phenotypes in offspring in the MIA rodent model. Thus, ROR $\gamma$ t and Th17 cells (as well as their cytokines) may serve as good therapeutic targets to prevent the development of ASD phenotypes in the children of susceptible mothers.

To further test this idea, we administered anti-IL-17a antibody to pregnant mice in a time window following MIA induction (Fig. 6). We injected pregnant mothers with PBS or poly(I:C) at E12.5, followed by injection of IgG isotype control or anti-IL-17a–blocking antibody at E14.5 (Fig. 6A), when the delayed expression of SAbT2 manifests in MIA-exposed fetal brains (Figs. 2A,C). Compared with PBS injection followed by control antibody treatment, poly(I:C) injection followed by anti-IL-17a antibody administration partially rescued USV and marble burying phenotypes (Figs. 6B,D). However, MIA-induced social interaction deficits were not corrected (Fig. 6C). As with the other experimental results reported here, these effects were not caused by group differences in mobility (Fig. 6E). Thus, treating pregnant mothers with anti-IL-17a after MIA can correct some of the ASD-like features, but pretreatment with anti-IL-17a antibody may have greater therapeutic potential.

## Conclusions

Our results identify a specific maternal immune cell population that may have direct roles in inducing ASD-like phenotypes by acting on the developing fetal brain. These findings raise the possibility that modulating the activity of a cytokine receptor, IL-17Ra, in the CNS can influence neuronal development, with implications as to specification of neuronal cell types and their connectivity. Further, it is worthwhile to note that the loss of certain genes, including *Wdfy3* and *Cntnap2*, that induce ASD-like phenotypes were also found with defects in cortical lamination (Penagarikano et al., 2011; Orosco et al., 2014). These observations raise the possibility that some genetic and environmental factors that have roles in the etiology of ASD function by way of similar physiological pathways. A related question is whether IL-17Ra signaling has a

normal physiological function in the fetal and adult brain, especially given the structural similarities observed between the IL-17 family cytokines and neurotrophin proteins (e.g., NGF) (Hymowitz et al., 2001; Zhang et al., 2011). Elucidating further downstream pathways of maternal IL-17a-producing T-cells in both MIA mothers and their offspring will likely yield a better understanding of the mechanisms by which inflammation *in utero* contributes to the development of neurodevelopmental disorders such as ASD. These pathways also may provide insights into the roles of cytokine receptors in the CNS.

## Acknowledgments

This chapter is a modified version of a previously published article: Choi, et al. (2016) The maternal interleukin-17a pathway in mice promotes autism-like phenotypes in offspring. *Science* 351:933–939. Copyright 2016, American Association for the Advancement of Science. G.B.C., Y.S.Y., and H.W. contributed equally to this work. Supplementary materials, including figures and references, are available at <https://www.ncbi.nlm.nih.gov/pmc/articles/PMC4782964>.

## References

- Al-Ayadhi LY, Mostafa GA (2012) Elevated serum levels of interleukin-17A in children with autism. *J Neuroinflammation* 9:158.
- Alcamo EA, Chirivella L, Dautzenberg M, Dobreva G, Fariñas I, Grosschedl R, McConnell SK (2008) *Satb2* regulates callosal projection neuron identity in the developing cerebral cortex. *Neuron* 57:364–377.
- Ashwood P, Wills S, Van de Water J (2006) The immune response in autism: a new frontier for autism research. *J Leukoc Biol* 80:1–15.
- Atladóttir HO, Pedersen MG, Thorsen P, Mortensen PB, Deleuran B, Eaton WW, Parner ET (2009) Association of family history of autoimmune diseases and autism spectrum disorders. *Pediatrics* 124:687–694.
- Atladóttir HO, Thorsen P, Østergaard L, Schendel DE, Lemcke S, Abdallah M, Parner ET (2010) Maternal infection requiring hospitalization during pregnancy and autism spectrum disorders. *J Autism Dev Disord* 40:1423–1430.
- Brown AS, Sourander A, Hinkka-Yli-Salomäki S, McKeague IW, Sundvall J, Surcel HM (2014) Elevated maternal C-reactive protein and autism in a national birth cohort. *Mol Psychiatry* 19:259–264.

- Casanova MF, El-Baz AS, Kamat SS, Dombroski BA, Khalifa F, Elnakib A, Soliman A, Allison-McNutt A, Switala AE (2013) Focal cortical dysplasias in autism spectrum disorders. *Acta Neuropathol Commun* 1:67.
- Choi GB, Yim YS, Wong H, Kim S, Kim H, Kim SV, Hoeffler CA, Littman DR, Huh JR (2016) The maternal interleukin-17a pathway in mice promotes autism-like phenotypes in offspring. *Science* 351:933–939.
- De Miranda J, Yaddanapudi K, Hornig M, Villar G, Serge R, Lipkin WI (2010) Induction of toll-like receptor 3-mediated immunity during gestation inhibits cortical neurogenesis and causes behavioral disturbances. *MBio* 1: e00176-10.
- Dehay C, Kennedy H (2007) Cell-cycle control and cortical development. *Nat Rev Neurosci* 8:438–450.
- Eberl G, Littman DR (2004) Thymic origin of intestinal alphabeta T cells revealed by fate mapping of RORgamma<sup>+</sup> cells. *Science* 305:248–251.
- Englund C, Fink A, Lau C, Pham D, Daza RA, Bulfone A, Kowalczyk T, Hevner RF (2005) Pax6, Tbr2, and Tbr1 are expressed sequentially by radial glia, intermediate progenitor cells, and postmitotic neurons in developing neocortex. *J Neurosci* 25:247–251.
- Hoeffler CA, Tang W, Wong H, Santillan A, Patterson RJ, Martinez LA, Tejada-Simon MV, Paylor R, Hamilton SL, Klann E (2008) Removal of FKBP12 enhances mTOR–Raptor interactions, LTP, memory, and perseverative/repetitive behavior. *Neuron* 60:832–845.
- Hsiao EY, Patterson PH (2011) Activation of the maternal immune system induces endocrine changes in the placenta via IL-6. *Brain Behav Immun* 25:604–615.
- Hsiao EY, McBride SW, Chow J, Mazmanian SK, Patterson PH (2012) Modeling an autism risk factor in mice leads to permanent immune dysregulation. *Proc Natl Acad Sci USA* 109:12776–12781.
- Hsiao EY, McBride SW, Hsien S, Sharon G, Hyde ER, McCue T, Codelli JA, Chow J, Reisman SE, Petrosino JF, Patterson PH, Mazmanian SK (2013) Microbiota modulate behavioral and physiological abnormalities associated with neurodevelopmental disorders. *Cell* 155:1451–1463.
- Huh JR, Leung MW, Huang P, Ryan DA, Krout MR, Malapaka RR, Chow J, Manel N, Ciofani M, Kim SV, Cuesta A, Santori FR, Lafaille JJ, Xu HE, Gin DY, Rastinejad F, Littman DR (2011) Digoxin and its derivatives suppress TH17 cell differentiation by antagonizing ROR $\gamma$ t activity. *Nature* 472:486–490.
- Hymowitz SG, Filvaroff EH, Yin JP, Lee J, Cai L, Risser P, Maruoka M, Mao W, Foster J, Kelley RF, Pan G, Gurney AL, de Vos AM, Starovasnik MA (2001) IL-17s adopt a cystine knot fold: structure and activity of a novel cytokine, IL-17F, and implications for receptor binding. *EMBO J* 20:5332–5341.
- Ivanov I, McKenzie B, Zhou L, Tadokoro C, Lepelley A, Lafaille J, Cua D, Littman D (2006) The orphan nuclear receptor ROR $\gamma$ t directs the differentiation program of proinflammatory IL-17<sup>+</sup> T helper cells. *Cell* 126:1121–1133.
- Iwakura Y, Ishigame H, Saijo S, Nakae S (2011) Functional specialization of interleukin-17 family members. *Immunity* 34:149–162.
- Kuchroo VK, Awasthi A (2012) Emerging new roles of Th17 cells. *Eur J Immunol* 42:2211–2214.
- Lee BK, Magnusson C, Gardner RM, Blomström A, Newschaffer CJ, Burstyn I, Karlsson H, Dalman C (2015) Maternal hospitalization with infection during pregnancy and risk of autism spectrum disorders. *Brain Behav Immun* 44:100–105.
- Leid M, Ishmael JE, Avram D, Shepherd D, Fraulob V, Dollé P (2004) CTIP1 and CTIP2 are differentially expressed during mouse embryogenesis. *Gene Expr Patterns* 4:733–739.
- Lochner M, Peduto L, Cherrier M, Sawa S, Langa F, Varona R, Riethmacher D, Si-Tahar M, Di Santo JP, Eberl G (2008) *In vivo* equilibrium of proinflammatory IL-17<sup>+</sup> and regulatory IL-10<sup>+</sup> Foxp3<sup>+</sup> RORgamma<sup>+</sup> T cells. *J Exp Med* 205:1381–1393.
- Malkova NV, Yu CZ, Hsiao EY, Moore MJ, Patterson PH (2012) Maternal immune activation yields offspring displaying mouse versions of the three core symptoms of autism. *Brain Behav Immun* 26:607–616.
- Mandal M, Marzouk AC, Donnelly R, Ponzio NM (2010) Preferential development of Th17 cells in offspring of immunostimulated pregnant mice. *J Reprod Immunol* 87:97–100.
- Manel N, Unutmaz D, Littman DR (2008) The differentiation of human T(H)-17 cells requires transforming growth factor-beta and induction of the nuclear receptor RORgamma<sup>+</sup>. *Nat Immunol* 9:641–649.
- Martínez-García EA, Chávez-Robles B, Sánchez-Hernández PE, Núñez-Atahualpa L, Martín-Máquez BT, Muñoz-Gómez A, González-López L, Gámez-Nava JI, Salazar-Páramo M, Dávalos-Rodríguez I, Petri MH, Zúñiga-Tamayo D, Vargas-Ramírez R, Vázquez-Del Mercado M (2011) IL-17 increased in the third trimester in healthy women with term labor. *Am J Reprod Immunol* 65:99–103.

- Molyneaux BJ, Arlotta P, Menezes JR, Macklis JD (2007) Neuronal subtype specification in the cerebral cortex. *Nat Rev Neurosci* 8:427–437.
- Nakashima A, Ito M, Yoneda S, Shiozaki A, Hidaka T, Saito S (2010) Circulating and decidual Th17 cell levels in healthy pregnancy. *Am J Reprod Immunol* 63:104–109.
- Orosco LA, Ross AP, Cates SL, Scott SE, Wu D, Sohn J, Pleasure D, Pleasure SJ, Adamopoulos IE, Zarbalis KS (2014) Loss of *Wdfy3* in mice alters cerebral cortical neurogenesis reflecting aspects of the autism pathology. *Nat Commun* 5:4692.
- Patterson PH (2009) Immune involvement in schizophrenia and autism: etiology, pathology and animal models. *Behav Brain Res* 204:313–321.
- Peñagarikano O, Abrahams BS, Herman EI, Winden KD, Gdalyahu A, Dong H, Sonnenblick LI, Gruver R, Almajano J, Bragin A, Golshani P, Trachtenberg JT, Peles E, Geschwind DH (2011) Absence of *CNTNAP2* leads to epilepsy, neuronal migration abnormalities, and core autism-related deficits. *Cell* 147:235–246.
- Schwartz JJ, Careaga M, Onore CE, Rushakoff JA, Berman RF, Ashwood P (2013) Maternal immune activation and strain specific interactions in the development of autism-like behaviors in mice. *Transl Psychiatry* 3:e240.
- Smith SE, Elliott RM, Anderson MP (2012) Maternal immune activation increases neonatal mouse cortex thickness and cell density. *J Neuroimmune Pharmacol* 7:529–532.
- Smith SEP, Li J, Garbett K, Mirmics K, Patterson PH (2007) Maternal immune activation alters fetal brain development through interleukin-6. *J Neurosci* 27:10695–10702.
- Spits H, Di Santo JP (2011) The expanding family of innate lymphoid cells: regulators and effectors of immunity and tissue remodeling. *Nat Immunol* 12:21–27.
- Stoner R, Chow ML, Boyle MP, Sunkin SM, Mouton PR, Roy S, Wynshaw-Boris A, Colamarino SA, Lein ES, Courchesne E (2014) Patches of disorganization in the neocortex of children with autism. *N Engl J Med* 370:1209–1219.
- Sun Z, Unutmaz D, Zou YR, Sunshine MJ, Pierani A, Brenner-Morton S, Mebius RE, Littman DR (2000) Requirement for *ROR $\gamma$*  in thymocyte survival and lymphoid organ development. *Science* 288:2369–2373.
- Suzuki K, Matsuzaki H, Iwata K, Kamenoy Y, Shimmura C, Kawai S, Yoshihara Y, Wakuda T, Takebayashi K, Takagai S, Matsumoto K, Tsuchiya KJ, Iwata Y, Nakamura K, Tsujii M, Sugiyama T, Mori N (2011) Plasma cytokine profiles in subjects with high-functioning autism spectrum disorders. *PLoS One* 6:e20470.
- van der Zwaag B, Franke L, Poot M, Hochstenbach R, Spierenburg HA, Vorstman JA, van Daalen E, de Jonge MV, Verbeek NE, Brilstra EH, van 't Slot R, Ophoff RA, van Es MA, Blauw HM, Veldink JH, Buizer-Voskamp JE, Beemer FA, van den Berg LH, Wijmenga C, van Amstel HK, et al. (2009) Gene-network analysis identifies susceptibility genes related to glycobiology in autism. *PLoS One* 4:e5324.
- Wilke CM, Bishop K, Fox D, Zou W (2011) Deciphering the role of Th17 cells in human disease. *Trends Immunol* 32:603–611.
- Wu HX, Jin LP, Xu B, Liang SS, Li DJ (2014) Decidual stromal cells recruit Th17 cells into decidua to promote proliferation and invasion of human trophoblast cells by secreting IL-17. *Cell Mol Immunol* 11:253–262.
- Yee N, Schwarting RK, Fuchs E, Wöhr M (2012) Increased affective ultrasonic communication during fear learning in adult male rats exposed to maternal immune activation. *J Psychiatr Res* 46:1199–1205.
- Zhang X, Angkasekwinai P, Dong C, Tang H (2011) Structure and function of interleukin-17 family cytokines. *Protein Cell* 2:26–40.

# ***TREM2* Variants: New Keys to Decipher Alzheimer's Disease Pathogenesis**

Marco Colonna, MD,<sup>1</sup> and Yaming Wang, PhD<sup>1,2</sup>

---

<sup>1</sup>Department of Pathology and Immunology  
Washington University School of Medicine  
St. Louis, Missouri

<sup>2</sup>Eli Lilly and Company, Lilly Corporate Center  
Indianapolis, Indiana

## Introduction

Triggering receptor expressed on myeloid cells 2 (TREM2) is a cell surface receptor of the Ig superfamily that is expressed on microglia in the CNS. Recent genetic studies (Benitez et al., 2013; Bertram et al., 2013; Guerreiro et al., 2013a; Jonsson et al., 2013; Reitz et al. 2013; Ruiz et al., 2014; Slattery et al., 2014) have identified a rare variant of TREM2 that is a risk factor for nonfamilial Alzheimer's disease (AD), the most common form of late-onset dementia. Moreover, TREM2 deficiency has been shown to alter microglial function in mouse models of AD (Ulrich et al., 2014; Jay et al., 2015; Wang et al., 2015). Here we review recent progress in our understanding of how TREM2 may control the microglial response to AD lesions and its impact on microglial senescence, as well as the interaction of TREM2 with other molecules encoded by gene variants associated with AD and the hypothetical consequences of its cleavage from the cell surface.

## TREM2 Expression and Signaling

TREM2 is a transmembrane receptor that belongs to the TREM family of proteins, which are encoded by genes clustered on human chromosome 6p21.1 and mouse chromosome 17 (Klesney-Tait et al., 2006; Ford and McVicar, 2009). TREM2 is found in various tissue macrophages, such as CNS microglia (Paloneva et al., 2002; Schmid et al., 2002); bone osteoclasts (Cella et al., 2003; Paloneva et al., 2003; Humphrey et al., 2006); and alveolar (Wu et al., 2015), peritoneal (Turnbull IR et al., 2006) and intestinal (Seno et al., 2009) macrophages. TREM2 is also present on cultured bone-marrow-derived macrophages (Daws et al., 2001) and monocyte-derived dendritic cells (Bouchon et al., 2001). Its expression *in vitro* is induced by macrophage colony-stimulating factor 1 (CSF-1), granulocyte-macrophage colony-stimulating factor (GM-CSF, also known as CSF-2), and interleukin-4 (IL-4) and is inhibited by toll-like receptors (TLRs) (Cella et al., 2003; Turnbull IR et al., 2006; Ji et al., 2009). *Trem2* transcription is also regulated by retinoid X receptors (RXRs) in mouse macrophages (Daniel et al., 2014). Accordingly, treatment of mice with the RXR agonist bexarotene augmented the cortical expression of *Trem2* mRNA in an AD mouse model (Lefterov et al., 2015).

The extracellular region of TREM2 contains a single Ig superfamily domain and binds polyanionic ligands, such as bacterial lipopolysaccharides (LPS) and phospholipids (Fig. 1) (Cannon et al., 2012; Poliani et al., 2015; Wang et al., 2015; Daws et al., 2016). Upon ligand binding, TREM2 transmits

intracellular signals through an adaptor, DAP12 (also known as TYRO protein tyrosine kinase-binding protein [TYROBP]), which is associated with the transmembrane region of TREM2 and recruits the protein tyrosine kinase SYK through its cytosolic immunoreceptor tyrosine-based activation motifs (ITAMs) (Fig. 1). SYK initiates a cascade of signaling events including protein tyrosine phosphorylation, phosphoinositide 3-kinase (PI3K) activation, Ca<sup>2+</sup> mobilization, and mitogen-activated protein kinase (MAPK) activation (Fig. 1). TREM2 also signals through DAP10 (also known as hematopoietic cell signal transducer), a DAP12-related adaptor that recruits PI3K (Peng et al., 2010) (Fig. 1). Together, these signals promote survival (Otero et al., 2012; Wang et al., 2015), proliferation (Otero et al., 2012), phagocytosis (Takahashi et al., 2005), and secretion of cytokines and chemokines (Bouchon et al., 2001). TREM2-induced signals also augment the activation of integrins that induce remodeling of the actin cytoskeleton, which controls adhesion and migration (Takahashi et al., 2005; Melchior et al., 2010; Forabosco et al., 2013). However, TREM2-induced signals interfere with the function of TLRs and hence curtail macrophage inflammatory responses to various TLR ligands, such as LPS, lipoteichoic acid, and unmethylated CpG oligodeoxyribonucleotides (Hamerman et al., 2006; Turnbull IR et al., 2006). Thus, TREM2 can perform both activating and inhibitory functions in tissue macrophages.

## Linking TREM2 and Dementia

Inactivating mutations of TREM2 were initially discovered in patients with a very rare form of autosomal recessive, inherited, early-onset dementia called Nasu-Hakola disease (NHD) (Paloneva et al., 2002; Klünemann et al., 2005). This disease causes brain and bone pathology consisting of sclerosing leukoencephalopathy and polycystic osteodysplasia, respectively (Paloneva et al., 2001). Based on these genetic studies and the observation that TREM2 is expressed in microglia and osteoclasts, it became apparent that these cells require TREM2 to perform their functions in the CNS and bone. More recently, Genome-wide association studies (GWAS) identified a low-frequency variant of *TREM2* as a genetic risk for nonfamilial AD. This variant, which results in an arginine-47-histidine (R47H) substitution in the extracellular Ig domain, significantly increased the risk for AD in two large cohorts of patients, a finding that was confirmed in other cohorts (Benitez et al., 2013; Bertram et al., 2013; Guerreiro et al., 2013a; Jonsson et al., 2013; Reitz et al. 2013; Ruiz et al., 2014; Slattery et al., 2014).

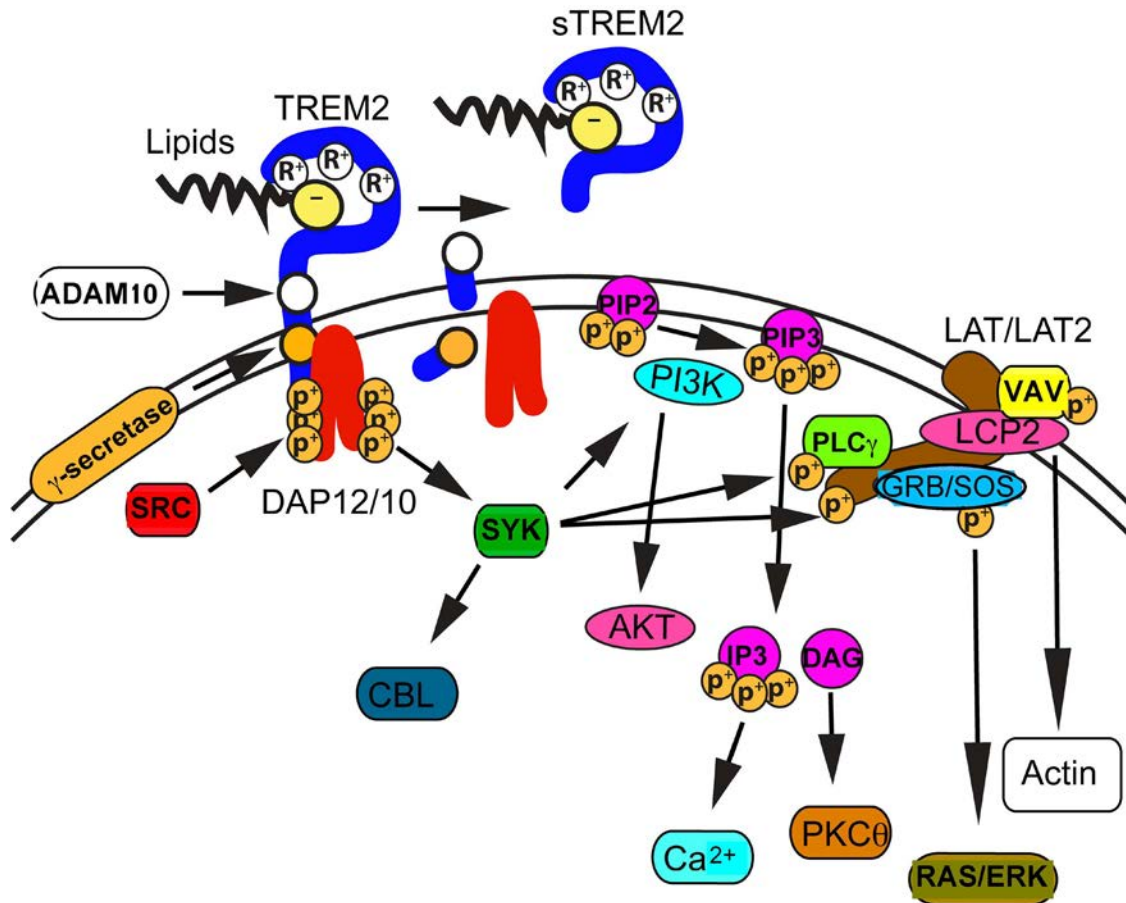


**Figure 1.** TREM2 signaling pathways. TREM2 binds negatively charged lipid ligands, most likely through the positively charged arginine residues ( $R^+$ ) present in its extracellular domain. During ligand binding, the TREM2-associated adapter DAP12 is tyrosine phosphorylated by the protein kinase SRC and recruits the tyrosine-protein kinase SYK. SYK phosphorylates the adapters LAT (linker for activation of T-cells family member 1) and LAT2, which in turn recruit various signaling mediators and adapters, including phospholipase  $C\gamma$  ( $PLC\gamma$ , which degrades phosphatidylinositol 3,4,5 trisphosphate [PIP3] into inositol trisphosphate [IP3] and diacylglycerol [DAG]); lymphocyte cytosolic protein 2 (LCP2, also known as SLP76); the proto-oncogene *vav* (VAV1); and growth factor receptor-bound protein 1 (GRB2) and/or son of sevenless homolog 2 (SOS2). Ultimately, these pathways lead to  $Ca^{2+}$  mobilization, activation of  $PKC\theta$ , activation of the RAS/ERK pathway, and actin remodeling. SYK also activates the phosphoinositide 3-kinase (PI3K)–AKT pathway as well as the E3 ubiquitin-protein ligase CBL, which negatively regulates the TREM2 pathway. TREM2 also associates with DAP10, which recruits and activates PI3K. TREM2 can be cleaved from the cell surface by ADAM10 and  $\gamma$ -secretase, thereby releasing sTREM2. Modified with permission from Colonna M and Wang Y (2016), Figure 1. Copyright 2016, Nature Publishing Group

The identification of TREM2 as a potential key molecule in AD pathogenesis was surprising, given the notable differences between NHD and AD. NHD is a rare form of early-onset dementia, whereas nonfamilial AD is the most common form of late-onset dementia (Holtzman et al., 2011). The pathological features of AD are also quite different from those of NHD: Whereas NHD consists of massive demyelination of the white matter of the frontal lobes (Paloneva et al., 2001), nonfamilial AD is characterized by the deposition of  $A\beta$  peptide

and hyperphosphorylated tau aggregates in the gray matter, which are associated with neuronal cell death as well as activation of microglia and astrocytes (Holtzman et al., 2011). Although rare forms of autosomal dominant, inherited AD result from mutations in proteins involved in the  $A\beta$  processing pathway, such as amyloid precursor protein (APP) and presenilin 1 (PS1), the origin of nonfamilial AD is less well understood and may depend on a combination of genetic and nongenetic risk factors (Tanzi, 2012).

The identification of a *TREM2* variant as a risk factor for AD supported the long-standing hypothesis that altered microglial function might significantly contribute to the pathogenesis of this disorder (Heneka et al., 2015; Meyer-Luehmann et al., 2015; Ransohoff and El Khoury, 2015). This hypothesis has also been corroborated by GWAS that have identified rare variants of other genes encoding immune receptors expressed by microglia as risk factors for AD. These include the inhibitory receptor myeloid cell surface antigen CD33 (CD33) (Bertram et al., 2008; Hollingworth et al., 2011; Naj et al., 2011; Bradshaw et al., 2013; Griciuc et al., 2013); the complement component (3b/4b) receptor 1 (CR1) (Lambert et al., 2009); the complement regulatory protein clusterin (Harold et al., 2009; Lambert et al., 2009); and the alternative activated macrophage marker MS4A4A (Hollingworth et al., 2011; Naj et al., 2011) (Table 1). Moreover, an integrated system approach has pinpointed immune-related gene networks as key regulators in AD. In particular, the role of *TREM2*, along with its associated adapter DAP12 and downstream signaling pathway, was highlighted (Zhang et al., 2013).

The identification of the R47H variant associated with AD has prompted extensive analyses of *TREM2* polymorphisms in the human population, leading to the identification of less frequent variants, such as the aspartic acid-87-asparagine (D87N) substitution (rs142232675 in Table 1) (Guerreiro et al., 2013).

Variants of genes encoding other TREM family receptors, such as Trem-like transcript protein 2 (TREM2) (Benitez et al., 2014) and TREM1 (Replogle et al., 2015), have also been found to be associated with protection or susceptibility to AD, respectively, independent of their genetic linkage with *TREM2* (Table 1). Although some variants were found in the exons encoding the extracellular portion of TREM receptors, others were found in intronic regions that may control gene expression and/or splicing. For example, a *TREM1* risk allele was associated with a reduced ratio of *TREM1*:*TREM2* expression (Chan et al., 2015). Further studies will be important to confirm these associations in various cohorts, determine the impact of these variants on TREM receptor expression and/or function, and assess their pathogenicity.

## TREM2 Function During AD

### Regulating microglial responses to A $\beta$ plaques

Beyond GWAS, the mechanistic link between *TREM2* variants, microglial dysfunction, and neurodegeneration has remained elusive. An initial study investigated the function of *TREM2* in microglia using overexpression and silencing approaches. In this *in vitro* study, microglia overexpressing *TREM2* were more efficient in removing apoptotic neurons through phagocytosis, whereas silencing of *TREM2* impaired this function (Takahashi et al., 2005). Thus, *TREM2*

**Table 1. Genetic association of innate immune genes with AD.**

SNP number	Locus	Odds ratio	Functional impact on the protein	Susceptibility to AD	References
rs75932628	TREM2	4.5, 4.66	Loss of function	Increased	Guerreiro et al., 2013; Jonsson et al., 2013; Kleinberger et al., 2014; Wang et al., 2015
rs142232675	TREM2	NA	ND	Increased	Guerreiro et al., 2013; Jonsson et al.
rs3826656	CD33	NA	ND	Increased	Bertram et al., 2008
rs3865444 <sup>T</sup>	CD33	0.89, 0.91	Reduced expression	Decreased	Hollingworth et al., 2011; Naj et al., 2011; Griciuc et al., 2013
rs3865444 <sup>C</sup>	CD33	NA	Increase expression	Increased	Bradshaw et al., 2013; Hollingworth et al., 2011; Naj et al., 2011
rs6701713	CR1	1.16	ND	Increased	Lambert et al., 2009
rs6656401	CR1	1.21	ND	Increased	Lambert et al., 2009
rs3747742	TREM2	0.89	ND	Decreased	Benitez et al., 2014
rs6910730	TREM1	NA	Reduced expression	Increased	Replogle et al., 2015

NA, not applicable; ND, not determined; SNP, single nucleotide polymorphism.

Modified with permission from Colonna M and Wang Y (2016), Copyright 2016, Nature Publishing Group.

was proposed to be a phagocytic receptor. This view was supported by studies showing that TREM2 contributes to macrophage phagocytosis of bacteria (N'Diaye et al., 2009) and that overexpression of TREM2 in a microglia cell line increases its capacity to phagocytose A $\beta$  (Melchior et al., 2009; Jiang et al., 2014). TREM2 was also found to curb myeloid cell secretion of pro-inflammatory cytokines (Takahashi et al., 2005; Hamerman et al., 2006; Turnbull et al., 2006). Thus, it was initially hypothesized that TREM2 might protect from neurodegeneration by promoting phagocytosis and clearance of apoptotic neurons while controlling detrimental inflammation (Fig. 2).

Recent studies analyzed the impact of TREM2 deficiency or haploinsufficiency on the microglial response to A $\beta$  deposition in two mouse models of AD: *APP/PS1-21* and *5XFAD* mice. These mice carry three or five mutations, respectively, in human transgenes encoding proteins involved in the A $\beta$  processing pathway, including APP PS1 (Ulrich et al., 2014; Jay et al., 2015; Wang et al., 2015). All studies found that A $\beta$  deposition induced robust microgliosis in TREM2-sufficient mice: that is, there was activation and accumulation of microglia around A $\beta$  plaques. In contrast, microglia failed to cluster around A $\beta$  plaques in TREM2-deficient or haploinsufficient mice, indicating a defective response to A $\beta$  accumulation. Moreover, gene expression analyses of microglia demonstrated that TREM2 deficiency reduced the expression of genes associated with microglial activation in response to A $\beta$  deposits, including phagocytic receptors, costimulatory molecules, inflammatory cytokines, and trophic factors (Ulrich et al., 2014; Jay et al., 2015; Wang et al., 2015). These results indicate that TREM2 promotes a broad array of microglial functions in response to A $\beta$  deposition, rather than just phagocytosis.

### Impact of TREM2 deficiency on A $\beta$ accumulation

Although the results from all the mouse studies described above demonstrated the importance of TREM2 in microgliosis, their findings on the impact of TREM2 deficiency on A $\beta$  accumulation were contradictory, which led to disparate interpretations of the mechanisms through which TREM2 deficiency impacts A $\beta$ -reactive microgliosis.

In the *5XFAD* model, TREM2-deficient microglia did not become activated or proliferate in response to A $\beta$  deposition, but rather underwent apoptosis (Wang et al., 2015). This defect resulted in A $\beta$  accumulation

at 8 months of age. A partial increase in A $\beta$ 1-40 and A $\beta$ 1-42 deposition was also evident in TREM2 haploinsufficient *5XFAD* mice. Moreover, this study found that TREM2 binds anionic and zwitterionic phospholipids that may become exposed during A $\beta$  accumulation owing to neuronal and glial apoptosis, myelin degradation, and the formation of aggregates between A $\beta$  and phospholipids. In contrast, microglia expressing the R47H variant of TREM2 associated with AD had a reduced capacity to bind phospholipids (Wang et al., 2015). The model that emerged from this study is that TREM2 senses changes in the lipid microenvironment that result from A $\beta$  accumulation and neuronal degeneration, and this response triggers signals that activate microglial capacity to limit A $\beta$  accumulation (Fig. 2). Consistent with this model, virally induced overexpression of TREM2 ameliorated neuropathology and rescued cognitive impairment in another mouse model of AD (Jiang et al., 2014).

In the *APP/PS1-21* model, TREM2 was found to be expressed on plaque-associated myeloid cells that lack phenotypic features of microglia, such as low expression of CD45 and high expression of the purinoceptor P2RY12 (Jay et al., 2015). Based on these results, Jay and colleagues proposed that the myeloid cells that cluster around A $\beta$  plaques originate from peripheral blood monocytes that are recruited to the brain rather than from resident microglia, and that TREM2 is required for such recruitment (Fig. 2). Interestingly, in this study, lack of TREM2 resulted in reduced accumulation of A $\beta$  in 4-month-old mice (Jay et al., 2015). Therefore, the authors posited a detrimental role for TREM2 in AD pathology, through a yet undefined mechanism.

In the third of these studies, haploinsufficiency of TREM2 in the *APP/PS1-21* model had no effect on A $\beta$  pathology in 3-month-old mice (Ulrich et al., 2014). Thus, although there is a consensus that TREM2 is required for microgliosis, the origin of the microglia surrounding A $\beta$  plaques and their impact on A $\beta$  accumulation remain controversial (Tanzi, 2015).

It is possible that, although the microglial response to A $\beta$  occurs very early in the progression of disease in these models, A $\beta$  accumulation itself may require much longer. Therefore, discrepancies in the effects of TREM2 deficiency on A $\beta$  accumulation may be the result of varied timing of the analyses performed in the different studies (8, 4, and 3 months in Wang et al., 2015; Ulrich et al., 2014; and Jay et al., 2015, respectively). A time-course analysis of

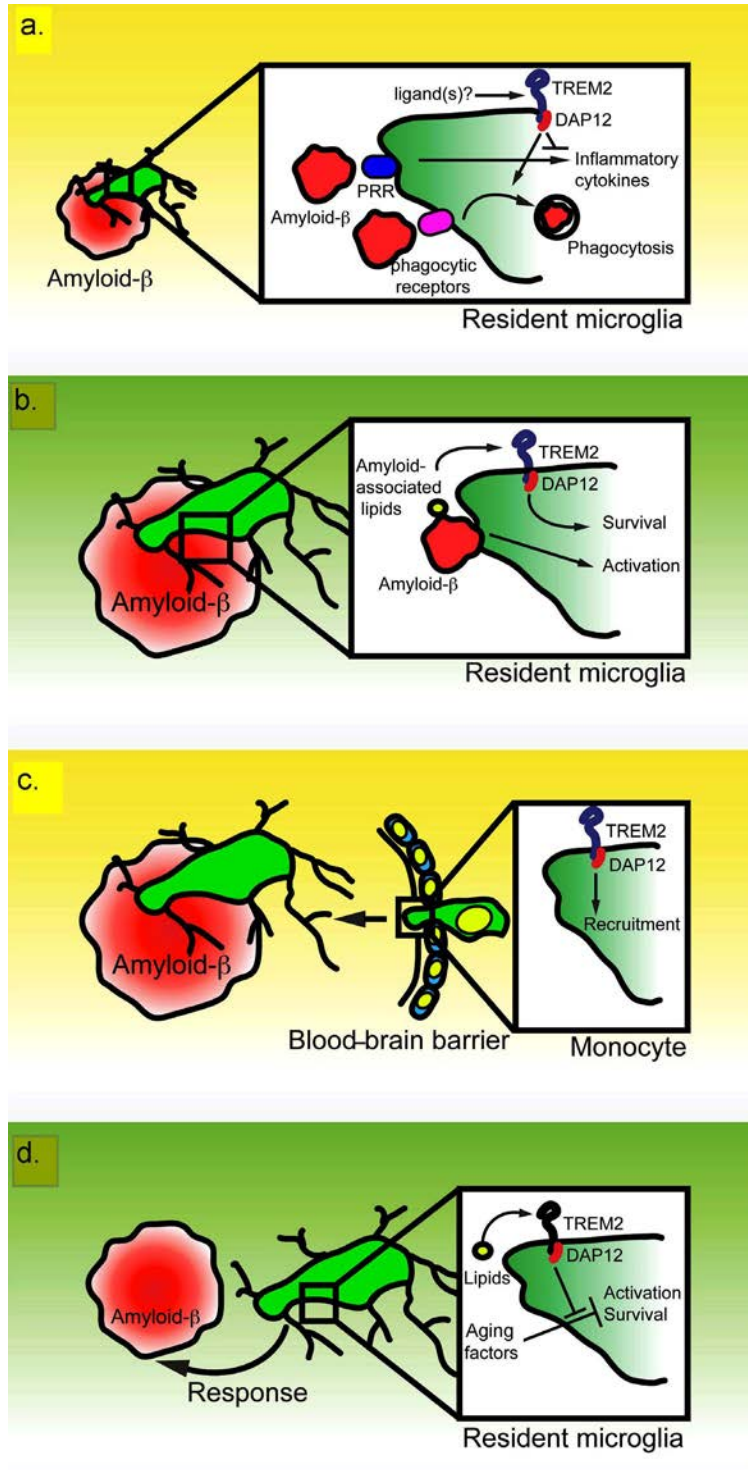


**Figure 2.** Potential models of TREM2 function in microglial response to AD. *a*, According to one model, TREM2 in resident microglia promotes phagocytosis and removal of apoptotic cells. Moreover, TREM2 limits inflammation by interfering with the ability of pattern recognition receptors (PRRs) to transmit pro-inflammatory signals at amyloid recognition; *b*, A second model suggests that TREM2 signals sustain the long-term survival of microglia in response to lipids that may become exposed during AD due to cell death, myelin degradation, and generation of A $\beta$  complexes with phospholipids. Thus, TREM2 enables and sustains activation of microglia by PRRs or other receptors that sense A $\beta$  deposition; *c*, A third model suggests that TREM2 expression on peripheral monocytes promotes their recruitment through the BBB to the A $\beta$  plaque; *d*, a fourth model suggests that, on sensing brain lipid components, TREM2 delivers a tonic signal that delays aging of microglia by contrasting yet undefined aging risk factors. Modified with permission from Colonna M and Wang Y (2016), Figure 2. Copyright 2016, Nature Publishing Group.

A $\beta$  accumulation may be helpful to settle these discrepancies. Furthermore, in these studies A $\beta$  accumulation was examined in two distinct *Trem2*<sup>-/-</sup> mouse lines in which the mutations targeted different regions of the *TREM2* gene. It is therefore possible that the discrepancies may be related to yet undefined disruptions of the *Trem* locus engendered during targeting, which may affect the expression of other TREM family members that are also involved in AD. Deriving the complete sequence of the targeted *Trem* locus will be necessary to address this possibility.

It is noteworthy that, beyond the discrepancies in the findings on A $\beta$  accumulation, all studies demonstrated pathological changes that occurred preferentially in the hippocampus, perhaps suggesting a region-specific role for TREM2 that should be further investigated. In addition to A $\beta$  pathology, it will be important to determine the impact of TREM2 deficiency on aggregates of hyperphosphorylated tau and neurite dystrophy. Behavioral studies may also be beneficial for evaluating the overall impact of TREM2 deficiency on A $\beta$  and tau-mediated neuronal damage (Rivest, 2015).

### Origin of A $\beta$ -reactive microglia

During embryogenesis, microglia progenitors develop in the yolk sac and migrate into the primitive brain, where they expand and differentiate into mature microglia that self-renew by slowly dividing throughout life (Gomez Perdiguero et al., 2013; Greter and Merad, 2013). However, in inflammatory conditions, microglia-like cells can be generated from circulating monocytes that cross the blood-brain barrier (BBB). It is unclear whether the A $\beta$ -reactive microgliosis that has been observed involves cells derived from resident microglia or infiltrating monocytes. This has been difficult to resolve for various reasons. In particular, surface marker-based identification of cellular origin has proven unreliable. Peripheral blood monocytes have unique phenotypic features, such as C-C chemokine receptor type 2 (CCR2) expression; however, once they infiltrate the brain, they quickly downregulate CCR2 and undergo molecular reprogramming to adopt features similar to those of resident microglia. These features include morphology, plaque association, and expression of allograft inflammatory factor 1 (AIF1, also known as IBA1) and TREM2 (Varvel et al., 2012). Additionally, although several novel microglia-specific markers have recently been identified (Hickman et al., 2013; Butovsky et al., 2014; Zhang et al., 2014), it is possible that their expression may be altered after activation or influenced by inflammatory stimuli, as shown for P2RY12, which is downregulated during LPS-induced inflammation and in the *SOD1* model

of amyotrophic lateral sclerosis (ALS) (Haynes et al., 2006; Butovsky et al., 2015).

Other techniques to distinguish between the contributions of brain resident microglia and bone-marrow-derived cells to reactive microgliosis are based on bone marrow grafts, which replace monocytes but not resident microglia. However, whole-body irradiation before bone marrow grafts increases permeability of the BBB, inducing an artificial influx of blood monocytes into the brain (Mildner et al., 2011). To overcome these obstacles, parabiosis experiments can be performed in which TREM2-sufficient and TREM2-deficient strains developing A $\beta$  accumulation are surgically joined to facilitate exchange of peripheral blood, leaving the BBB unaltered. Preliminary data suggest that, in these settings, myeloid cells clustered around A $\beta$  plaques derive from resident microglia (Wang et al., 2016). Two very recent studies examined an experimental model in which resident microglia are depleted by intracranial administration of gangliocyclovir and replaced with blood monocytes. These studies showed that the blood monocytes that repopulate the brain after microglial depletion express TREM2 and cluster around A $\beta$  deposits only after a long period of time. Moreover, these myeloid cells fail to modify the A $\beta$  load, despite adopting features of microglia (Prokop et al., 2015; Varvel et al., 2015). Thus, peripheral monocytes may be incapable of becoming fully functional microglia or may require a yet undefined process of maturation.

### TREM2 expression in blood monocytes during AD

Early work in healthy donors detected TREM2 only in tissue macrophages as well as dendritic cells and macrophages cultured *in vitro*, but not in appreciable quantities in blood monocytes (Bouchon et al., 2001; Cella et al., 2003). However, more recent studies reported increased TREM2 expression on blood monocytes from some AD patients (Hu et al., 2014) as well as a decrease in the TREM1:TREM2 expression ratio in these cells (Chan et al., 2015). The mechanisms by which TREM2 expression may be controlled during AD remains unclear. TREM2 could be induced on human monocytes by CSF-2 and IL-4 (Bouchon et al., 2001; Cella et al., 2003) and/or RXR ligands (Daniel et al., 2014; Lefterov et al., 2015). Moreover, a recent study proposed that CD33 signaling can promote TREM2 expression in monocytes (Chan et al., 2015). Whether these mechanisms are active in AD and the pathogenetic impact of altered TREM2 expression on blood monocytes remain to be investigated.

## TREM2's role in preventing microglial aging

Aging is the most important risk factor for AD. It has been proposed that microglial dysfunction is part of the normal aging process and contributes to AD pathology (Streit, 2006; Streit et al., 2009; Hefendehl et al., 2014). Can TREM2 deficiency accelerate senescence by progressively disabling the capacity of microglia to respond to degenerative processes? A recent study revealed that aged TREM2-deficient mice have significantly reduced numbers of microglia in the white matter (Poliani et al., 2015). Moreover, microglia of aged TREM2-deficient mice acquire a dystrophic morphology that is reminiscent of senescent microglia in humans (Streit, 2006; Poliani et al., 2015). A similar phenotype was also observed in aged DAP12-deficient mice (Otero et al., 2009). These studies suggest that the TREM2–DAP12 complex, stimulated by the lipid-rich environment of the brain, may deliver a continuous tonic signal that sustains microglial survival and preserves normal microglial function over time (Fig. 2).

## A possible role for soluble TREM2

One intriguing feature of TREM2 biology is that the extracellular portion of TREM2 is shed by proteases like ADAM10 (a disintegrin and metalloproteinase domain-containing protein 10) and  $\gamma$ -secretase (Wunderlich et al., 2013; Kleinberger et al., 2014). This has two consequences. First, a soluble form of TREM2 (sTREM2) is released into the CNS, which can then be detected in the cerebrospinal fluid (Piccio et al., 2008; Kleinberger et al., 2014). Second, a C-terminal fragment of TREM2 remains inserted in the microglial plasma membrane in association with DAP12. This C-terminal fragment is cleaved by  $\gamma$ -secretase, releasing bound DAP12 (Wunderlich et al., 2013). It has been observed that the concentration of sTREM2 in the cerebrospinal fluid correlates with the levels of tau in the cerebrospinal fluid (Lill et al., 2015). Thus, sTREM2 may be an effective biomarker of microglial activation in response to neurodegeneration and neuronal injury. Whether sTREM2 and/or the C-terminal fragment has any biological function remains unclear. It is possible that sTREM2 acts as a decoy or scavenger receptor, binding phospholipids and/or apoptotic cells. Cleavage of the C-terminal fragment may increase the bioavailability of DAP12 for native TREM2 or other DAP12-associated receptors (Wunderlich et al., 2013). Failure of this cleavage may lead to sequestration of DAP12 at the cell surface, altering DAP12 signaling. Thus, it is important to investigate the biological significance of TREM2 shedding and whether AD-associated TREM2 variants affect this process.

## TREM2 and Other AD Risk Factors

Because TREM2 is one of multiple immune-related genes expressed in microglia and implicated in the pathogenesis of AD, it is possible that some of these genes are functionally connected and belong to common pathways that may be targeted for future therapeutic intervention. Using network analysis, highly preserved immune and/or microglia modules in normal and AD human brains have been detected in which TREM2, DAP12, CD33, and the gamma chain of Fc receptors are key nodes (Forabosco et al., 2013; Zhang et al., 2013). More recent data provide some experimental support for this systems biology data. CD33 is an inhibitory receptor expressed on microglia that recruits protein tyrosine phosphatases through cytoplasmic tyrosine-based inhibitory motifs (ITIMs). A variant that confers enhanced expression of CD33 is associated with increased risk for AD (Bertram et al., 2008; Hollingworth et al., 2011; Naj et al., 2011; Bradshaw et al., 2013; Griciuc et al., 2013). This CD33 variant was shown to be associated with increased expression of TREM2 and antibody-mediated suppression of CD33-moderated TREM2 expression on blood monocytes (Chan et al., 2015). Thus, TREM2 may lie downstream of CD33 (Chan et al., 2015). Alternatively, because TREM2 sustains microglial activation through ITAM signaling, and CD33 inhibits microglial activation through ITIM signaling, either impaired TREM2 function or increased CD33 function may result in altered intracellular tyrosine phosphorylation that facilitates microglial dysfunction and AD. In addition to TREM2 and CD33, TREM1 has been linked to AD (Replogle et al., 2015). Because TREM2 and TREM1 share DAP12 as a signaling adapter, it is possible that variants affecting the expression of TREM1 may impact the expression and signaling properties of TREM2 and vice versa.

Given that TREM2 is a lipid sensor, it is possible that TREM2 interacts with AD risk factors involved in lipid metabolism, such as apolipoprotein E (ApoE). The  $\epsilon 4$  allele of ApoE is a major risk factor for non-autosomal dominant forms of early-onset AD (Corder et al., 1993; Strittmatter et al., 1993). Moreover, ApoE is the most abundant lipoprotein in the brain for lipid transport and can aggregate with amyloid plaques (Namba et al., 1991; Wisniewski and Frangione, 1992). Thus, the association of both TREM2 and APOE polymorphisms with AD may reflect a functional interface. Accordingly, recent biochemical approaches have shown interactions between TREM2 and ApoE *in vitro* (Atagi et al., 2015; Bailey et al., 2015), suggesting that ApoE may act as a ligand to stimulate microglial function through

TREM2. Future *in vivo* studies will be important to determine whether functional deficiencies of ApoE and TREM2 have similar impact on AD pathology.

### TREM2 in Other Diseases

In addition to AD, *TREM2* variants have been found to be associated with other neurodegenerative diseases, such as frontotemporal lobar degeneration (FTD) (Guerreiro et al., 2013b,c; Lattante et al., 2013; Borroni et al., 2014; Cuyvers et al., 2014; Le Ber et al., 2014; Ruiz et al., 2014), ALS (Cady et al., 2014; Lill et al., 2015), and Parkinson's disease (Rayaprolu et al., 2013; Lill et al., 2015), suggesting that *TREM2* deficiency may be a general risk factor for microglial dysfunction and neurodegeneration. However, the precise impact of *TREM2* in these human pathologies is not clear because *TREM2* variants are extremely rare and the analysis of small cohorts has generated conflicting results (Thelen et al., 2014; Lill et al., 2015).

Studies of a mouse model of demyelination caused by administration of cuprizone, a toxic agent that kills oligodendrocytes, showed that *TREM2* deficiency impairs the ability of microglia to remove damaged myelin and hinders subsequent remyelination (Cantoni et al., 2015; Poliani et al., 2015). *TREM2* deficiency in mouse models of stroke also resulted in reduced inflammatory response (Sieber et al., 2013) as well as reduced microglial activation and phagocytosis of injured neurons, impaired neurological recovery, and ultimately, less viable brain tissue (Kawabori et al., 2015). Finally, clinical symptoms in an experimental mouse model of autoimmune encephalitis improved after adoptive transfer of myeloid cells expressing *TREM2* but became worse after *TREM2* blockade with a monoclonal antibody (Piccio et al., 2007; Takahashi et al., 2007). These *in vivo* studies support a general role for *TREM2* in controlling the microglial response to pathological changes in the CNS.

### Future Perspectives

Although it is now well established that *TREM2* binds lipids and that the R47H mutation impairs this capacity, it remains to be determined whether the other *TREM2* variants found in AD patients are also hypofunctional. These variants might also affect protein expression or folding, as reported for the glutamine-33-stop (Q33X) and threonine-66-methionine (T66M) mutations associated with NHD and FTD (Kleinberger et al., 2014). Elucidating the crystal structure of *TREM2* will provide a structural

basis for the involvement of particular amino acid residues, such as R47, in lipid binding. In addition to *TREM2*–lipid interactions, several studies have indicated that *TREM2* may bind to nonlipidic ligands, such as heat shock protein 60 (Stefano et al., 2009) or act in concert with PlexinA1 as a coreceptor for the transmembrane semaphorin Sema6D (Takegahara et al., 2006). Moreover, it was shown that soluble fusion proteins containing the *TREM2* extracellular domain can bind to the surface of multiple cells, especially in regions immediately surrounding amyloid plaques (Hsieh et al., 2009; Melchior et al., 2010). Future investigation will determine whether *TREM2* recognizes alternative ligands and whether these interactions impact microglial function and AD pathogenesis. Finally, the identification of *TREM2* as a potential protective factor in AD has prompted the design of drugs that may promote microglial responses to A $\beta$ . It is likely that agonistic antibodies and activating ligands of *TREM2* will contribute to therapeutic strategies in AD.

### Acknowledgments

This chapter was modified from a previously published article: Colonna M, Wang Y (2016) *TREM2* variants: new keys to decipher Alzheimer's disease pathogenesis. *Nat Rev Neurosci* 17:201–207. Copyright 2016, Nature Publishing Group.

### References

- Atagi Y, Liu CC, Painter MM, Chen XF, Verbeeck C, Zheng H, Li X, Rademakers R, Kang SS, Xu H, Younkin S, Das P, Fryer JD, Bu G (2015) Apolipoprotein E is a ligand for triggering receptor expressed on myeloid cells 2 (*TREM2*). *J Biol Chem* 290:26043–26050.
- Bailey CC, DeVaux LB, Farzan M (2015) The triggering receptor expressed on myeloid cells 2 binds apolipoprotein E. *J Biol Chem* 290:26033–26042.
- Benitez BA, Cooper B, Pastor P, Jin SC, Lorenzo E, Cervantes S, Cruchaga C (2013) *TREM2* is associated with the risk of Alzheimer's disease in Spanish population. *Neurobiol Aging* 34:1711.e15–e17.
- Benitez BA, Jin SC, Guerreiro R, Graham R, Lord J, Harold D, Sims R, Lambert JC, Gibbs JR, Brás J, Sassi C, Harari O, Bertelsen S, Lupton MK, Powell J, Bellenguez C, Brown K, Medway C, Haddick PC, van der Brug MP, et al. (2014) Missense variant in *TREML2* protects against Alzheimer's disease. *Neurobiol Aging* 35:1510.e19–e26.

- Bertram L, Lange C, Mullin K, Parkinson M, Hsiao M, Hogan MF, Schjeide BM, Hooli B, Divito J, Ionita I, Jiang H, Laird N, Moscarillo T, Ohlsen KL, Elliott K, Wang X, Hu-Lince D, Ryder M, Murphy A, Wagner SL, et al. (2008) Genome-wide association analysis reveals putative Alzheimer's disease susceptibility loci in addition to APOE. *Am J Hum Genet* 83:623–632.
- Bertram L, Parrado AR, Tanzi RE (2013) TREM2 and neurodegenerative disease. *N Engl J Med* 369:1565.
- Borroni B, Ferrari F, Galimberti D, Nacmias B, Barone C, Bagnoli S, Fenoglio C, Piaceri I, Archetti S, Bonvicini C, Gennarelli M, Turla M, Scarpini E, Sorbi S, Padovani A (2014) Heterozygous TREM2 mutations in frontotemporal dementia. *Neurobiol Aging* 35:934.e7–e10.
- Bouchon A, Hernández-Munain C, Cella M, Colonna M (2001) A DAP12-mediated pathway regulates expression of CC chemokine receptor 7 and maturation of human dendritic cells. *J Exp Med* 194:1111–1122.
- Bradshaw EM, Chibnik LB, Keenan BT, Ottoboni L, Raj T, Tang A, Rosenkrantz LL, Imboywa S, Lee M, Von Korff A; Alzheimer Disease Neuroimaging Initiative, Morris MC, Evans DA, Johnson K, Sperling RA, Schneider JA, Bennett DA, De Jager PL (2013) CD33 Alzheimer's disease locus: altered monocyte function and amyloid biology. *Nat Neurosci* 16:848–850.
- Butovsky O, Jedrychowski MP, Moore CS, Cialic R, Lanser AJ, Gabriely G, Koeglsperger T, Dake B, Wu PM, Doykan CE, Fanek Z, Liu L, Chen Z, Rothstein JD, Ransohoff RM, Gygi SP, Antel JP, Weiner HL (2014) Identification of a unique TGF- $\beta$ -dependent molecular and functional signature in microglia. *Nat Neurosci* 17:131–143.
- Butovsky O, Jedrychowski MP, Cialic R, Krasemann S, Murugaiyan G, Fanek Z, Greco DJ, Wu PM, Doykan CE, Kiner O, Lawson RJ, Frosch MP, Pochet N, Fatimy RE, Krichevsky AM, Gygi SP, Lassmann H, Berry J, Cudkowicz ME, Weiner HL (2015) Targeting miR-155 restores abnormal microglia and attenuates disease in SOD1 mice. *Ann Neurol* 77:75–99.
- Cady J, Koval ED, Benitez BA, Zaidman C, Jockel-Balsarotti J, Allred P, Baloh RH, Ravits J, Simpson E, Appel SH, Pestronk A, Goate AM, Miller TM, Cruchaga C, Harms MB (2014) TREM2 variant p.R47H as a risk factor for sporadic amyotrophic lateral sclerosis. *JAMA Neurol* 71:449–453.
- Cannon JP, O'Driscoll M, Litman GW (2012) Specific lipid recognition is a general feature of CD300 and TREM molecules. *Immunogenetics* 64:39–47.
- Cantoni C, Bollman B, Licastro D, Xie M, Mikesell R, Schmidt R, Yuede CM, Galimberti D, Olivecrona G, Klein RS, Cross AH, Otero K, Piccio (2015) TREM2 regulates microglial cell activation in response to demyelination *in vivo*. *Acta Neuropathol* 129:429–447.
- Cella M, Buonsanti C, Strader C, Kondo T, Salmaggi A, Colonna M (2003) Impaired differentiation of osteoclasts in TREM-2-deficient individuals. *J Exp Med* 198:645–651.
- Chan G, White CC, Winn PA, Cimpean M, Replogle JM, Glick LR, Cuedon NE, Ryan KJ, Johnson KA, Schneider JA, Bennett DA, Chibnik LB, Sperling RA, Bradshaw EM, De Jager P (2015) CD33 modulates TREM2: convergence of Alzheimer loci. *Nat Neurosci* 18:1556–1558.
- Colonna M, Wang Y (2016) TREM2 variants: new keys to decipher Alzheimer's disease pathogenesis. *Nat Rev Neurosci* 17:201–207.
- Corder EH, Saunders AM, Strittmatter WJ, Schmechel DE, Gaskell PC, Small GW, Roses AD, Haines JL, Pericak-Vance M (1993) Gene dose of apolipoprotein E type 4 allele and the risk of Alzheimer's disease in late onset families. *Science* 261:921–923.
- Cuyvers E, Bettens K, Philtjens S, Van Langenhove T, Gijssels I, van der Zee J, Engelborghs S, Vandenbulcke M, Van Dongen J, Geerts N, Maes G, Mattheijssens M, Peeters K, Cras P, Vandenberghe R, De Deyn PP, Van Broeckhoven C, Cruts M, Sleegers K; BELNEU consortium (2014) Investigating the role of rare heterozygous TREM2 variants in Alzheimer's disease and frontotemporal dementia. *Neurobiol Aging* 35:726.e11–e9.
- Daniel B, Nagy G, Hah N, Horvath A, Czimmerer Z, Poliska S, Gyuris T, Keirsse J, Gysemans C, Van Ginderachter JA, Balint BL, Evans RM, Barta E, Nagy L (2014) The active enhancer network operated by liganded RXR supports angiogenic activity in macrophages. *Genes Dev* 28:1562–1577.
- Daws MR, Lanier LL, Seaman WE, Ryan JC (2001) Cloning and characterization of a novel mouse myeloid DAP12-associated receptor family. *Eur J Immunol* 31:783–791.

- Daws MR, Sullam PM, Niemi EC, Chen TT, Tchao NK, Seaman WE (2003) Pattern recognition by TREM-2: binding of anionic ligands. *J Immunol* 171:594–599.
- Forabosco P, Ramasamy A, Trabzuni D, Walker R, Smith C, Brás J, Levine AP, Hardy J, Pocock JM, Guerreiro R, Weale ME, Ryten M (2013) Insights into TREM2 biology by network analysis of human brain gene expression data. *Neurobiol Aging* 34:2699–2714.
- Ford JW, McVicar DW (2009) TREM and TREM-like receptors in inflammation and disease. *Curr Opin Immunol* 21:38–46.
- Gomez Perdiguero E, Schulz C, Geissmann F (2013) Development and homeostasis of “resident” myeloid cells: the case of the microglia. *Glia* 61:112–120.
- Greter M, Merad M (2013) Regulation of microglia development and homeostasis. *Glia* 61:121–127.
- Griciuc A, Serrano-Pozo A, Parrado AR, Lesinski AN, Asselin CN, Mullin K, Hooli B, Choi SH, Hyman BT, Tanzi RE (2013) Alzheimer's disease risk gene CD33 inhibits microglial uptake of amyloid beta. *Neuron* 78:631–643.
- Guerreiro R, Wojtas A, Brás J, Carrasquillo M, Rogaeve E, Majounie E, Cruchaga C, Sassi C, Kauwe JS, Younkin S, Hazrati L, Collinge J, Pocock J, Lashley T, Williams J, Lambert JC, Amouyel P, Goate A, Rademakers R, Morgan K, et al. (2013a) TREM2 variants in Alzheimer's disease. *N Engl J Med* 368:117–127.
- Guerreiro R, Bilgic B, Guven G, Brás J, Rohrer J, Lohmann E, Hanagasi H, Gurvit H, Emre M (2013b) Novel compound heterozygous mutation in TREM2 found in a Turkish frontotemporal dementia-like family. *Neurobiol Aging* 34:2890.e1–e5.
- Guerreiro RJ, Lohmann E, Brás JM, Gibbs JR, Rohrer JD, Guranlian N, Dursun B, Bilgic B, Hanagasi H, Gurvit H, Emre M, Singleton A, Hardy J (2013c) Using exome sequencing to reveal mutations in TREM2 presenting as a frontotemporal dementia-like syndrome without bone involvement. *JAMA Neurol* 70:78–84.
- Hamerman JA, Jarjoura JR, Humphrey MB, Nakamura MC, Seaman WE, Lanier LL (2006) Cutting edge: inhibition of TLR and FcR responses in macrophages by triggering receptor expressed on myeloid cells (TREM)-2 and DAP12. *J Immunol* 177:2051–2055.
- Harold D, Abraham R, Hollingworth P, Sims R, Gerrish A, Hamshere ML, Pahwa JS, Moskvina V, Dowzell K, Williams A, Jones N, Thomas C, Stretton A, Morgan AR, Lovestone S, Powell J, Proitsi P, Lupton MK, Brayne C, Rubinsztein DC, et al. (2009) Genome-wide association study identifies variants at CLU and PICALM associated with Alzheimer's disease. *Nat Genet* 41:1088–1093.
- Haynes SE, Hollopeter G, Yang G, Kurpius D, Dailey ME, Gan WB, Julius D (2006) The P2Y12 receptor regulates microglial activation by extracellular nucleotides. *Nat Neurosci* 9:1512–1519.
- Hefendehl JK, Neher JJ, Sühs RB, Kohsaka S, Skodras A, Jucker M (2014) Homeostatic and injury-induced microglia behavior in the aging brain. *Aging Cell* 13:60–69.
- Heneka MT, Golenbock DT, Latz E (2015) Innate immunity in Alzheimer's disease. *Nat Immunol* 16:229–236.
- Hickman SE, Kingery ND, Ohsumi TK, Borowsky ML, Wang LC, Means TK, El Khoury J (2013) The microglial sensome revealed by direct RNA sequencing. *Nat Neurosci* 16:1896–1905.
- Hollingworth P, Harold D, Sims R, Gerrish A, Lambert JC, Carrasquillo MM, Abraham R, Hamshere ML, Pahwa JS, Moskvina V, Dowzell K, Jones N, Stretton A, Thomas C, Richards A, Ivanov D, Widdowson C, Chapman J, Lovestone S, Powell J (2011) Common variants at ABCA7, MS4A6A/MS4A4E, EPHA1, CD33 and CD2AP are associated with Alzheimer's disease. *Nat Genet* 43:429–435.
- Holtzman DM, Morris JC, Goate AM (2011) Alzheimer's disease: the challenge of the second century. *Sci Transl Med* 3:77sr71.
- Hsieh CL, Koike M, Spusta SC, Niemi EC, Yenari M, Nakamura MC, Seaman WE (2009) A role for TREM2 ligands in the phagocytosis of apoptotic neuronal cells by microglia. *J Neurochem* 109:1144–1156.
- Hu N, Tan MS, Yu JT, Sun L, Tan L, Wang YL, Jiang T, Tan L (2014) Increased expression of TREM2 in peripheral blood of Alzheimer's disease patients. *J Alzheimers Dis* 38:497–501.
- Humphrey MB, Daws MR, Spusta SC, Niemi EC, Torchia JA, Lanier LL, Seaman WE, Nakamura MC (2006) TREM2, a DAP12-associated receptor, regulates osteoclast differentiation and function. *J Bone Miner Res* 21:237–245.

- Jay TR, Miller CM, Cheng PJ, Graham LC, Bemiller S, Broihier ML, Xu G, Margevicius D, Karlo JC, Sousa GL, Cotleur AC, Butovsky O, Bekris L, Staugaitis SM, Leverenz JB, Pimplikar SW, Landreth GE, Howell GR, Ransohoff RM, Lamb BT (2015) TREM2 deficiency eliminates TREM2+ inflammatory macrophages and ameliorates pathology in Alzheimer's disease mouse models. *J Exp Med* 212:287–295.
- Ji JD, Park-Min KH, Shen Z, Fajardo RJ, Goldring SR, McHugh KP, Ivashkiv LB (2009) Inhibition of RANK expression and osteoclastogenesis by TLRs and IFN-gamma in human osteoclast precursors. *J Immunol* 183:7223–7233.
- Jiang T, Tan L, Zhu XC, Zhang QQ, Cao L, Tan MS, Gu LZ, Wang HF, Ding ZZ, Zhang YD, Yu JT (2014) Upregulation of TREM2 ameliorates neuropathology and rescues spatial cognitive impairment in a transgenic mouse model of Alzheimer's disease. *Neuropsychopharmacology* 39:2949–2962.
- Jonsson T, Stefansson H, Steinberg S, Jonsdottir I, Jonsson PV, Snaedal J, Bjornsson S, Huttenlocher J, Levey AI, Lah JJ, Rujescu D, Hampel H, Giegling I, Andreassen OA, Engedal K, Ulstein I, Djurovic S, Ibrahim-Verbaas C, Hofman A, Ikram MA, et al. (2013) Variant of TREM2 associated with the risk of Alzheimer's disease. *N Engl J Med* 368:107–116.
- Kawabori M, Kacimi R, Kauppinen T, Calosing C, Kim JY, Hsieh CL, Nakamura MC, Yenari MA (2015) Triggering receptor expressed on myeloid cells 2 (TREM2) deficiency attenuates phagocytic activities of microglia and exacerbates ischemic damage in experimental stroke. *J Neurosci* 35:3384–3396.
- Kleinberger G, Yamanishi Y, Suárez-Calvet M, Czirr E, Lohmann E, Cuyvers E, Struyfs H, Pettkus N, Weninger-Weinzierl A, Mazaheri F, Tahirovic S, Lleó A, Alcolea D, Forstea J, Willem M, Lammich S, Molinuevo JL, Sánchez-Valle R, Antonell A, Ramirez A, et al. (2014) TREM2 mutations implicated in neurodegeneration impair cell surface transport and phagocytosis. *Sci Transl Med* 6:243ra286.
- Klesney-Tait J, Turnbull IR, Colonna M (2006) The TREM receptor family and signal integration. *Nat Immunol* 7:1266–1273.
- Klünemann HH, Ridha BH, Magy L, Wherrett JR, Hemelsoet DM, Keen RW, De Bleecker JL, Rossor MN, Marienhagen J, Klein HE, Peltonen L, Paloneva J (2005) The genetic causes of basal ganglia calcification, dementia, and bone cysts: DAP12 and TREM2. *Neurology* 64:1502–1507.
- Lambert JC, Heath S, Even G, Campion D, Sleegers K, Hiltunen M, Combarros O, Zelenika D, Bullido MJ, Tavernier B, Letenneur L, Bettens K, Berr C, Pasquier F, Fiévet N, Barberger-Gateau P, Engelborghs S, De Deyn P, Mateo I, Franck A, et al. (2009) Genome-wide association study identifies variants at CLU and CR1 associated with Alzheimer's disease. *Nat Genet* 41:1094–1099.
- Lattante S, Le Ber I, Camuzat A, Dayan S, Godard C, Van Bortel I, De Septenville A, Ciura S, Brice A, Kabashi E; French Research Network on FTD and FTD-ALS (2013) TREM2 mutations are rare in a French cohort of patients with frontotemporal dementia. *Neurobiol Aging* 34:2443.e1–e2.
- Le Ber I, De Septenville A, Guerreiro R, Brás J, Camuzat A, Caroppo P, Lattante S, Couarch P, Kabashi E, Bouya-Ahmed K, Dubois B, Brice A (2014) Homozygous TREM2 mutation in a family with atypical frontotemporal dementia. *Neurobiol Aging* 35:2419.e23–e2415.
- Lefterov I, Schug J, Mounier A, Nam KN, Fitz NF, Koldamova R (2015) RNA-sequencing reveals transcriptional up-regulation of Trem2 in response to bexarotene treatment. *Neurobiol Dis* 82:132–140.
- Lill CM, Rengmark A, Pihlstrøm L, Fogh I, Shatunov A, Sleiman PM, Wang LS, Liu T, Lassen CF, Meissner E, Alexopoulos P, Calvo A, Chio A, Dizdar N, Faltraco F, Forsgren L, Kirchheiner J, Kurz A, Larsen JP, Liebsch M, et al. (2015) The role of TREM2 R47H as a risk factor for Alzheimer's disease, frontotemporal lobar degeneration, amyotrophic lateral sclerosis, and Parkinson's disease. *Alzheimers Dement* 11:1407–1416.
- Melchior B, Garcia AE, Hsiung BK, Lo KM, Doose JM, Thrash JC, Stalder AK, Staufenbiel M, Neumann H, Carson MJ (2010) Dual induction of TREM2 and tolerance-related transcript, Tmem176b, in amyloid transgenic mice: implications for vaccine-based therapies for Alzheimer's disease. *ASN Neuro* 2:e00037.
- Meyer-Luehmann M, Prinz M (2015) Myeloid cells in Alzheimer's disease: culprits, victims or innocent bystanders? *Trends Neurosci* 38:659–668.

- Mildner A, Schlevogt B, Kierdorf K, Böttcher C, Erny D, Kummer MP, Quinn M, Brück W, Bechmann I, Heneka MT, Priller J, Prinz M (2011) Distinct and non-redundant roles of microglia and myeloid subsets in mouse models of Alzheimer's disease. *J Neurosci* 31, 11159–11171.
- Naj AC, Jun G, Beecham GW, Wang LS, Vardarajan BN, Buros J, Gallins PJ, Buxbaum JD, Jarvik GP, Crane PK, Larson EB, Bird TD, Boeve BF, Graff-Radford NR, De Jager PL, Evans D, Schneider JA, Carrasquillo MM, Ertekin-Taner N, Younkin SG, et al. (2011) Common variants at MS4A4/MS4A6E, CD2AP, CD33 and EPHA1 are associated with late-onset Alzheimer's disease. *Nat Genet* 43:436–441.
- Namba Y, Tomonaga M, Kawasaki H, Otomo E, Ikeda K (1991) Apolipoprotein E immunoreactivity in cerebral amyloid deposits and neurofibrillary tangles in Alzheimer's disease and kuru plaque amyloid in Creutzfeldt-Jakob disease. *Brain Res* 541:163–166.
- N'Diaye EN, Branda CS, Branda SS, Nevarez L, Colonna M, Lowell C, Hamerman JA, Seaman WE (2009) TREM-2 (triggering receptor expressed on myeloid cells 2) is a phagocytic receptor for bacteria. *J Cell Biol.* 184:215–223.
- Otero K, Turnbull IR, Poliani PL, Vermi W, Cerutti E, Aoshi T, Tassi I, Takai T, Stanley SL, Miller M, Shaw AS, Colonna M (2009) Macrophage colony-stimulating factor induces the proliferation and survival of macrophages via a pathway involving DAP12 and beta-catenin. *Nat Immunol* 10:734–743.
- Otero K, Shinohara M, Zhao H, Cella M, Gilfillan S, Colucci A, Faccio R, Ross FP, Teitelbaum SL, Takayanagi H, Colonna M (2012) TREM2 and  $\beta$ -catenin regulate bone homeostasis by controlling the rate of osteoclastogenesis. *J Immunol* 188:2612–2621.
- Paloneva J, Autti T, Raininko R, Partanen J, Salonen O, Puranen M, Hakola P, Haltia M (2001) CNS manifestations of Nasu-Hakola disease: a frontal dementia with bone cysts. *Neurology* 56:1552–1558.
- Paloneva J, Mandelin J, Kiialainen A, Bohling T, Prudlo J, Hakola P, Haltia M, Konttinen YT, Peltonen L (2003) DAP12/TREM2 deficiency results in impaired osteoclast differentiation and osteoporotic features. *J Exp Med* 198:669–675.
- Paloneva J, Manninen T, Christman G, Hovanes K, Mandelin J, Adolfsson R, Bianchin M, Bird T, Miranda R, Salmaggi A, Tranebjaerg L, Konttinen Y, Peltonen L (2002) Mutations in two genes encoding different subunits of a receptor signaling complex result in an identical disease phenotype. *Am J Hum Genet* 71:656–662.
- Peng Q, Malhotra S, Torchia JA, Kerr WG, Coggeshall KM, Humphrey MB (2010) TREM2- and DAP12-dependent activation of PI3K requires DAP10 and is inhibited by SHIP1. *Sci Signal* 3:ra38.
- Piccio L, Buonsanti C, Mariani M, Cella M, Gilfillan S, Cross AH, Colonna M, Panina-Bordignon P (2007) Blockade of TREM-2 exacerbates experimental autoimmune encephalomyelitis. *Eur J Immunol* 37:1290–1301.
- Piccio L, Buonsanti C, Cella M, Tassi I, Schmidt RE, Fenoglio C, Rinker J 2nd, Naismith RT, Panina-Bordignon P, Passini N, Galimberti D, Scarpini E, Colonna M, Cross AH (2008) Identification of soluble TREM-2 in the cerebrospinal fluid and its association with multiple sclerosis and CNS inflammation. *Brain* 131(Pt 11):3081–3091.
- Poliani PL, Wang Y, Fontana E, Robinette ML, Yamanishi Y, Gilfillan S, Colonna (2015) TREM2 sustains microglial expansion during aging and response to demyelination. *J Clin Invest* 125:2161–2170.
- Prokop S, Miller KR, Drost N, Handrick S, Mathur V, Luo J, Wegner A, Wyss-Coray T, Heppner F (2015) Impact of peripheral myeloid cells on amyloid- $\beta$  pathology in Alzheimer's disease-like mice. *J Exp Med* 212:1811–1818.
- Ransohoff RM, El Khoury J (2015) Microglia in health and disease. *Cold Spring Harb Perspect Biol* 8:a020560.
- Rayaprolu S, Mullen B, Baker M, Lynch T, Finger E, Seeley WW, Hatanpaa KJ, Lomen-Hoerth C, Kertesz A, Bigio EH, Lippa C, Josephs KA, Knopman DS, White CL 3rd, Caselli R, Mackenzie IR, Miller BL, Boczarska-Jedynak M, Opala G, Krygowska-Wajs A, et al. (2013) TREM2 in neurodegeneration: evidence for association of the p.R47H variant with frontotemporal dementia and Parkinson's disease. *Mol Neurodegener* 8:19.
- Reitz C, Mayeux R, Alzheimer's Disease Genetics Consortium (2013) TREM2 and neurodegenerative disease. *N Engl J Med* 369:1564–1565.

- Replogle JM, Chan G, White CC, Raj T, Winn PA, Evans DA, Sperling RA, Chibnik LB, Bradshaw EM, Schneider JA, Bennett DA, De Jager P (2015) A TREM1 variant alters the accumulation of Alzheimer-related amyloid pathology. *Ann Neurol* 77:469–477.
- Rivest S (2015) TREM2 enables amyloid  $\beta$  clearance by microglia. *Cell Res* 25:535–536.
- Ruiz A, Dols-Icardo O, Bullido MJ, Pastor P, Rodríguez-Rodríguez E, López de Munain A, de Pancorbo MM, Pérez-Tur J, Alvarez V, Antonell A, López-Arrieta J, Hernández I, Tárraga L, Boada M, Lleó A, Blesa R, Frank-García A, Sastre I, Razquin C, Ortega-Cubero S, et al. (2014) Assessing the role of the TREM2 p.R47H variant as a risk factor for Alzheimer's disease and frontotemporal dementia. *Neurobiol Aging* 35:444.e1–e4.
- Schmid CD, Sautkulis LN, Danielson PE, Cooper J, Hasel KW, Hilbush BS, Sutcliffe JG, Carson MJ (2002) Heterogeneous expression of the triggering receptor expressed on myeloid cells-2 on adult murine microglia. *J Neurochem* 83:1309–1320.
- Seno H, Miyoshi H, Brown SL, Geske MJ, Colonna M, Stappenbeck TS (2009) Efficient colonic mucosal wound repair requires Trem2 signaling. *Proc Natl Acad Sci USA* 106, 256–261.
- Sieber MW, Jaenisch N, Brehm M, Guenther M, Linnartz-Gerlach B, Neumann H, Witte OW, Frahm C (2013) Attenuated inflammatory response in triggering receptor expressed on myeloid cells 2 (TREM2) knock-out mice following stroke. *PLoS One* 8:e52982.
- Slattery C, Beck J, Harper L, Adamson G, Abdi Z, Uphill J, Campbell T, Druyeh R, Mahoney CJ, Rohrer JD, Kenny J, Lowe L, Leung KK, Barnes J, Clegg SL, Blair M, Nicholas JM, Guerreiro RJ, Rowe JB, Ponto C, et al. (2014) Trem2 variants increase risk of typical early-onset Alzheimer's disease but not of prion or frontotemporal dementia. *J Neurol Neurosurg Psychiatry* 85:e3.
- Stefano L, Racchetti G, Bianco F, Passini N, Gupta RS, Panina Bordignon P, Meldolesi J (2009) The surface-exposed chaperone, Hsp60, is an agonist of the microglial TREM2 receptor. *J Neurochem* 110:284–294.
- Streit WJ (2006) Microglial senescence: does the brain's immune system have an expiration date? *Trends Neurosci* 29:506–510.
- Streit WJ, Braak H, Xue QS, Bechmann I (2009) Dystrophic (senescent) rather than activated microglial cells are associated with tau pathology and likely precede neurodegeneration in Alzheimer's disease. *Acta Neuropathol* 118:475–485.
- Strittmatter WJ, Saunders AM, Schmechel D, Pericak-Vance M, Enghild J, Salvesen GS, Roses AD (1993) Apolipoprotein E: high-avidity binding to beta-amyloid and increased frequency of type 4 allele in late-onset familial Alzheimer disease. *Proc Natl Acad Sci USA* 90:1977–1981.
- Takahashi K, Rochford CD, Neumann H (2005) Clearance of apoptotic neurons without inflammation by microglial triggering receptor expressed on myeloid cells-2. *J Exp Med* 201:647–657.
- Takahashi K, Prinz M, Stagi M, Chechneva O, Neumann H (2007) TREM2-transduced myeloid precursors mediate nervous tissue debris clearance and facilitate recovery in an animal model of multiple sclerosis. *PLoS Med* 4:e124.
- Takegahara N, Takamatsu H, Toyofuku T, Tsujimura T, Okuno T, Yukawa K, Mizui M, Yamamoto M, Prasad DV, Suzuki K, Ishii M, Terai K, Moriya M, Nakatsuji Y, Sakoda S, Sato S, Akira S, Takeda K, Inui M, Takai T, et al. (2006) Plexin-A1 and its interaction with DAP12 in immune responses and bone homeostasis. *Nat Cell Biol* 8:615–622.
- Tanzi RE (2012) The genetics of Alzheimer disease. *Cold Spring Harb Perspect Med* 2 pii: a006296.
- Tanzi RE (2015) TREM2 and risk of Alzheimer's disease—friend or foe? *N Engl J Med* 372:2564–2565.
- Thelen M, Razquin C, Hernández I, Gorostidi A, Sánchez-Valle R, Ortega-Cubero S, Wolfgruber S, Driichel D, Fliessbach K, Duenkel T, Damian M, Heilmann S, Slotosch A, Lennarz M, Seijo-Martínez M, Rene R, Kornhuber J, Peters O, Luckhaus C, Jahn H, et al. (2014) Investigation of the role of rare TREM2 variants in frontotemporal dementia subtypes. *Neurobiol Aging* 35:2657.e13–e9.
- Turnbull IR, Gilfillan S, Cella M, Aoshi T, Miller M, Piccio L, Hernández M, Colonna M (2006) Cutting edge: TREM-2 attenuates macrophage activation. *J Immunol* 177:3520–3524.
- Ulrich JD, Finn MB, Wang Y, Shen A, Mahan TE, Jiang H, Stewart FR, Piccio L, Colonna M, Holtzman DM (2014) Altered microglial response to A $\beta$  plaques in APPPS1-21 mice heterozygous for TREM2. *Mol Neurodegener* 9:20.

- Varvel NH, Grathwohl SA, Baumann F, Liebig C, Bosch A, Brawek B, Thal DR, Charo IF, Heppner FL, Aguzzi A, Garaschuk O, Ransohoff RM, Jucker M (2012) Microglial repopulation model reveals a robust homeostatic process for replacing CNS myeloid cells. *Proc Natl Acad Sci USA* 109:18150–18155.
- Varvel NH, Grathwohl SA, Degenhardt K, Resch C, Bosch A, Jucker M, Neher JJ (2015) Replacement of brain-resident myeloid cells does not alter cerebral amyloid- $\beta$  deposition in mouse models of Alzheimer's disease. *J Exp Med* 212:1803–1809.
- Wang Y, Cella M, Mallinson K, Ulrich JD, Young KL, Robinette ML, Gilfillan S, Krishnan GM, Sudhakar S, Zinselmeyer BH, Holtzman DM, Cirrito JR, Colonna M (2015) TREM2 lipid sensing sustains the microglial response in an Alzheimer's disease model. *Cell* 160:1061–1071.
- Wang Y, Ulland TK, Ulrich JD, Song W, Tzaferis JA, Hole JT, Yuan P, Mahan TE, Shi Y, Gilfillan S, Cella M, Grutzendler J, DeMattos RB, Cirrito JR, Holtzman DM, Colonna M (2016) TREM2-mediated early microglial response limits diffusion and toxicity of amyloid plaques. *J Exp Med* 213:667–675.
- Wisniewski T, Frangione B (1992) Apolipoprotein E: a pathological chaperone protein in patients with cerebral and systemic amyloid. *Neurosci Lett* 135:235–238.
- Wu K, Byers DE, Jin X, Agapov E, Alexander-Brett J, Patel AC, Cella M, Gilfillan S, Colonna M, Kober DL, Brett TJ, Holtzman M (2015) TREM-2 promotes macrophage survival and lung disease after respiratory viral infection. *J Exp Med* 212:681–697.
- Wunderlich P, Glebov K, Kemmerling N, Tien NT, Neumann H, Walter J (2013) Sequential proteolytic processing of the triggering receptor expressed on myeloid cells-2 (TREM2) protein by ectodomain shedding and  $\gamma$ -secretase-dependent intramembranous cleavage. *J Biol Chem* 288:33027–33036.
- Zhang B, Gaiteri C, Bodea LG, Wang Z, McElwee J, Podtelezchnikov AA, Zhang C, Xie T, Tran L, Dobrin R, Fluder E, Clurman B, Melquist S, Narayanan M, Suver C, Shah H, Mahajan M, Gillis T, Mysore J, MacDonald ME, et al. (2013) Integrated systems approach identifies genetic nodes and networks in late-onset Alzheimer's disease. *Cell* 153:707–720.
- Zhang Y, Chen K, Sloan SA, Bennett ML, Scholze AR, O'Keeffe S, Phatnani HP, Guarnieri P, Caneda C, Ruderisch N, Deng S, Liddelow SA, Zhang C, Daneman R, Maniatis T, Barres BA, Wu JQ (2014) An RNA-sequencing transcriptome and splicing database of glia, neurons, and vascular cells of the cerebral cortex. *J Neurosci* 34:11929–11947.

# **Microglia: Phagocytosing to Clean, Sculpt, and Destroy**

Soyon Hong, PhD,<sup>1</sup> and Beth Stevens, PhD<sup>1,2</sup>

---

<sup>1</sup>F.M. Kirby Neurobiology Center  
Boston Children's Hospital and Harvard Medical School  
Boston, Massachusetts

<sup>2</sup>Stanley Center for Psychiatric Research  
Broad Institute of MIT and Harvard  
Cambridge, Massachusetts

## Introduction

Microglia are the resident macrophages and primary phagocytes of the CNS. Unlike other phagocytes, which function primarily in immunity, microglia are immune cells that are heavily involved in not only supporting brain tissue, but also shaping it. Using phagocytosis, they destroy excess functional connections between neurons (synaptic pruning) to sculpt neuronal and synaptic circuits during development and throughout adulthood. They use classical immune molecules, such as complement, to signal to neurons and glia, and they survey their microenvironment using their dynamic processes. We now appreciate that microglia are key modulators of neuronal development and plasticity, yet details about their normal homeostatic role in the healthy brain and how they contribute to disease remain elusive. Several neurodegenerative disorders involve synapse loss, and emerging evidence from several mouse models suggests that microglia mediate this loss. Although pruning is not their only role, understanding how microglia recognize and prune synapses during development is providing new insight into synapse loss and dysfunction in disease, potentially nominating new therapeutic candidates.

## What Defines Microglia

Microglia were first characterized by del Rio-Hortega as a population of migratory phagocytic cells within the CNS. A long-standing mission has been to determine what defines microglia and to assess how they vary—not only across cell populations, but also across time, space, and individuals. It is becoming increasingly clear that microglia are a distinct macrophage population, differentiated and specialized from other tissue macrophages by microenvironment cues unique to the CNS (Gosselin et al., 2014; Lavin et al., 2014). Even so, the transcriptional profiles of microglia are remarkably diverse. Their profiles appear to vary by cell age, developmental stage, resident brain region, sex, and even gut microbiota (Butovsky et al., 2013; Hickman et al., 2013; Grabert et al., 2016; Matcovitch-Natan et al., 2016), suggesting that the cells' functional roles are shaped by complex regulatory networks in their local milieu. An intriguing question is whether this microglial heterogeneity shapes circuit wiring (or vice versa) in the developing brain and whether this underlies region-specific vulnerability in disease. Further studies are needed to obtain a more comprehensive profile of microglia, and particularly to assess how that profile changes in disease. This would provide insight into their remarkable plasticity in the living brain and the molecular pathways that underlie it.

## Phagocytic Functions in the Brain

Microglia are the local phagocytes of brain parenchyma, where they rapidly and efficiently clear dead or dying cells and debris. They have many roles, but being our brain's innate immune cells, they react to damage signals (Ransohoff and Cardona, 2010). They migrate to injury, extend their processes to it, and produce cytokines, chemokines, and other pro-inflammatory and anti-inflammatory signals for repairing injury and maintaining homeostasis. In addition, because they enter the brain early in development (embryonic day ~9.5 in mouse) (Ginhoux et al., 2010), they are well poised to impact the developing brain. Indeed, deletion of microglia-related genes or dysregulation of inflammatory markers leads to altered brain wiring and produces behavioral deficits associated with neuropsychiatric or neurodevelopmental disorders (Frost and Schafer, 2016). Microglia are also involved in spatial patterning, engulfing cells undergoing apoptosis (programmed cell death) as the embryonic brain matures and clearing apoptotic cells during adult neurogenesis. Together, these findings suggest that microglia play an important role in shaping the brain; however, signaling mechanisms underlying the crosstalk between microglia and other cell types, including neurons and astrocytes, still remain unclear.

## Microglia Shape Brain Wiring by Targeting Synapses

Microglia and immune-related proteins are critical for the refinement of neuronal connectivity in the developing brain. Manipulating microglia or microglia-related functions leads to sustained defects in synaptic connectivity, brain wiring, and plasticity-associated tasks (Hong et al., 2016b). Under healthy basal conditions, microglia connect with synapses using their highly motile processes (Fig. 1). The frequency of these connections is regulated by neuronal activity or sensory (visual) experience, suggesting that these contacts have functional implications. Indeed, microglia sculpt synaptic connectivity by engulfing the neuronal terminals that form the synapse, a process known as synaptic pruning (Tremblay et al., 2010; Paolicelli et al., 2011; Schafer et al., 2012).

## Complement as an “Eat Me” Signal for Synaptic Engulfment

How do microglia target synapses for phagocytosis? One mechanism involved in both neural development and models of neurodegeneration is the classical

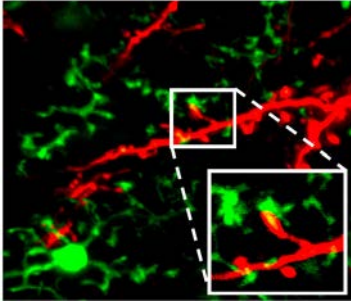


**Figure 1.** Microglia dynamically interact with synaptic elements in the healthy brain. Two-photon imaging in the olfactory bulb of adult mice shows processes of CX3CR1-GFP-positive microglia connecting to tdTomato-labeled neurons. Image courtesy of Jenelle Wallace at Harvard University. Reprinted with permission from Hong S and Stevens S (2016), Figure 1. Copyright 2016, Elsevier.

complement cascade (Stevens et al., 2007; Schafer et al., 2012; Hong et al., 2016a; Lui et al., 2016). In the peripheral immune system, classical complement proteins are “eat me” signals that promote rapid clearance of invading pathogens or cellular debris, which is done in part by macrophages expressing complement receptors (CRs) including CR3. In the developing visual thalamus, C1q (the initiating protein of the cascade) and C3 (a downstream protein) localize to subsets of immature synapses, likely marking them for elimination (Stevens et al., 2007). Microglia, which express CR3, phagocytose these synaptic inputs through the C3–CR3 signaling pathway (Schafer et al., 2012). Significantly, mice deficient in C1q, C3, or CR3 have sustained defects in synaptic connectivity. This complement-dependent synaptic pruning is significantly downregulated in the mature brain, suggesting that it is a highly regulated process, likely restricted to refinement stages of development.

### When Synapses Are (Wrongly) Marked as Debris

Reactive microglia and neuroinflammation are hallmarks of Alzheimer’s disease (AD) and other neurodegenerative disorders, including Parkinson’s disease, ALS, and frontotemporal dementia (Ransohoff, 2016). Long considered to be events secondary to neurodegeneration, microglia-related pathways have been identified by emerging genetic and transcriptomic studies as central to AD risk and pathogenesis (Guerreiro et al., 2013; Jonsson et al., 2013; Lambert et al., 2013; Zhang et al., 2013; Karch and Goate, 2015; Villegas-Llerena et al., 2016; Efthymiou et al., 2017). Large-scale

genome-wide association studies (GWAS) have identified more than 20 loci that are causally linked to AD. Of these, approximately half are expressed or exclusively expressed in microglia or myeloid cells, including TREM2 (triggering receptor expressed on myeloid cells 2), CD33 and members of the classical complement cascade, apolipoprotein J (ApoJ)/Clusterin, and complement receptor 1 (CR1) (Colonna and Wang, 2016; Villegas-Llerena et al., 2016). These findings (Griciuc et al., 2013) implicate microglia as critical or even causal players in AD pathogenesis; however, their biological significance remains elusive.

Region-specific synapse loss and dysfunction are early hallmarks of AD. Microglia and immune-related pathways have been implicated in AD pathogenesis through GWAS, but their role in synapse loss and cognitive impairment remains elusive (Hong et al., 2016b). Complement proteins are often upregulated in AD and localize to neuritic plaques along with microglia, but these processes have been regarded largely as secondary to plaque-related neuroinflammation. However, in multiple AD mouse models, C1q and C3 have been associated with synapses before overt plaque deposition and are localized to brain regions vulnerable to synapse loss (Hong et al., 2016a). In addition, microglia in adult mice phagocytose synaptic material in the presence of soluble oligomeric amyloid- $\beta$ , a key synaptotoxic species in AD. This engulfment is dependent on CR3, and blocking the complement cascade (C1q, C3, and CR3) protects the synapses (Hong et al., 2016a). Similarly, complement activation and microglia-mediated synaptic pruning are drivers of neurodegeneration caused by progranulin deficiency in mice (Lui et al., 2016). Together, these results suggest that a key developmental pruning pathway involving complement and microglia is reactivated early in the disease process to “mark” vulnerable synapses for destruction (Fig. 2).

It is important to understand what other pathways, besides complement, are critical for pruning. For example, CX3C chemokine receptor 1 (CX3CR1, also known as the microglial fractalkine receptor) is necessary for synapse maturation, elimination, and functional connectivity (Paolicelli et al., 2011, Zhan et al., 2014); however, whether or how fractalkine signaling regulates synaptic engulfment is not yet clear. Another pathway could involve neuronal activity that modulates synaptic engulfment in the developing brain (Schafer et al., 2012). Several other immune-related molecules have recently been identified as mediators of synaptic refinement and plasticity in the

## NOTES

developing and mature brain (Boulanger 2009). These include neuronal pentraxins (NP1, NP2), neuronal activity-regulated pentraxin (Narp), and components of the adaptive immune system (e.g., the major histocompatibility class I [MHC I] family of proteins and receptors) (Huh et al., 2000; Bjartmar et al., 2006; Syken et al., 2006; Lee et al., 2014).

It is intriguing to speculate that components of the complement pathway may be interacting with one of several of these immune-related molecules to mediate CNS synapse elimination in health and disease. In neurodegenerative diseases, there is aberrant neuronal activity in distinct brain networks (Seeley et al., 2009), perhaps triggering region-specific microglial phagocytosis of synapses. Knowing the positive and negative signals that regulate pruning, as well as those that guide microglia to specific synapses, will be important for nominating therapeutic candidates.

## Redefining the Role of Microglia in Health and Disease

Loss of synaptic integrity has been linked to a host of developmental and neurodegenerative diseases, potentially implicating microglia-mediated pruning. Indeed, data from multiple models of neurological diseases, including AD, frontotemporal dementia, glaucoma, and West Nile virus-induced memory impairment, suggest that region-specific activation of the microglia-complement signaling pathway leads to synapse loss (Stevens et al., 2007; Hong et al., 2016a; Lui et al., 2016; Vasek et al., 2016). In addition, C4 (complement component 4) is a strong risk factor for schizophrenia (Sekar et al., 2016), indicating that this pathway could also underlie neurodevelopmental and neuropsychiatric diseases such as autism and schizophrenia. Microglia-mediated pruning may thus be involved in a variety of diseases, but its activation may differ in time, place, and magnitude. As such, it is imperative that we catalog pruning activity in the healthy brain and understand how microglia recognize

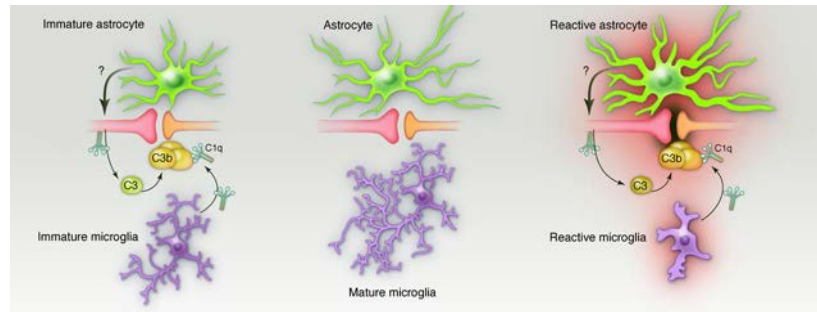


**Figure 2.** Complement-mediated synapse elimination during development and in neurodegenerative diseases. Left, In the developing brain, astrocytes induce the production of C1q in neurons through a molecular signal (?) that was recently identified as TGF- $\beta$  (Bialas et al., 2013). Neuronal and microglia-derived C1q tags the weak or superfluous synapses for removal through the classical complement pathway, resulting in C3 cleavage and synaptic C3b deposition. Complement-tagged synapses are removed through phagocytosis by microglia. Center, In the absence of activated complement, synapses remain stable. Right, We propose that complement-mediated synapse elimination drives the development and/or progression of neurodegenerative diseases. As observed in the developing brain, reactive astrocytes release signal(s) (?) that induce C1q production in neurons. Neuronal and microglia-derived C1q is then recruited to synapses, which triggers the activation of downstream classical complement components, produced in excess by reactive astrocytes and microglia, and neurons, resulting in microglia-mediated synapse elimination. Modified with permission from Stephan et al. (2012), Fig. 2. Copyright 2012, Annual Reviews.

and engulf specific synapses. This knowledge could not only lead to novel biomarkers for disease severity (e.g., of cognitive decline) but could also identify the time and place where intervention to protect synapses may be the most efficient. Further, learning how to modulate microglial functions may lead to drug candidates with broad therapeutic potential across multiple diseases.

## Acknowledgments

This chapter was adapted in part from three previously published articles: Stephan et al. (2012) The complement system: An unexpected role in synaptic pruning during development and disease. *Annu Rev Neurosci* 25: 369-389. Copyright 2015, Annual Reviews; Hong and Stevens (2016) Microglia: phagocytosing to clear, sculpt, and eliminate. *Dev Cell* 38:126-128. Copyright 2016, Elsevier; and Hong, et al. (2016b) New insights on the role of microglia in synaptic pruning in health and disease. *Curr Opin Neurobiol* 36:128-134. Copyright 2016, Elsevier.

## References

Bialas A, Stevens B (2013) TGF- $\beta$  signaling regulates neuronal C1q expression and developmental synaptic refinement. *Nat Neurosci* 16:1773-1782.

- Bjartmar L, Huberman AD, Ullian EM, Renteria RC, Liu X, Xu W, Prezioso J, Susman MW, Stellwagen D, Stokes CC, Cho R, Worley P, Malenka RC, Ball S, Peachey NS, Copenhagen D, Chapman B, Nakamoto M, Barres BA, Perin MS (2006) Neuronal pentraxins mediate synaptic refinement in the developing visual system. *J Neurosci* 26:6269–6281.
- Butovsky O, Jedrychowski MP, Moore CS, Cialic R, Lanser AJ, Gabriely G, Koeglsperger T, Dake B, Wu PM, Doykan CE, Fanek Z, Liu L, Chen Z, Rothstein JD, Ransohoff RM, Gygi SP, Antel JP, Weiner HL (2013) Identification of a unique TGF- $\beta$ -dependent molecular and functional signature in microglia. *Nat Neurosci* 17:131–143.
- Colonna M, Wang Y (2016) TREM2 variants: new keys to decipher Alzheimer disease pathogenesis. *Nat Rev Neurosci* 17:201–207.
- Efthymiou AG, Goate AM (2017) Late onset Alzheimer's disease genetics implicates microglial pathways in disease risk. *Mol Neurodegener* 12:43.
- Frost JL, Schafer DP (2016) Microglia: architects of the developing nervous system. *Trends Cell Biol* 26:587–597.
- Ginhoux F, Greter M, Leboeuf M, Nandi S, See P, Gokhan S, Mehler MF, Conway SJ, Ng LG, Stanley ER, Samokhvalov IM, Merad M (2010) Fate mapping analysis reveals that adult microglia derive from primitive macrophages. *Science* 330:841–845.
- Gosselin D, Link VM, Romanoski CE, Fonseca GJ, Eichenfield DZ, Spann NJ, Stender JD, Chun HB, Garner H, Geissmann F, Glass CK (2014) Environment drives selection and function of enhancers controlling tissue-specific macrophage identities. *Cell* 159:1327–1340.
- Grabert K, Michael T, Karavolos MH, Clohisey S, Baillie JK, Stevens MP, Freeman TC, Summers KM, McColl BW (2016) Microglial brain region-dependent diversity and selective regional sensitivities to aging. *Nat Neurosci* 19:504–516.
- Griciuc A, Serrano-Pozo A, Parrado AR, Lesinski AN, Asselin CN, Mullin K, Hooli B, Choi SH, Hyman BT, Tanzi RE (2013) Alzheimer's disease risk gene *CD33* inhibits microglial uptake of amyloid beta. *Neuron* 78:631–643.
- Guerreiro R, Wojtas A, Bras J, Carrasquillo M, Rogaeva E, Majounie E, Cruchaga C, Sassi C, Kauwe JS, Younkin S, Hazrati L, Collinge J, Pocock J, Lashley T, Williams J, Lambert JC, Amouyel P, Goate A, Rademakers R, Morgan K, et al. (2013) TREM2 variants in Alzheimer's disease. *N Engl J Med* 368:117–127.
- Hickman SE, Kingery ND, Ohsumi TK, Borowsky ML, Wang LC, Means TK, El Khoury J (2013) The microglial sensome revealed by direct RNA sequencing. *Nat Neurosci* 16:1896–1905.
- Hong S, Stevens B (2016) Microglia: phagocytosing to clear, sculpt, and eliminate. *Dev Cell* 38:126–128.
- Hong S, Beja-Glasser VF, Nfonoyim BM, Frouin A, Li S, Ramakrishnan S, Merry KM, Shi Q, Rosenthal A, Barres BA, Lemere CA, Selkoe DJ, Stevens B (2016a) Complement and microglia mediate early synapse loss in Alzheimer mouse models. *Science* 352:712–716.
- Hong S, Dissing-Olesen L, Stevens B (2016b) New insights on the role of microglia in synaptic pruning in health and disease. *Curr Opin Neurobiol* 36:128–134.
- Huh GS, Boulanger LM, Du H, Riquelme PA, Brotz TM, Shatz CJ (2000) Functional requirement for class I MHC in CNS development and plasticity. *Science* 290:2155–2159.
- Jonsson T, Stefansson H, Steinberg S, Jonsdottir I, Jonsson PV, Snaedal J, Bjornsson S, Huttenlocher J, Levey AI, Lah JJ, Rujescu D, Hampel H, Giegling I, Andreassen OA, Engedal K, Ulstein I, Djurovic S, Ibrahim-Verbaas C, Hofman A, Ikram MA, et al. (2013) Variant of TREM2 associated with the risk of Alzheimer's disease. *N Engl J Med* 368:107–116.
- Karch CM, Goate AM (2015) Alzheimer's disease risk genes and mechanisms of disease pathogenesis. *Biol Psychiatry* 77:43–51.
- Lambert JC, Ibrahim-Verbaas CA, Harold D, Naj AC, Sims R, Bellenguez C, DeStafano AL, Bis JC, Beecham GW, Grenier-Boley B, Russo G, Thornton-Wells TA, Jones N, Smith AV, Chouraki V, Thomas C, Ikram MA, Zelenika D, Vardarajan BN, Kamatani Y, et al. (2013) Meta-analysis of 74,046 individuals identifies 11 new susceptibility loci for Alzheimer's disease. *Nat Genet* 45:1452–1458.

- Lavin Y, Winter D, Blecher-Gonen R, David E, Keren-Shaul H, Merad M, Jung S, Amit I (2014) Tissue-resident macrophage enhancer landscapes are shaped by the local microenvironment. *Cell* 159:1312–1326.
- Lee H, Brott BK, Kirkby LA, Adelson JD, Cheng S, Feller MB, Datwani A, Shatz CJ (2014) Synapse elimination and learning rules co-regulated by MHC class I H2-Db. *Nature* 509:195–200.
- Lui H, Zhang J, Makinson SR, Cahill MK, Kelley KW, Huang HY, Shang Y, Oldham MC, Martens LH, Gao F, Coppola G, Sloan SA, Hsieh CL, Kim CC, Bigio EH, Weintraub S, Mesulam MM, Rademakers R, Mackenzie IR, Seeley WW, et al. (2016) Progranulin deficiency promotes circuit-specific synaptic pruning by microglia via complement activation. *Cell* 165:921–935.
- Matcovitch-Natan O, Winter DR, Giladi A, Vargas Aguilar S, Spinrad A, Sarrazin S, Ben-Yehuda H, David E, Zelada González F, Perrin P, Keren-Shaul H, Gury M, Lara-Astaiso D, Thaiss CA, Cohen M, Bahar Halpern K, Baruch K, Deczkowska A, Lorenzo-Vivas E, et al. (2016) Microglia development follows a stepwise program to regulate brain homeostasis. *Science* 353:aad8670.
- Paolicelli RC, Bolasco G, Pagani F, Maggi L, Scianni M, Panzanelli P, Giustetto M, Ferreira TA, Guiducci E, Dumas L, Ragozzino D, Gross CT (2011) Synaptic pruning by microglia is necessary for normal brain development. *Science* 333:1456–1458.
- Ransohoff RM (2016) How neuroinflammation contributes to neurodegeneration. *Science* 353:777–783.
- Ransohoff, RM, Cardona AE (2010) The myeloid cells of the central nervous system parenchyma. *Nature* 468:253–262.
- Schafer DP, Lehrman EK, Kautzman AG, Koyama R, Mardinly AR, Yamasaki R, Ransohoff RM, Greenberg ME, Barres BA, Stevens B (2012) Microglia sculpt postnatal neural circuits in an activity and complement-dependent manner. *Neuron* 74:691–705.
- Seeley WW, Crawford RK, Zhou J, Miller BL, Greicius MD (2009) Neurodegenerative diseases target large-scale human brain networks. *Neuron* 62:42–52.
- Sekar A, Bialas AR, de Rivera H, Davis A, Hammond TR, Kamitaki N, Tooley K, Presumey J, Baum M, Van Doren V, Genovese G, Rose SA, Handsaker RE, Schizophrenia Working Group of the Psychiatric Genomics Consortium, Daly MJ, Carroll MC, Stevens B, McCarroll SA (2016) Schizophrenia risk from complex variation of complement component 4. *Nature* 530:177–183.
- Stephan AH, Barres BA, Stevens B (2012) The complement system: an unexpected role in synaptic pruning during development and disease. *Annu Rev Neurosci* 35:369–389.
- Stevens B, Allen NJ, Vazquez LE, Howell GR, Christopherson KS, Nouri N, Micheva KD, Mehalow AK, Huberman AD, Stafford B, Sher A, Litke AM, Lambris JD, Smith SJ, John SWM, Barres BA (2007) The classical complement cascade mediates CNS synapse elimination. *Cell* 131:1164–1178.
- Syken J, Grandpre T, Kanold PO, Shatz CJ (2006) PirB restricts ocular-dominance plasticity in visual cortex. *Science* 313:1795–1800.
- Tremblay MÈ, Lowery RL, Majewska AK (2010) Microglial interactions with synapses are modulated by visual experience. *PLoS Biol* 8:e1000527.
- Vasek MJ, Garber C, Dorsey D, Durrant DM, Bollman B, Soung A, Yu J, Perez-Torres C, Frouin A, Wilton DK, Funk K, DeMasters BK, Jiang X, Bowen JR, Mennerick S, Robinson JK, Garbow JR, Tyler KL, Suthar MS, Schmidt RE, et al. (2016) A complement–microglial axis drives synapse loss during virus-induced memory impairment. *Nature* 534:538–543.
- Villegas-Llerena C, Phillips A, Garcia-Reitboeck P, Hardy J, Pocock JM (2016) Microglial genes regulating neuroinflammation in the progression of Alzheimer’s disease. *Curr Opin Neurobiol* 36:74–81.
- Zhan Y, Paolicelli RC, Sforzini F, Weinhard L, Bolasco G, Pagani F, Vyssotski AL, Bifone A, Gozzi A, Ragozzino D, Gross CT (2014) Deficient neuron-microglia signaling results in impaired functional brain connectivity and social behavior. *Nat Neurosci* 17:400–406.
- Zhang B, Gaiteri C, Bodea LG, Wang Z, McElwee J, Podtelezchnikov AA, Zhang C, Xie T, Tran L, Dobrin R, Fluder E, Clurman B, Melquist S, Narayanan M, Suver C, Shah H, Mahajan M, Gillis T, Mysore J, MacDonald ME, et al. (2013) Integrated systems approach identifies genetic nodes and networks in late-onset Alzheimer’s disease. *Cell* 153:707–720.

# **Synapse Elimination and Learning Rules Coregulated by Major Histocompatibility Class I Protein H2-D<sup>b</sup>**

Hanmi Lee, PhD,<sup>1</sup> Lowry A. Kirkby, PhD,<sup>2</sup>  
Barbara K. Brott, PhD,<sup>1</sup> Jaimie D. Adelson, PhD,<sup>1</sup>  
Sarah Cheng, BS,<sup>1</sup> Marla B. Feller, PhD,<sup>2</sup>  
Akash Datwani, PhD,<sup>1</sup> and Carla J. Shatz, PhD<sup>1</sup>

---

<sup>1</sup>Departments of Biology and Neurobiology and Bio-X  
The James H. Clark Center  
Stanford, California

<sup>2</sup>Department of Molecular and Cell Biology  
Helen Wills Neuroscience Institute  
University of California, Berkeley  
Berkeley, California

## Introduction

The formation of precise connections between retina and LGN involves the activity-dependent elimination of some synapses and the strengthening and retention of others. Here we show that the major histocompatibility class I (MHCI) molecule H2-Db is necessary and sufficient for synapse elimination in the retinogeniculate system. In mice lacking both H2-Kb and H2-Db (KbDb<sup>-/-</sup>) despite intact retinal activity and basal synaptic transmission, the developmentally regulated decrease in functional convergence of retinal ganglion cell synaptic inputs to LGN neurons fails, and eye-specific layers do not form. Neuronal expression of just H2-Db in KbDb<sup>-/-</sup> mice rescues both synapse elimination and eye-specific segregation despite a compromised immune system. When patterns of stimulation mimicking endogenous retinal waves are used to probe synaptic learning rules at retinogeniculate synapses, long-term synaptic potentiation (LTP) is intact but long-term synaptic depression (LTD) is impaired in KbDb<sup>-/-</sup> mice. This change is the result of an increase in Ca<sup>2+</sup>-permeable (CP) AMPA receptors. Restoring H2-Db to KbDb<sup>-/-</sup> neurons renders AMPA receptors Ca<sup>2+</sup> impermeable and rescues LTD. These observations reveal an MHC I-mediated link between developmental synapse pruning and balanced synaptic learning rules enabling both LTD and LTP. They also demonstrate a direct requirement for H2-Db in functional and structural synapse pruning in CNS neurons.

Early in development before photoreceptors function, retinal ganglion cells (RGCs) spontaneously generate correlated bursts of action potentials called “retinal waves” (Meister et al., 1991; Wong et al., 1993; Feller et al., 1996). Postsynaptic LGN neurons in turn are driven to fire in similar patterns (Mooney et al., 1996; Weliky and Katz, 1999), and this endogenous activity is even relayed further into the visual system (Ackman et al., 2012). Although there is consensus that retinal waves and correlated activity are needed for RGC synapse remodeling and segregation of RGC axons into eye-specific layers (Penn et al., 1998; Huberman et al., 2008), little is known at synaptic or molecular levels about how natural patterns of activity are read out to drive elimination and structural remodeling prior to sensory experience. It is assumed that synaptic learning rules are present at retinogeniculate synapses and that implementation of these rules leads ultimately to either synapse stabilization or elimination. Efforts to discover molecular mechanisms of developmental synapse elimination have implicated several unexpected candidates, all with links to the immune system, including neuronal pentraxins, complement

C1q, and MHC I family members (Huh et al., 2000; Bjartmar et al., 2006; Stevens et al., 2007). However, it is not known whether any of these molecules regulate plasticity rules at developing synapses. Moreover, because germline knock-out mice were examined in each of these examples, it is not known whether neuronal or immune function is required for synapse elimination *in vivo*. Here we examine these questions and test whether genetically restoring H2-Db expression selectively to CNS neurons *in vivo* can rescue synapse elimination in mice that nevertheless lack an intact immune system.

## Defective Synapse Elimination in KbDb<sup>-/-</sup> LGN

MHC I genes *H2-Db* and *H2-Kb*, members of a polymorphic family of more than 50, are expressed in LGN neurons (Huh et al., 2000) and were discovered in an unbiased screen *in vivo* for genes regulated by retinal waves: Blocking this endogenous neural activity not only prevents RGC axonal remodeling (Penn et al., 1998) but also downregulates the expression of MHC I mRNA (Corriveau et al., 1998). Previous studies have suggested that MHC I molecules regulate synapse number in cultured neurons (Glynn et al., 2001) and are needed for anatomical segregation of RGC axons into LGN layers *in vivo* (Huh et al., 2000; Datwani et al., 2009). To examine whether H2-Kb and H2-Db are involved in functional synapse elimination, whole-cell microelectrode recordings were made from individual neurons in wild-type (WT) or KbDb<sup>-/-</sup> LGN slices (Fig. 1a) (Chen and Regehr, 2000; Hooks and Chen, 2006). Adult mouse LGN neurons normally receive strong monosynaptic inputs from one to three RGC axons, but in development, many weak synaptic inputs are present. The majority are eliminated between postnatal day 5 (P5) and P12 before eye opening, while the few remaining inputs strengthen, resulting in adult-like synaptic innervation by P24–P30 (Chen and Regehr, 2000). By gradually increasing optic tract (OT) stimulation intensity, individual RGC axons with progressively higher firing thresholds can be recruited (Chen and Regehr, 2000), generating a stepwise series of EPSCs recorded in each LGN neuron. For example, at P21 in WT mice, only two steps are present (Fig. 1b), indicating that just two RGC axons provide input to this LGN neuron, as expected. In contrast, in KbDb<sup>-/-</sup> LGN neurons, there are many EPSC steps (Fig. 1c), a pattern similar to that in much younger WT mice before synapse elimination (Chen and Regehr, 2000; Hooks and Chen, 2006).

To obtain more quantitative information, minimal stimulation was used to estimate single-fiber AMPA

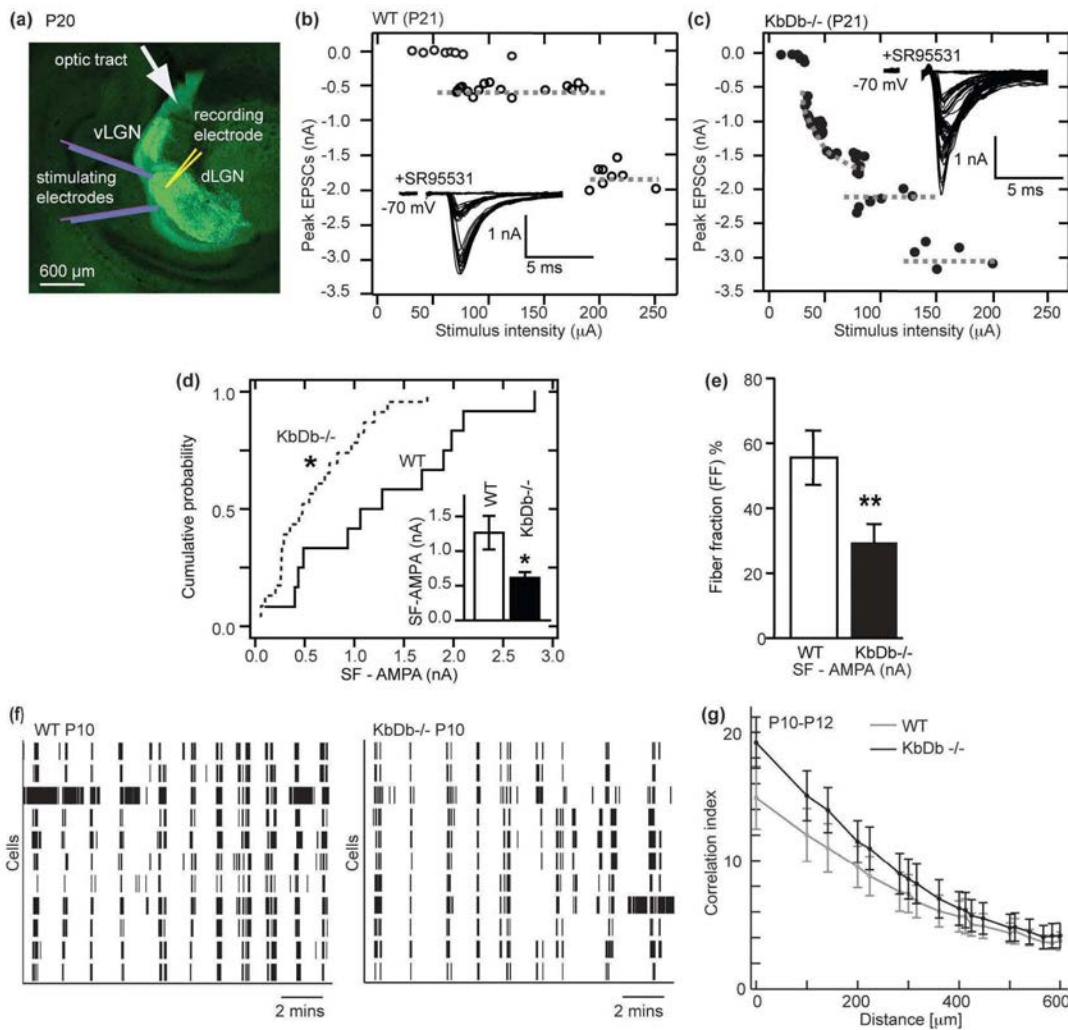


**Figure 1.** Failure of retinogeniculate synapse elimination despite intact retinal waves in *KbdB*<sup>-/-</sup> mice. **a–e**, Impaired synapse elimination in *KbdB*<sup>-/-</sup> neurons at P20–P24. **a**, Slice preparation used for whole-cell recording from dLGN neurons and stimulation of RGC axons in the OT. The retinogeniculate projection is visualized by injecting CTb AF488 (green) into the contralateral eye. Scale bar, 600  $\mu$ m. **b, c**, EPSC amplitude versus OT stimulus intensity. Insets, example traces. **d**, Cumulative probability histograms of SF-AMPA. Inset, mean  $\pm$  SEM for WT mice ( $n = 12/N = 6$ ); *KbdB*<sup>-/-</sup> mice ( $n = 23/N = 8$ ); \* $p < 0.05$ . **e**, Fiber fraction (FF) for WT mice ( $n = 12/N = 6$ ); *KbdB*<sup>-/-</sup> mice ( $n = 21/N = 8$ ); \*\* $p < 0.01$ ; *t*-test for **d–g**. Intact retinal waves in RGCs of *KbdB*<sup>-/-</sup> mice at P10–P12. **f**, Raster plots of single-unit spike trains recorded from 10 representative RGCs during retinal waves. **g**, Correlation indices vs interelectrode distance for all cell pairs for WT ( $N = 5$ ) vs *KbdB*<sup>-/-</sup> mice ( $N = 6$ ). Data correspond to mean values of medians from individual datasets, and error bars represent SEM.  $n = \text{cells}/N = \text{animals}$ ; dLGN, dorsal lateral geniculate nucleus; vLGN, ventral lateral geniculate nucleus. Reprinted with permission from Lee H et al. (2014), Figure 1. Copyright 2014, Nature Publishing Group.

(SF-AMPA) strength (Stevens and Wang, 1994) (see Methods and Extended Data for Figs. 1a,b, available at <https://www.ncbi.nlm.nih.gov/pmc/articles/PMC4016165>). On average, the amplitude of SF-AMPA in *KbdB*<sup>-/-</sup> mice is almost half that of WT mice, and the cumulative probability distribution of EPSC amplitudes recorded from *KbdB*<sup>-/-</sup> LGN neurons is also consistent with the presence of smaller EPSCs (Fig. 1d) (note that onset latency of SF-AMPA is similar in both genotypes; Extended Data, Fig. 1c). In contrast, *maximal* synaptic input (Max-AMPA) does

not differ between WT and *KbdB*<sup>-/-</sup> mice (Extended Data, Fig. 1d). Fiber fraction, an index of how much each input contributes to total synaptic response (Chen and Regehr, 2000) (Methods), is half as large in *KbdB*<sup>-/-</sup> mice as in WT mice (Fig. 1e), consistent with the idea that the number of RGC synapses in *KbdB*<sup>-/-</sup> LGN neurons is greater than in WT neurons. An alternative possibility—that differences can arise from altered probability of release—is unlikely because paired-pulse ratio (an index of presynaptic release probability) is similar in WT and *KbdB*<sup>-/-</sup> neurons

at a variety of stimulus intervals (Extended Data, Figs. 1e–h). Together, these experiments, which directly measure the functional status of synaptic innervation, demonstrate that either or both H2-Kb and H2-Db are required for retinogeniculate synapse elimination.

## Intact Retinal Wave Activity in KbDb<sup>-/-</sup> Mice

Many previous studies have shown that retinogeniculate synapse elimination and eye-specific segregation in LGN fail if retinal waves are blocked or perturbed (Feller et al., 1996; Penn et al., 1998; Huberman et al., 2008). Thus, waves could be absent or abnormal in KbDb<sup>-/-</sup> mice. To examine this possibility, waves were recorded using a multielectrode array to monitor action potential activity from many ganglion cells in KbDb<sup>-/-</sup> or WT retinas between P5 and P12—the peak period of extensive RGC synapse remodeling requiring waves. The spatiotemporal pattern of waves in KbDb<sup>-/-</sup> retina is indistinguishable from WT retina (Fig. 1f; Extended Data, Figs. 2a–e). Moreover, the correlation index between all RGC pairs (a measure of the distance over which cells fire together; Meister et al., 1991; Wong et al., 1993; Torborg et al., 2005) is almost identical (Fig. 1g; Extended Data, Fig. 2a). Retinal wave activity also transitioned normally from cholinergic-dependent stage II (P5–P8) to glutamatergic-dependent stage III (P10–P12) (Extended Data, Figs. 2a–e) (Huberman et al., 2008). After eye opening, vision in KbDb<sup>-/-</sup> mice is also normal (Datwani et al., 2009). Thus, synapse elimination and eye-specific segregation fail to occur despite intact retinal activity patterns in KbDb<sup>-/-</sup> mice, implying that one or both of these MHC I proteins acts downstream of activity to drive synapse remodeling.

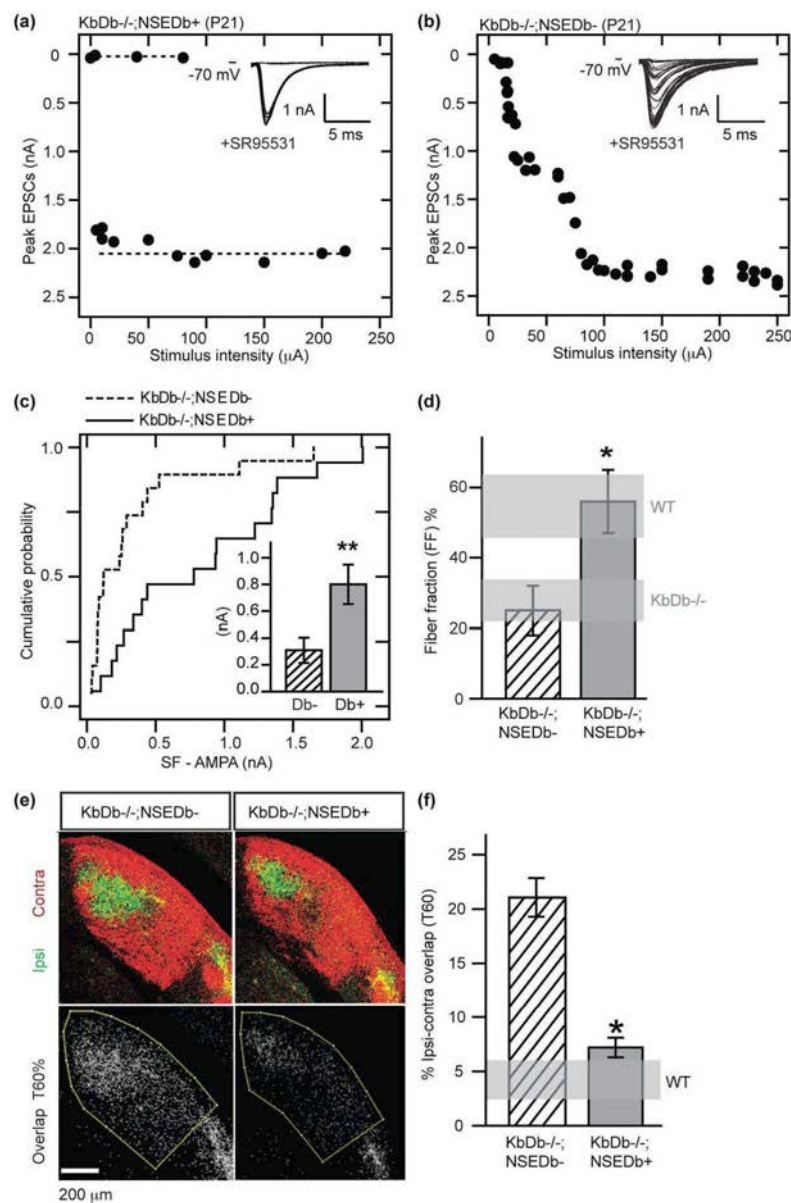


**Figure 2.** H2-Db expression in neurons rescues synapse elimination and eye-specific segregation in KbDb<sup>-/-</sup> LGN. **a–d**, Rescue of synapse elimination at P20–P24. **a, b**, EPSC amplitudes vs OT stimulus intensity. Insets: example traces. **c**, Cumulative probability histogram of SF-AMPA. Inset, mean ± SEM for control: Db<sup>-</sup> (KbDb<sup>-/-</sup>;NSEDb<sup>-</sup>; n = 19/N = 5). Rescue, Db<sup>+</sup> (KbDb<sup>-/-</sup>;NSEDb<sup>+</sup>; n = 17/N = 7), \*\**p* < 0.01. **d**, FF is also rescued in KbDb<sup>-/-</sup>;NSEDb<sup>+</sup> mice (n = 16/N = 7) compared with KbDb<sup>-/-</sup>;NSEDb<sup>-</sup> animals (n = 18/N = 5); \**p* < 0.05; Mann–Whitney *U* test for **c–d**. Horizontal gray bars delineate Fig. 1e data (mean ± SEM). **e, f**, Rescue of eye-specific segregation in KbDb<sup>-/-</sup>;NSEDb<sup>+</sup> mice at P34. **e**, Top, Coronal sections of dLGN showing pattern of retinogeniculate projections from the ipsilateral (green) and contralateral (red) eyes. Bottom, Region of ipsi-contra pixel (white) overlap between the two channels at 60% intensity threshold (T60%). Scale bar, 200 μm. **f**, Percentage of dLGN area occupied by ipsi-contra overlap. mean ± SEM for KbDb<sup>-/-</sup>;NSEDb<sup>-</sup> (N = 3) and KbDb<sup>-/-</sup>;NSEDb<sup>+</sup> (N = 4) mice (T60%); \**p* < 0.05; 2-way ANOVA [Lee H et al., (2014) Extended Data, Fig. 5]. Horizontal gray bar indicates WT value at T60% (Datwani et al., 2009). n = cells/N = animals. Reprinted with permission from Lee H et al. (2014), Figure 2. Copyright 2014, Nature Publishing Group.

## Neuronal H2-Db Rescues Elimination and Segregation

H2-Db and H2-Kb are also critical for immune function and CD8 T-cell development (Vugmeyster et al., 1998). Both MHCI molecules are expressed in LGN during the period of retinogeniculate synaptic refinement, with H2-Db higher than H2-Kb (Huh et al., 2000; Datwani et al., 2009). To separate a contribution of the immune system, and to examine whether neuronal expression is sufficient for synapse elimination, H2-Db expression was restored exclusively to neurons by crossing *KbDb*<sup>-/-</sup> mice to *NSEDb*<sup>+</sup> mice in which H2-Db expression is regulated under the neuron-specific enolase (NSE) promoter (Rall et al., 1995). “Rescued” offspring littermates have H2-Db expression restored to CNS neurons, while the rest of the body remains *KbDb*<sup>-/-</sup> (*KbDb*<sup>-/-</sup>; *NSEDb*<sup>+</sup>); “control” littermates (*KbDb*<sup>-/-</sup>; *NSEDb*<sup>-</sup>) lack H-2Kb and H2-Db everywhere (Extended Data, Fig. 3a). Genomic rescue as well as low but highly significant levels of H2-Db mRNA ( $p = 0.0001$ ) and protein can be detected in *KbDb*<sup>-/-</sup>; *NSEDb*<sup>+</sup> thalamus at P10 (Extended Data, Figs. 3b–e). In contrast, no H2-Db can be detected in spleen, gut, or liver, with little if any expression in retina, hippocampus, and cortex of *KbDb*<sup>-/-</sup>; *NSEDb*<sup>+</sup> mice.

In *KbDb*<sup>-/-</sup>; *NSEDb*<sup>+</sup> LGN neurons, only one to two EPSC steps could be evoked in response to increasing OT stimulus intensity (Fig. 2a), similar to the mature WT innervation pattern (compare Fig. 1b) but very different from littermate *KbDb*<sup>-/-</sup>; *NSEDb*<sup>-</sup> controls (Fig. 2b). Minimal stimulation also revealed an increase in SF-AMPA strength (Fig. 2c; Extended Data, Figs. 1c, 4b). Max-AMPA is similar between these genotypes (Extended Data, Fig. 4a); thus, fiber fraction in *KbDb*<sup>-/-</sup>; *NSEDb*<sup>+</sup> LGN neurons is 56% versus 25% in *KbDb*<sup>-/-</sup>; *NSEDb*<sup>-</sup> neurons (Fig. 2d): strikingly similar to WT (cf. Fig. 1e). Therefore, expression of H2-Db in neurons rescues RGC synapse elimination in *KbDb*<sup>-/-</sup> LGN close to WT levels.

The formation of the adult anatomical pattern of eye-specific segregation in the LGN involves synapse elimination: Initially intermixed RGC axons from the right and left eyes remodel, eventually restricting their terminal arbors to the appropriate LGN layer (Shatz and Kirkwood, 1984; Shatz, 1996). To examine whether eye-specific segregation in the LGN is also rescued, anatomical tract-tracing methods (Torborg and Feller, 2004; Datwani et al., 2009) were used at P34, an age chosen because it is more than 3 weeks after segregation is normally complete as assessed anatomically. The retinogeniculate projections in LGN of *KbDb*<sup>-/-</sup>; *NSEDb*<sup>+</sup> mice appear almost

indistinguishable from WT mice, both in eye-specific pattern (Fig. 2e) and in the percentage of overlap between ipsilateral and contralateral projections (Fig. 2f; Extended Data, Figs. 5a,b). Segregation is impaired in control *KbDb*<sup>-/-</sup>; *NSEDb*<sup>-</sup> littermates (Fig. 2e), as expected from previous studies of *KbDb*<sup>-/-</sup> mice (Datwani et al., 2009). These anatomical results support the electrophysiological studies mentioned earlier and strongly suggest that both RGC synapse elimination and eye-specific segregation require neuronal H2-Db.

## Impaired LTD with Natural Activity Patterns

Synapse elimination is thought to involve cellular processes leading to synaptic weakening such as LTD (Zhou et al., 2004; Baskrikova et al., 2008); conversely, LTP-like mechanisms are postulated to strengthen and stabilize synapses (Yuste and Bonhoeffer, 2001; Malenka and Bear, 2004). In addition, spike-timing-dependent mechanisms are crucial in *Xenopus* tectum for visually driven tuning of receptive fields (Mu and Poo, 2006). In mammalian LGN, LTP (Mooney et al., 1993) or LTD (Ziburkus et al., 2009) can be induced at retinogeniculate synapses using 100 Hz OT stimulation, which is far different from the endogenous bursting patterns generated by retinal waves (Figs. 1f,g) (Meister et al., 1991; Wong et al., 1993; Feller et al., 1996; Mooney et al., 1996). However, realistic patterns of OT stimulation mimicking waves, paired with postsynaptic depolarization of LGN neurons, have also been used. Results revealed a synaptic learning rule that generates LTP when presynaptic and postsynaptic activity coincide (Butts et al., 2007; Shah and Crair, 2008) but generates LTD when presynaptic OT activity precedes postsynaptic LGN depolarization within a broad window corresponding to the 60–90 s duty cycle of retinal waves (Figs. 3a–c; Extended Data, Fig. 2b) (Butts et al., 2007). Moreover, using these timing patterns in conjunction with optogenetic stimulation of retina is sufficient to either drive or prevent segregation of RGC axons, depending on the pattern (Zhang et al., 2011).

To determine whether synaptic learning rules based on natural activity patterns are altered at *KbDb*<sup>-/-</sup> retinogeniculate synapses, perforated patch recordings were made in LGN slices from WT versus *KbDb*<sup>-/-</sup> mice at P8–P13, the relevant period when extensive synapse elimination and eye-specific segregation are actually occurring. First, paired pulse stimulation was used to examine release probability: The same amount of synaptic depression was observed in WT and *KbDb*<sup>-/-</sup> mice, implying similar probabilities (Extended Data, Fig. 6). Next, synchronous activity

patterns were used in which 10 Hz OT stimulation was paired with LGN depolarization (Figs. 3a,b: 0 ms latency), generating 10–20 Hz bursts of action potentials in LGN neurons mimicking retinal waves (Mooney et al., 1996; Weliky and Katz, 1999). In WT neurons, synchronous stimulation induced LTP (Figs. 3d,f; 117%  $\pm$  8% over baseline;  $p < 0.001$ ). In KbDb $^{-/-}$  LGN neurons, the same protocol elicited LTP indistinguishable from WT neurons (Figs. 3e,f).

In contrast, induction using asynchronous activity patterns reveals a defect in LTD. In WT mice, when OT stimulation precedes LGN neuron depolarization by 1.1 s (Figs. 3a,c: 1100 ms latency), LTD results (Figs. 3g,i: 12% decrease from baseline;  $p < 0.001$ ). In contrast, in KbDb $^{-/-}$  mice, the same induction protocol failed to induce synaptic depression; if anything, a slight but significant potentiation was seen (Figs. 3h,i: 5% increase from baseline;  $p < 0.005$ ). Thus, although LTD using asynchronous presynaptic and postsynaptic activity patterns is a robust feature of WT retinogeniculate synapses during the period of synapse elimination and eye-specific layer formation, it appears to be absent in KbDb $^{-/-}$  mice. This impairment is consistent with the failure of synapse elimination and axonal remodeling in KbDb $^{-/-}$  mice.

### Ca<sup>2+</sup>-Permeable AMPA Receptors at KbDb $^{-/-}$ Synapses

Impaired LTD in KbDb $^{-/-}$  mice could result from altered regulation of NMDA-receptor-mediated synaptic responses because LTP and LTD are known to depend on NMDA receptors at a variety of synapses (Malenka and Bear, 2004). Surprisingly, the NMDA:AMPA ratio did not differ between genotypes (Extended Data, Figs. 7a,b). However, the kinetics of  $I_{AMPA}$  recorded in KbDb $^{-/-}$  LGN neurons are markedly prolonged compared with WT neurons (Figs. 4a–d). The slowed decay in KbDb $^{-/-}$  EPSCs is unlikely to result from different peak  $I_{AMPA}$  amplitudes ( $p > 0.1$ ) (Fig. 4d) but could occur if there were greater Ca<sup>2+</sup> influx through AMPA receptors.

CP-AMPA receptors are blocked selectively by bath-applying the specific antagonist NASPM (1-naphthyl acetyl spermine), a synthetic homologue of Joro spider toxin (Liu and Cull-Candy, 2000). Indeed, in KbDb $^{-/-}$  LGN neurons, 100  $\mu$ M NASPM blocked 40% of the current recorded at  $-70$  mV but only 20% in WT neurons (Fig. 4e; Extended Data, Fig. 7c), confirming a twofold increase in CP-AMPA receptor-mediated currents in KbDb $^{-/-}$  neurons. Another diagnostic feature of CP-AMPA receptors is rectification in the current–voltage (I–V) relationship when spermine

is present in the internal recording solution (Liu and Cull-Candy, 2000; Cull-Candy et al., 2006; Isaac et al., 2007). In WT neurons, the I–V relationship is linear; however in KbDb $^{-/-}$  LGN neurons, rectification is very prominent (Figs. 4f,g; Extended Data, Fig. 7d), though it can be linearized close to WT levels by bath application of NASPM (Figs. 4f,g). This implies that the prominent I–V rectification in KbDb $^{-/-}$  arises from an increase in CP-AMPA receptors.

Differences in composition of GluR subunits are known to modulate AMPA receptor Ca<sup>2+</sup> permeability, and tetramers containing GluR2 confer Ca<sup>2+</sup> impermeability (Cull-Candy et al., 2006). Indeed, the ratio of GluR1:GluR2, the most prevalent subunits (Hohnke et al., 2000; Cull-Candy et al., 2006; Goel et al., 2006), is slightly increased by 30% in developing thalamus from KbDb $^{-/-}$  mice ( $p = 0.07$ ; Extended Data, Fig. 7e). The thalamus is highly heterogeneous, so we also examined cortical neuronal cultures: the ratio of GluR1:GluR2 also significantly increased by 230% in KbDb $^{-/-}$  mice ( $p = 0.03$ ; Extended Data, Fig. 7f). Elevated levels of GluR1 subunits suggest that AMPA receptors in KbDb $^{-/-}$  mice are more likely to be composed of GluR1 homomers, yielding increased Ca<sup>2+</sup> permeability. Together, these results point to an increase in CP-AMPA receptors in KbDb $^{-/-}$  mice. Similar increases in CP-AMPA receptors at other synapses are known to shift synaptic learning rules away from LTD and toward LTP (Jia et al., 1996; Toyoda et al., 2007). If so, the deficit in LTD observed with the asynchronous pairing protocol (Figs. 3c,i) in KbDb $^{-/-}$  LGN should be rescued using NASPM to block CP-AMPA receptors—exactly what was observed (Extended Data, Fig. 8).

### Neuronal H2-Db Rescues Synaptic Function and LTD

If H2-Db affects synapse elimination by regulating the properties of AMPA receptors, then retinogeniculate EPSCs should be rescued to WT in the LGN of KbDb $^{-/-}$ ;NSEDb<sup>+</sup> mice. Indeed, the kinetics of  $I_{AMPA}$  are significantly faster in KbDb $^{-/-}$ ;NSEDb<sup>+</sup> LGN neurons than in KbDb $^{-/-}$ ;NSEDb<sup>-</sup> neurons (Figs. 5a–c; Extended Data, Fig. 9a), implying a decrease in CP-AMPA receptors. Accordingly, NASPM-dependent inhibition of  $I_{AMPA}$  is only 20% in KbDb $^{-/-}$ ;NSEDb<sup>+</sup> mice, significantly reduced from the 40% inhibition observed in littermate KbDb $^{-/-}$ ;NSEDb<sup>-</sup> mice (Fig. 5d; Extended Data, Fig. 9a). Moreover, the I–V relationship is linearized in KbDb $^{-/-}$ ;NSEDb<sup>+</sup> LGN neurons when spermine is present in the internal recording solution, and bath application of NASPM has little additional

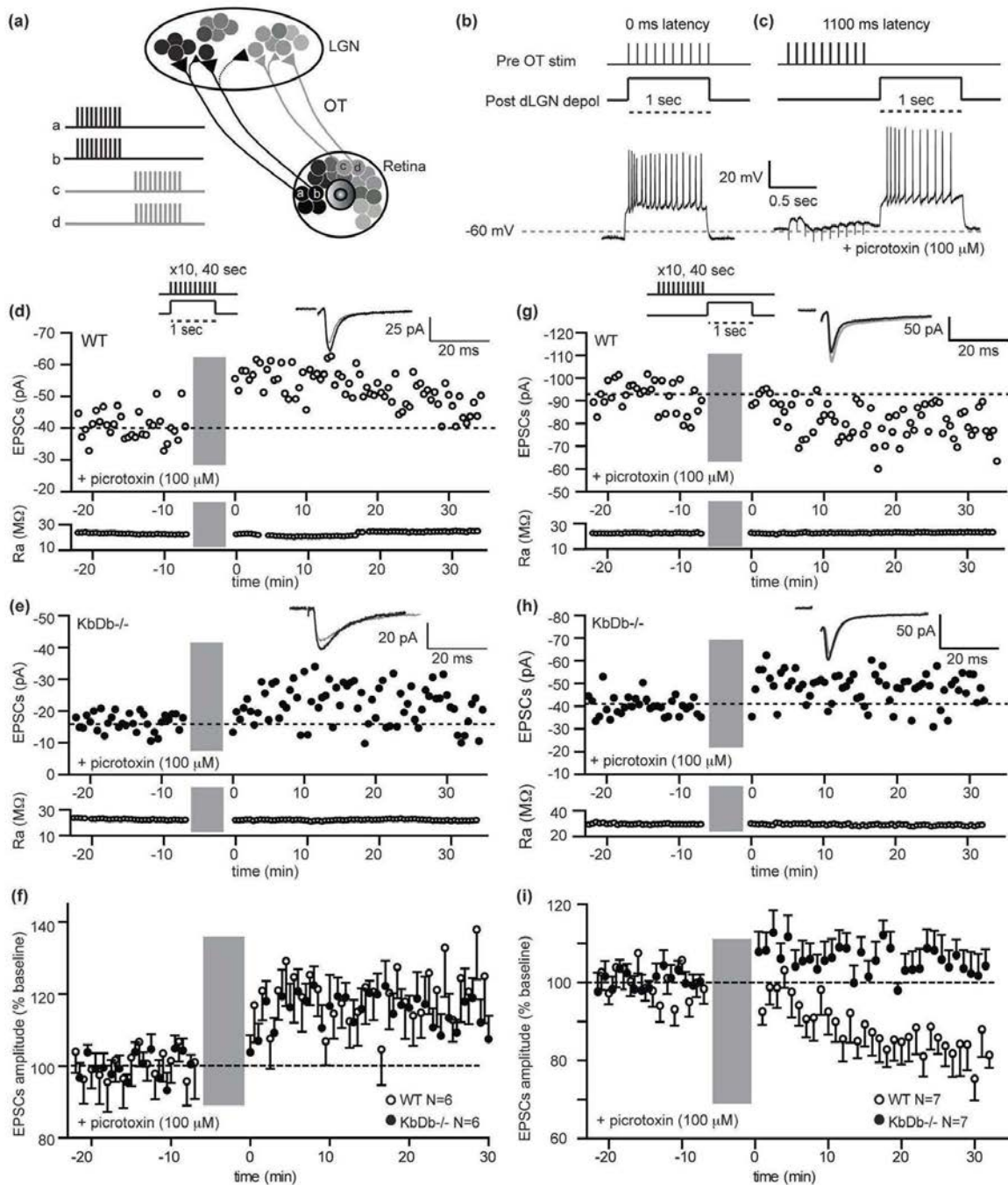


**Figure 3.** Impaired LTD but intact LTP at retinogeniculate synapses in KbDb<sup>-/-</sup> neurons induced with natural activity patterns. **a**, Diagram illustrating basis for timing-dependent plasticity at developing RGC synapses. Inset, Spontaneous retinal waves propagate from “a, b” toward “c, d”; neighboring RGCs fire synchronously but asynchronously with respect to RGCs located elsewhere. Waves drive action potentials in postsynaptic LGN neurons with varying time delays between presynaptic and postsynaptic activity. Ages P8–P13 studied. **b–c**, Top, Conditioning protocol for LTP (0 ms latency) (**b**) or LTD (1100 ms latency) (**c**). Bottom, example membrane potential changes recorded in LGN neuron during conditioning protocol. **d–f**, Intact LTP in KbDb<sup>-/-</sup> mice. Single experiment showing LTP in WT (**d**) and KbDb<sup>-/-</sup> (**e**) mice. EPSC peak amplitude vs. time. **f**, Summary of all 0 ms latency experiments: EPSC peak amplitude (% change from baseline) vs. time ( $n = 6/N = 6$  for each;  $p > 0.1$ ;  $t$ -test). **g–i**, Deficient LTD in KbDb<sup>-/-</sup> mice. Single experiment for WT (**g**) and KbDb<sup>-/-</sup> (**h**) mice. EPSC peak amplitude vs. time. **i**, Summary of all 1100 ms latency experiments: EPSC peak amplitude (% change from baseline) vs. time ( $n = 7/N = 7$  for each;  $p < 0.01$ ;  $t$ -test). Gray bars, induction period. Insets, Average EPSCs (30 traces) before (gray) and after (black) induction. **f**, **i**, 1 min data binning.  $n = \text{cells}/N = \text{animals}$ ; depol, depolarization; Ra, access resistance (MΩ); stim, stimulation. Reprinted with permission from Lee H et al. (2014), Figure 3. Copyright 2014, Nature Publishing Group.

effect ( $p > 0.5$  at +40 mV), similar to WT neurons (Fig. 5e; Extended Data, Fig. 9b). Because the  $\text{Ca}^{2+}$  permeability of AMPA receptors is close to WT levels in  $\text{KbDb}^{-/-};\text{NSEDb}^{+}$  LGN, it is possible that LTD is also rescued. Indeed, the same asynchronous activity pattern that failed to induce LTD in  $\text{KbDb}^{-/-}$  LGN (Fig. 3) induces robust LTD (15%;  $p < 0.001$ ) in  $\text{KbDb}^{-/-};\text{NSEDb}^{+}$  neurons, similar to WT neurons (Figs. 5f,g). Together, these observations suggest that restoring expression of H2-Db in neurons is sufficient to rescue LTD at retinogeniculate synapses by decreasing the  $\text{Ca}^{2+}$  permeability of AMPA receptors.

## Discussion

A major finding of this study is that the link between activity-dependent synapse pruning during development, and regulation of LTD and CP-AMPA receptors, requires neuronal MHCI function. It is notable that synapse elimination fails despite the fact that retinal waves and retinogeniculate basal synaptic transmission are intact. The persistence of multiple innervation in  $\text{KbDb}^{-/-}$  LGN neurons is highly reminiscent of the immature synaptic connectivity in the LGN of younger WT mice (Chen and Regehr, 2000) as well as abnormal connectivity observed in the LGNs of dark-reared or TTX-treated WT mice (Hooks and Chen, 2006). Together, these considerations imply that H2-Db and H2-Kb act downstream of neural activity. In studying the synaptic plasticity at RGC synapses, we imposed plasticity induction protocols that mimic natural patterns of spiking activity present in the retinogeniculate system during synapse elimination and eye-specific segregation. Our observation that in  $\text{KbDb}^{-/-}$  mice, LTD is impaired while LTP is intact can explain the failure in retinogeniculate synapse elimination: If synapses cannot undergo weakening, then they cannot be eliminated. Immunostaining for MHCI proteins H2-Db and H2-Kb is colocalized with synaptic markers in array tomography (Datwani et al., 2009) and at synapses in immunoelectron microscopy (Datwani et al., 2009; Needleman et al., 2010). Thus, these observations also argue strongly that H2-Db and/or H2-Kb at synapses regulate mechanisms of LTD, which in turn are required for synapse elimination. It would be useful to know whether other molecules implicated in RGC synapse elimination, such as C1q (Stevens et al., 2007), which colocalizes with H2-Db and H2-Kb at synapses (Datwani et al., 2009), also alter LTD or instead act downstream of MHCI to target already weakened synapses for removal.

The rescue experiments performed here imply that a single MHCI molecule—H2-Db, when expressed

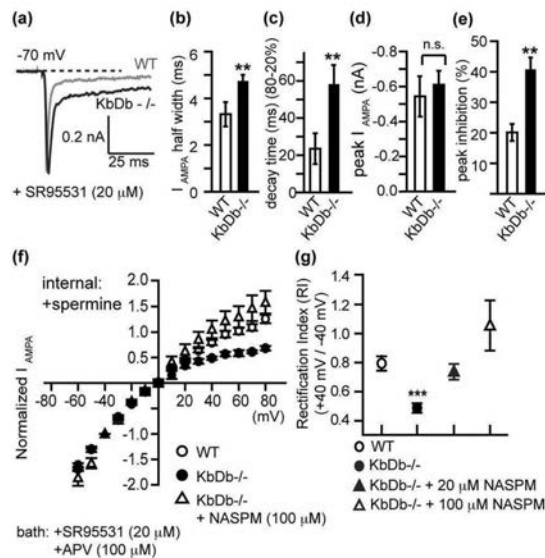


**Figure 4.** Increased CP-AMPA receptors at RGC synapses in  $\text{KbDb}^{-/-}$  LGN. **a–d**, Prolonged decay kinetics of  $I_{\text{AMPA}}$  in  $\text{KbDb}^{-/-}$  LGN neurons. **a**, Average  $I_{\text{AMPA}}$  (5–10 EPSCs) for WT vs  $\text{KbDb}^{-/-}$  LGN neurons **b**,  $I_{\text{AMPA}}$  half width (ms), **c**,  $I_{\text{AMPA}}$  decay time (ms) and **d**, Peak amplitude (nA) for WT vs  $\text{KbDb}^{-/-}$  mice (WT:  $n = 16/N = 4$ ;  $\text{KbDb}^{-/-}$ :  $n = 22/N = 5$ ). **e**, Increased inhibition of peak  $I_{\text{AMPA}}$  by NASPM in  $\text{KbDb}^{-/-}$  ( $n = 13/N = 4$ ) vs WT ( $n = 9/N = 3$ ) mice (\*\* $p < 0.01$ ; n.s., not significant; Mann-Whitney  $U$  test for **b–c**). **f**,  $I_{\text{AMPA}}$  I–V curves (normalized to –40 mV). **g**, Rectification index (RI) for WT ( $n = 14/N = 3$ ),  $\text{KbDb}^{-/-}$  ( $n = 9/N = 3$ ),  $\text{KbDb}^{-/-}$  + 20  $\mu\text{M}$  NASPM ( $n = 16/N = 4$ ), or  $\text{KbDb}^{-/-}$  + 100  $\mu\text{M}$  NASPM ( $n = 6/N = 2$ ) (\*\* $p < 0.001$  for WT vs  $\text{KbDb}^{-/-}$ ;  $p > 0.05$  for WT vs  $\text{KbDb}^{-/-}$  + NASPM [20 or 100  $\mu\text{M}$ ]; Mann-Whitney  $U$  test). Ages studied: P8–P13. See also Lee H et al. (2014) Extended Data, Fig. 7.  $n = \text{cells}/N = \text{animals}$ . Reprinted with permission from Lee H et al. (2014), Figure 4. Copyright 2014, Nature Publishing Group.

in neurons—is sufficient for functional synapse elimination and anatomical eye-specific segregation in the LGN. By crossing  $\text{KbDb}^{-/-}$  mice to  $\text{NSEDb}^{+}$  transgenic mice, expression of H2-Db alone was restored to neurons but not elsewhere in the body, rescuing LTD, functional synapse elimination,  $\text{Ca}^{2+}$ -impermeable AMPA receptors, and structural remodeling at retinogeniculate synapses. Notably, these brain phenotypes are rescued even though the immune system is still impaired in  $\text{KbDb}^{-/-};\text{NSEDb}^{+}$  mice. Until this experiment, it was not known whether any one MHCI molecule is sufficient either *in vitro* or *in vivo*, nor has it been possible to separate the general effects of immune compromise from the absence of H2-Db and/or H2-Kb in neurons. Together, these observations argue for a key role for H2-Db in reading out endogenous activity patterns into a lasting structural framework. In the human genome,

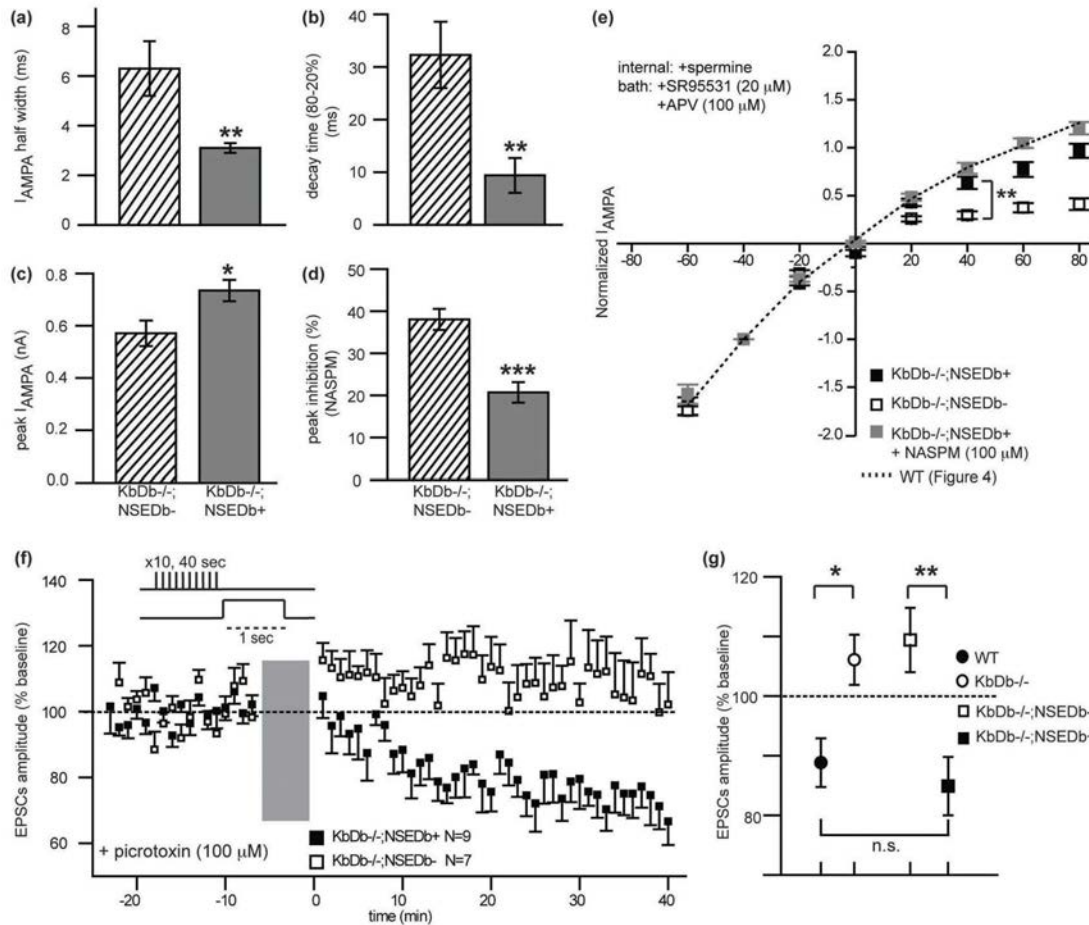


**Figure 5.** Neuronal expression of H2-Db restores  $Ca^{2+}$ -impermeable AMPA receptors and rescues LTD. **a**,  $I_{AMPA}$  half width (ms), **b**,  $I_{AMPA}$  decay time (ms), and **c**, Peak amplitude (nA) for  $KbDb^{-/-}; NSEDb^{-}$  ( $n = 9/N = 2$ ) and  $KbDb^{-/-}; NSEDb^{+}$  ( $n = 11/N = 4$ ) LGN. **d**, Reduced percentage inhibition of peak  $I_{AMPA}$  by NASPM (100  $\mu$ M) in  $KbDb^{-/-}; NSEDb^{+}$  ( $n = 10/N = 3$ ) compared with  $KbDb^{-/-}; NSEDb^{-}$  ( $n = 8/N = 2$ ) LGN; \* $p < 0.05$ , \*\* $p < 0.01$ , \*\*\* $p < 0.001$ ; Mann-Whitney  $U$  test for **a-d**. **e**, Rescue of  $I_{AMPA}$  linear I-V relationship in  $KbDb^{-/-}; NSEDb^{+}$  LGN. Rectification index at +40 mV for  $KbDb^{-/-}; NSEDb^{-}$  ( $n = 11/N = 3$ ) and  $KbDb^{-/-}; NSEDb^{+}$  ( $n = 13/N = 5$ ) LGN shows significant difference (\*\* $p < 0.005$ ); in contrast,  $KbDb^{-/-}; NSEDb^{+}$  (+NASPM) ( $n = 7/N = 3$ ) is not significantly different from  $KbDb^{-/-}; NSEDb^{+}$  ( $p > 0.05$ ), Mann-Whitney  $U$  test. See also Extended Data, Fig. 9. Mean  $\pm$  SEM. **f**, **g**, LTD rescued in  $KbDb^{-/-}; NSEDb^{+}$  LGN neurons. **f**, Ensemble average of all experiments at P8-P9 (Fig. 3). Gray bar, LTD induction period. 1 min data binning. **g**, Average percentage change (mean  $\pm$  SEM) for WT ( $N = 7$ ),  $KbDb^{-/-}$  ( $N = 7$ ), or  $KbDb^{-/-}; NSEDb^{-}$  ( $N = 7$ ) and  $KbDb^{-/-}; NSEDb^{+}$  ( $N = 9$ ) neurons. \* $p < 0.05$ , \*\* $p < 0.01$ , n.s., not significant;  $t$ -test. Ages studied: P8-P13.  $n = \text{cells}/N = \text{animals}$ . Reprinted with permission from Lee H et al. (2014), Figure 5. Copyright 2014, Nature Publishing Group.

as in mice, the MHC I (human leukocyte antigen) locus is large and highly polymorphic. Recent genome-wide association studies have consistently linked specific single nucleotide polymorphisms in MHC I to schizophrenia (Stefansson et al., 2009; Ripke et al., 2013). Our observations offer possible mechanistic insight: Alterations in expression levels of specific MHC I at neuronal synapses could trigger changes in activity-dependent plasticity and synaptic pruning during critical periods of human development, generating lasting alterations in circuits and behavior.

## Methods Summary

$KbDb^{-/-}$  mice were maintained on C57BL/6 backgrounds. Crosses of these two lines generated  $KbDb^{-/-}; NSEDb^{+}$  mice plus littermate controls. Electrophysiological recordings were made from LGN neurons by cutting parasagittal brain slices containing dorsal LGN and optic tract; synaptic transmission and degree of innervation were assessed as previously described (Chen and Regehr, 2000). For plasticity experiments at retinogeniculate synapses, perforated patch-clamp technique and induction protocols with natural activity patterns were used (Butts et al., 2007). Multielectrode array

recordings of retinal waves and anatomical labeling of retinogeniculate projections to determine status of eye-specific segregation were carried out according to Torborg et al. (2005) and Datwani et al. (2009). Pharmacological investigation of CP-AMPA receptors was made according to Liu and Cull-Candy (2000). All experiments were conducted and analyzed blind to genotype except in Figure 4 (in which genotype was obvious to the experimenter because of phenotype). Sample sizes were chosen for each experiment to reach statistical significance ( $p \leq 0.05$ ).

## Acknowledgments

All experimental protocols were approved by Stanford University Animal Care and Use Committees. KbdB<sup>-/-</sup> mice were generously provided by H. Ploegh (Vugmeyster et al., 1998) and NSEDb mice by Michael B.A. Oldstone (Rall et al., 1995). We thank members of the Shatz Lab for helpful comments. For technical assistance, thanks to N. Sotelo-Kury, C. Chechelski, and P. Kemper. For training in retinogeniculate slice methods, we thank Dr. Chinfei Chen (Boston Children's Hospital, Harvard Medical School) and Drs. Patrick Kanold and Dan Butts (University of Maryland, College Park). This work was supported by National Institutes of Health (NIH) Grants R01 MH071666 and EY02858; the G. Harold and Leila Y. Mathers Charitable Foundation (C.J.S.); NIH Grant R01 EY13528 (M.B.F.); National Defense Science and Engineering Graduate and National Science Foundation (NSF) Graduate Research Fellowships (J.D.A.); and an NSF Predoctoral Fellowship (L.A.K.). This chapter was modified from a previously published version: Lee, et al. (2014) Synapse elimination and learning rules coregulated by MHC Class I H2-Db. *Nature* 509:195–200. Copyright 2014, Nature Publishing Group. Supplementary materials, including Extended Data and complete Methods, are available at <https://www.ncbi.nlm.nih.gov/pmc/articles/PMC4016165>.

## References

Ackman JB, Burbridge, TJ, Crair MC (2012) Retinal waves coordinate patterned activity throughout the developing visual system. *Nature* 490:219–225.

Bastrikova N, Gardner GA, Reece JM, Jeromin A, Dudek SM (2008) Synapse elimination accompanies functional plasticity in hippocampal neurons. *Proc Natl Acad Sci USA* 105:3123–3127.

Bjartmar L, Huberman AD, Ullian EM, Rentería RC, Liu X, Xu W, Prezioso J, Susman MW, Stellwagen D, Stokes CC, Cho R, Worley P, Malenka RC, Ball S, Peachey NS, Copenhagen D, Chapman B, Nakamoto M, Barres BA, Perin MS (2006) Neuronal pentraxins mediate synaptic refinement in the developing visual system. *J Neurosci* 26:6269–6281.

Butts DA, Kanold PO, Shatz CJ (2007) A burst-based “Hebbian” learning rule at retinogeniculate synapses links retinal waves to activity-dependent refinement. *PLoS Biol* 5:e61.

Chen C, Regehr WG (2000) Developmental remodeling of the retinogeniculate synapse. *Neuron* 28:955–966.

Corriveau RA, Huh GS, Shatz CJ (1998) Regulation of class I MHC gene expression in the developing and mature CNS by neural activity. *Neuron* 21:505–520.

Cull-Candy S, Kelly L, Farrant M (2006) Regulation of Ca<sup>2+</sup>-permeable AMPA receptors: synaptic plasticity and beyond. *Curr Opin Neurobiol* 16:288–297.

Datwani A, McConnell MJ, Kanold PO, Micheva KD, Busse B, Shamloo M, Smith SJ, Shatz CJ (2009) Classical MHCI molecules regulate retinogeniculate refinement and limit ocular dominance plasticity. *Neuron* 64:463–470.

Feller MB, Wellis DP, Stellwagen D, Werblin FS, Shatz CJ (1996) Requirement for cholinergic synaptic transmission in the propagation of spontaneous retinal waves. *Science* 272:1182–1187.

Glynn MW, Elmer BM, Garay PA, Liu XB, Needleman LA, El-Sabeawy F, McAllister AK (2011) MHCI negatively regulates synapse density during the establishment of cortical connections. *Nat Neurosci* 14:442–451.

Goel A, Jiang B, Xu LW, Song L, Kirkwood A, Lee HK (2006) Cross-modal regulation of synaptic AMPA receptors in primary sensory cortices by visual experience. *Nat Neurosci* 9:1001–1003.

Hohnke CD, Oray S, Sur M (2000) Activity-dependent patterning of retinogeniculate axons proceeds with a constant contribution from AMPA and NMDA receptors. *J Neurosci* 20:8051–8060.

- Hooks BM, Chen C (2006) Distinct roles for spontaneous and visual activity in remodeling of the retinogeniculate synapse. *Neuron* 52:281–291.
- Huberman AD, Feller MB, Chapman B (2008) Mechanisms underlying development of visual maps and receptive fields. *Annu Rev Neurosci* 31:479–509.
- Huh GS, Boulanger LM, Du H, Riquelme PA, Brotz TM, Shatz CJ (2000) Functional requirement for class I MHC in CNS development and plasticity. *Science* 290:2155–2159.
- Isaac JT, Ashby MC, McBain CJ (2007) The role of the GluR2 subunit in AMPA receptor function and synaptic plasticity. *Neuron* 54:859–871.
- Jia Z, Agopyan N, Miu P, Xiong Z, Henderson J, Gerlai R, Taverna FA, Velumian A, MacDonald J, Carlen P, Abramow-Newerly W, Roder J (1996) Enhanced LTP in mice deficient in the AMPA receptor GluR2. *Neuron* 17:945–956.
- Lee H, Kirkby L, Brott BK, Adelson JD, Cheng S, Feller MB, Datwani A, Shatz CJ (2004) Synapse elimination and learning rules coregulated by MHC class I H2-Db. *Nature* 509:195–200.
- Liu SQ, Cull-Candy SG (2000) Synaptic activity at calcium-permeable AMPA receptors induces a switch in receptor subtype. *Nature* 405:454–458.
- Malenka RC, Bear MF (2004) LTP and LTD: an embarrassment of riches. *Neuron* 44:5–21.
- Meister M, Wong RO, Baylor DA, Shatz CJ (1991) Synchronous bursts of action potentials in ganglion cells of the developing mammalian retina. *Science* 252:939–943.
- Mooney R, Madison DV, Shatz CJ (1993) Enhancement of transmission at the developing retinogeniculate synapse. *Neuron* 10:815–825.
- Mooney R, Penn AA, Gallego R, Shatz CJ (1996) Thalamic relay of spontaneous retinal activity prior to vision. *Neuron* 17:863–874.
- Mu Y, Poo MM (2006) Spike timing-dependent LTP/LTD mediates visual experience-dependent plasticity in a developing retinotectal system. *Neuron* 50:115–125.
- Needleman LA, Liu XB, El-Sabeawy F, Jones EG, McAllister AK (2010) MHC class I molecules are present both pre- and postsynaptically in the visual cortex during postnatal development and in adulthood. *Proc Natl Acad Sci USA* 107:16999–17004.
- Penn AA, Riquelme PA, Feller MB, Shatz CJ (1998) Competition in retinogeniculate patterning driven by spontaneous activity. *Science* 279:2108–2112.
- Rall GF, Mucke L, Oldstone MB (1995) Consequences of cytotoxic T lymphocyte interaction with major histocompatibility complex class I-expressing neurons *in vivo*. *J Exp Med* 182:1201–1212.
- Ripke S, O'Dushlaine C, Chambert K, Moran JL, Kähler AK, Akterin S, Bergen SE, Collins AL, Crowley JJ, Fromer M, Kim Y, Lee SH, Magnusson PK, Sanchez N, Stahl EA, Williams S, Wray NR, Xia K, Bettella F, Borglum AD, et al. (2013) Genome-wide association analysis identifies 13 new risk loci for schizophrenia. *Nat Genet* 45:1150–1159.
- Shah RD, Crair MC (2008) Retinocollicular synapse maturation and plasticity are regulated by correlated retinal waves. *J Neurosci* 28:292–303.
- Shatz CJ, Kirkwood PA (1984) Prenatal development of functional connections in the cat's retinogeniculate pathway. *J Neurosci* 4:1378–1397.
- Shatz CJ (1996) Emergence of order in visual system development. *Proc Natl Acad Sci USA* 93:602–608.
- Stefansson H, Ophoff RA, Steinberg S, Andreassen OA, Cichon S, Rujescu D, Werge T, Pietiläinen OP, Mors O, Mortensen PB, Sigurdsson E, Gustafsson O, Nyegaard M, Tuulio-Henriksson A, Ingason A, Hansen T, Suvisaari J, Lonnqvist J, Paunio T, Børglum AD, et al. (2009) Common variants conferring risk of schizophrenia. *Nature* 460:744–747.
- Stevens B, Allen NJ, Vazquez LE, Howell GR, Christopherson KS, Nouri N, Micheva KD, Mehalow AK, Huberman AD, Stafford B, Sher A, Litke AM, Lambris JD, Smith SJ, John SW, Barres BA (2007) The classical complement cascade mediates CNS synapse elimination. *Cell* 131:1164–1178.
- Stevens CF, Wang Y (1994) Changes in reliability of synaptic function as a mechanism for plasticity. *Nature* 371:704–707.
- Torborg CL, Feller MB (2004) Unbiased analysis of bulk axonal segregation patterns. *J Neurosci Methods* 135:17–26.
- Torborg CL, Hansen KA, Feller MB (2005) High frequency, synchronized bursting drives eye-specific segregation of retinogeniculate projections. *Nat Neurosci* 8:72–78.

- Toyoda H, Wu LJ, Zhao MG, Xu H, Jia Z, Zhuo M (2007) Long-term depression requires postsynaptic AMPA GluR2 receptor in adult mouse cingulate cortex. *J Cell Physiol* 211:336–343.
- Vugmeyster Y, Glas R, Pérarnau B, Lemonnier FA, Eisen H, Ploegh H (1998) Major histocompatibility complex (MHC) class I K<sup>b</sup>D<sup>b</sup>-/- deficient mice possess functional CD8<sup>+</sup> T cells and natural killer cells. *Proc Natl Acad Sci USA* 95:12492–12497.
- Weliky M, Katz LC (1999) Correlational structure of spontaneous neuronal activity in the developing lateral geniculate nucleus *in vivo*. *Science* 285:599–604.
- Wong RO, Meister M, Shatz CJ (1993) Transient period of correlated bursting activity during development of the mammalian retina. *Neuron* 11:923–938.
- Yuste R, Bonhoeffer T (2001) Morphological changes in dendritic spines associated with long-term synaptic plasticity. *Annu Rev Neurosci* 24:1071–1089.
- Zhang J, Ackman JB, Xu HP, Crair MC (2011) Visual map development depends on the temporal pattern of binocular activity in mice. *Nat Neurosci* 15:298–307.
- Zhou Q, Homma KJ, Poo MM (2004) Shrinkage of dendritic spines associated with long-term depression of hippocampal synapses. *Neuron* 44:749–757.
- Ziburkus J, Dilger EK, Lo FS, Guido W (2009) LTD and LTP at the developing retinogeniculate synapse. *J Neurophysiol* 102:3082–3090.